

**EFFICIENCY COMPARISON OF MAXIMUM POWER POINT
TRACKING ON PHOTOVOLTAIC USING FUZZY LOGIC AND
PERTURB & OBSERVE METHODS**

THESIS

**MAGISTER PROGRAM OF ELECTRICAL ENGINEERING
POWER SYSTEM ENGINEERING**

Submitted to Qualify for a Master's Degree in Engineering



OSAMA AHMED A. ELGWEAL

156060308111001

**UNIVERSITY OF BRAWIJAYA
FACULTY OF ENGINEERING
MALANG**

2019

TITLE OF THE THESIS:

EFFICIENCY COMPARISON OF MAXIMUM POWER POINT TRACKING ON PHOTOVOLTAIC USING FUZZY LOGIC AND PERTURB & OBSERVE

METHODS

Name of Student : Osama Ahmed A. Elgweal

SID : 156060308111001

Department : Master Program of Electrical Engineering

Sub Department Interest : Power System

COMMISSION OF SUPERVISORS

Main Supervisor : Ir. Wijono, M.T., Ph.D.

Second Supervisor : Dr. Rini Nur Hasanah, S.T., M.Sc.

COMMISSION OF EXAMINERS

Examiner I : Ir. Hadi Suyono, S.T., M.T., Ph.D., IPM.

Examiner II : Dr. Ir. Harry Soekotjo Dachlan, M.Sc.

Examination Date : 27 May 2019

Assessment Letter of Examiners : 1077 Year 2019

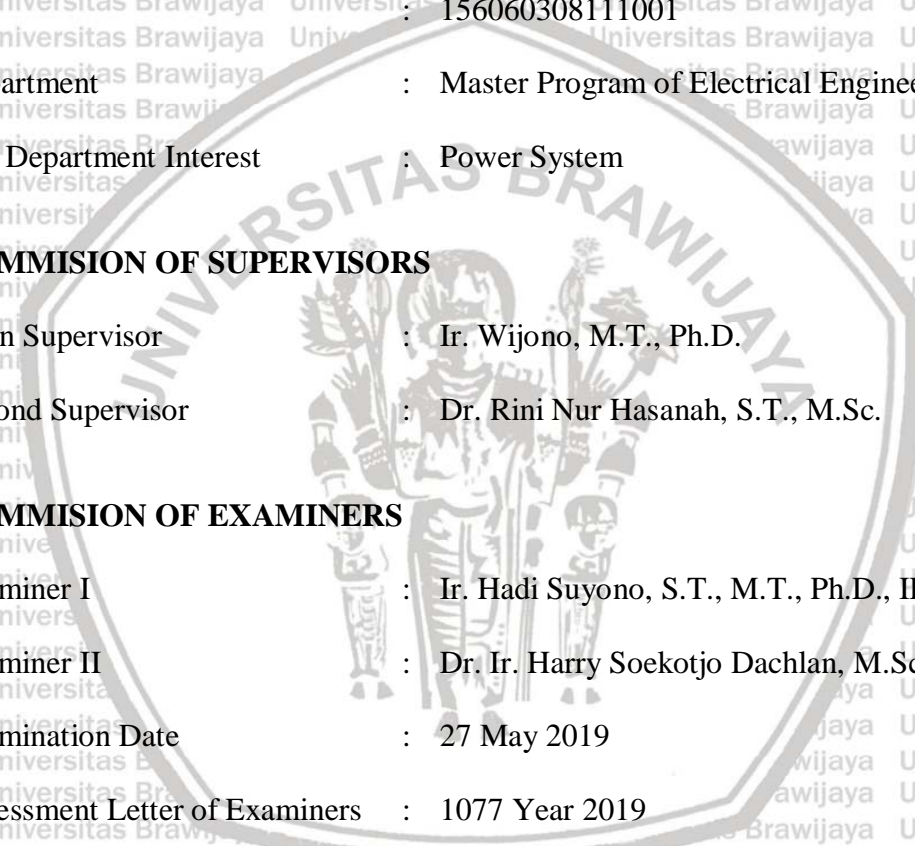


TABLE OF CONTENTS

SHEET OF VALIDATION	Error! Bookmark not defined.
IDENTITY OF THESIS EXAMINERS.....	Error! Bookmark not defined.
STATEMENT OF THESIS RESEARCH ORIGINALITIES	Error! Bookmark not defined.
SHEET OF TRIBUTE	Error! Bookmark not defined.
BIOGRAPHY.....	Error! Bookmark not defined.
ACKNOWLEDGEMENTS	Error! Bookmark not defined.
SUMMARY	Error! Bookmark not defined.
FOREWORD	Error! Bookmark not defined.
TABLE OF CONTENTS	1
LIST OF TABLES	3
LIST OF FIGURES	4
CHAPTER I PRELIMINARY	Error! Bookmark not defined.
1.1 Background	Error! Bookmark not defined.
1.2 Formulations of Problem	Error! Bookmark not defined.
1.3 Objectives of Research	Error! Bookmark not defined.
1.4 Scopes of Problem.....	Error! Bookmark not defined.
1.5 Benefits of Research.....	Error! Bookmark not defined.
CHAPTER II LITERATURE REVIEW	Error! Bookmark not defined.
2.1 Relevant Research Results.....	Error! Bookmark not defined.
2.2 Solar Cell	Error! Bookmark not defined.
2.3 Power and Efficiency of a Photovoltaic System.....	Error! Bookmark not defined.
2.4 Maximum Power Point Tracking (MPPT)	Error! Bookmark not defined.
2.5 MPPT Techniques	Error! Bookmark not defined.
2.6 Pulse Width Modulation (PWM)	Error! Bookmark not defined.
2.7 DC-DC Converter	Error! Bookmark not defined.
CHAPTER III RESEARCH CONCEPTUAL FRAMEWORK.....	Error! Bookmark not defined.
3.1 Framework of the Research	Error! Bookmark not defined.
3.2 The MPP Control Principles using P&O Algorithm and FLC Method	Error! Bookmark not defined.
3.3 Modeling of the PV System.....	Error! Bookmark not defined.
3.4 Determination of the Common Simulation Parameters.....	Error! Bookmark not defined.
3.5 Hypothesis	Error! Bookmark not defined.

CHAPTER IV RESEARCH METHODS Error! Bookmark not defined.

4.1 The Methods Comparison Study..... **Error! Bookmark not defined.**

4.2 The Expected Result of this Research..... **Error! Bookmark not defined.**

CHAPTER V RESULTS AND ANALYSIS Error! Bookmark not defined.

5.1 The Photovoltaic Parameters **Error! Bookmark not defined.**

5.2 Photovoltaic Testing without MPPT Implementation..... **Error! Bookmark not defined.**

5.3 General Simulation Parameters..... **Error! Bookmark not defined.**

5.4 Perturb and Observe Algorithm MPPT Simulation**Error! Bookmark not defined.**

5.5 Fuzzy Logic Control Method MPPT Simulation**Error! Bookmark not defined.**

5.6 Analysis of Result Comparison between P&O Algorithm and FLC Method**Error! Bookmark not defined.**

CHAPTER VI CONCLUSIONS AND PROPOSITIONS Error! Bookmark not defined.

6.1 Conclusions..... **Error! Bookmark not defined.**

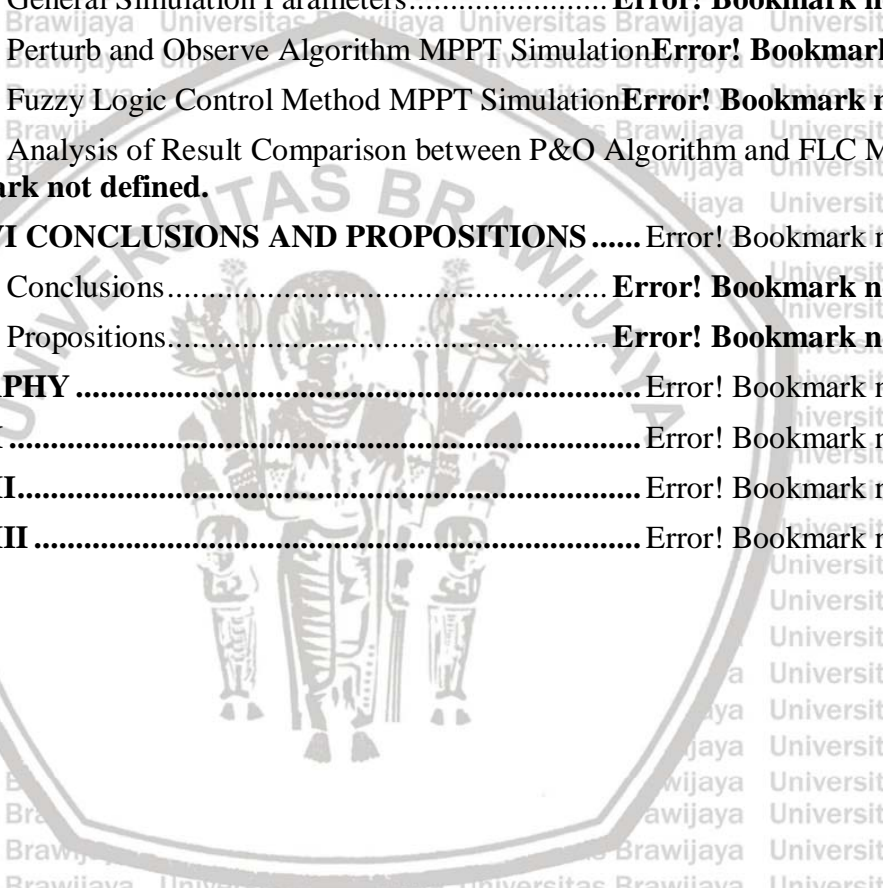
6.2 Propositions..... **Error! Bookmark not defined.**

BIBLIOGRAPHY Error! Bookmark not defined.

APPENDIX I Error! Bookmark not defined.

APPENDIX II..... Error! Bookmark not defined.

APPENDIX III Error! Bookmark not defined.



LIST OF TABLES

No.	Table Name	Page
Table 5.1	Example of P&O Algorithm Calculation Result from 0 Millisecond to 3 Milliseconds	Error! Bookmark not defined.
Table 5.2	FLC Rule for MPPT	Error! Bookmark not defined.
Table 5.3	Example of FLC Method Calculation Result from 0 Millisecond to 3 Milliseconds	Error! Bookmark not defined.
Table 5.4	Summary of P&O Algorithm and FLC Method on Photovoltaic MPPT	Error! Bookmark not defined.



LIST OF FIGURES

No.	Figure Name	Page
Figure 2.1	Solar cell basic principle operation.	Error! Bookmark not defined.
Figure 2.2	Equivalent circuit of solar cell.	Error! Bookmark not defined.
Figure 2.3	I-V characteristics for a PV module at specific atmospheric conditions. ..	Error! Bookmark not defined.
Figure 2.4	I-V characteristics of a solar cell showing the open-circuit voltage.	Error! Bookmark not defined.
Figure 2.5	I-V characteristics of a solar cell showing the short-circuit current.	Error! Bookmark not defined.
Figure 2.6	Important points in the characteristic curves of a solar panel.	Error! Bookmark not defined.
Figure 2.7	Fill factor of solar cell.	Error! Bookmark not defined.
Figure 2.8	I-V curve and P-V curve showing MPP.	Error! Bookmark not defined.
Figure 2.9	A scheme of hill-climbing technique in PV MPPT.....	Error! Bookmark not defined.
Figure 2.10	Flowchart of P&O algorithm.	Error! Bookmark not defined.
Figure 2.11	P&O MPPT technique.....	Error! Bookmark not defined.
Figure 2.12	Stages of an FLC method.....	Error! Bookmark not defined.
Figure 2.13	Membership functions for inputs and output of FLC.....	Error! Bookmark not defined.
Figure 2.14	The slope of P-V curve of PV module in accordance to power derivative and voltage derivative.....	Error! Bookmark not defined.
Figure 2.15	The P-V curve area division as named by linguistic variables.	Error! Bookmark not defined.
Figure 2.16	The flowchart of general FLC method.	Error! Bookmark not defined.
Figure 2.17	Schematic of a boost converter.	Error! Bookmark not defined.
Figure 3.1	Block system concept framework that will be created. The grayed boxes are the parts that will be done in this study.....	Error! Bookmark not defined.
Figure 3.2	The principle of MPPT controller using P&O algorithm.	Error! Bookmark not defined.
Figure 3.3	The principle of MPPT controller using FLC method.	Error! Bookmark not defined.
Figure 3.4	Kyocera Solar KC200GT PV module modeling in Matlab/Simulink.....	Error! Bookmark not defined.
Figure 4.1	Flowchart of the research methodology.	Error! Bookmark not defined.

- Figure 5.1 Kyocera Solar KC200GT I-V curve, with $1,000 \text{ W}\cdot\text{m}^{-2}$ irradiance and 25°C temperature. **Error! Bookmark not defined.**
- Figure 5.2 Kyocera Solar KC200GT P-V curve, with $1,000 \text{ W}\cdot\text{m}^{-2}$ irradiance and 25°C temperature. **Error! Bookmark not defined.**
- Figure 5.3 Simulink PV circuit diagram without MPPT implementation. **Error! Bookmark not defined.**
- Figure 5.4 The output voltage profile on PV, without the MPPT..... **Error! Bookmark not defined.**
- Figure 5.5 Matlab/Simulink PV MPPT circuit diagram for P&O algorithm. **Error! Bookmark not defined.**
- Figure 5.6 The graphical representation of the example of P&O algorithm result from 0 millisecond to 3 milliseconds..... **Error! Bookmark not defined.**
- Figure 5.7 The output of voltage, current, and power profile simulation on PV MPPT using P&O algorithm in the first 3 s..... **Error! Bookmark not defined.**
- Figure 5.8 The output voltage profile simulation on PV MPPT using P&O algorithm in the first 3 s..... **Error! Bookmark not defined.**
- Figure 5.9 The output current profile simulation on PV MPPT using P&O algorithm in the first 3 s..... **Error! Bookmark not defined.**
- Figure 5.10 The output power profile simulation on PV MPPT using P&O algorithm in the first 3 seconds..... **Error! Bookmark not defined.**
- Figure 5.11 The output of power profile simulation on PV MPPT using P&O algorithm in the first 100 ms..... **Error! Bookmark not defined.**
- Figure 5.12 Matlab/Simulink PV MPPT circuit diagram for FLC method. **Error! Bookmark not defined.**
- Figure 5.13 Simulink PV MPPT detailed circuit diagram for FLC method. **Error! Bookmark not defined.**
- Figure 5.14 Membership functions of voltage derivative (ΔV). **Error! Bookmark not defined.**
- Figure 5.15 Membership functions of power derivative (ΔP). **Error! Bookmark not defined.**
- Figure 5.16 The surface view of FLC rules for MPPT. **Error! Bookmark not defined.**
- Figure 5.17 Membership functions of duty cycle action (ΔD) as control action..... **Error! Bookmark not defined.**
- Figure 5.18 The graphical representation of the example of FLC method result from 0 millisecond to 3 milliseconds..... **Error! Bookmark not defined.**
- Figure 5.19 The output of voltage, current, and power profile simulation on PV MPPT using FLC method in the first 3 s. **Error! Bookmark not defined.**
- Figure 5.20 The output of voltage profile simulation on PV MPPT using FLC method in the first 3 s..... **Error! Bookmark not defined.**
- Figure 5.21 The output of current profile simulation on PV MPPT using FLC method in the first 3 s..... **Error! Bookmark not defined.**

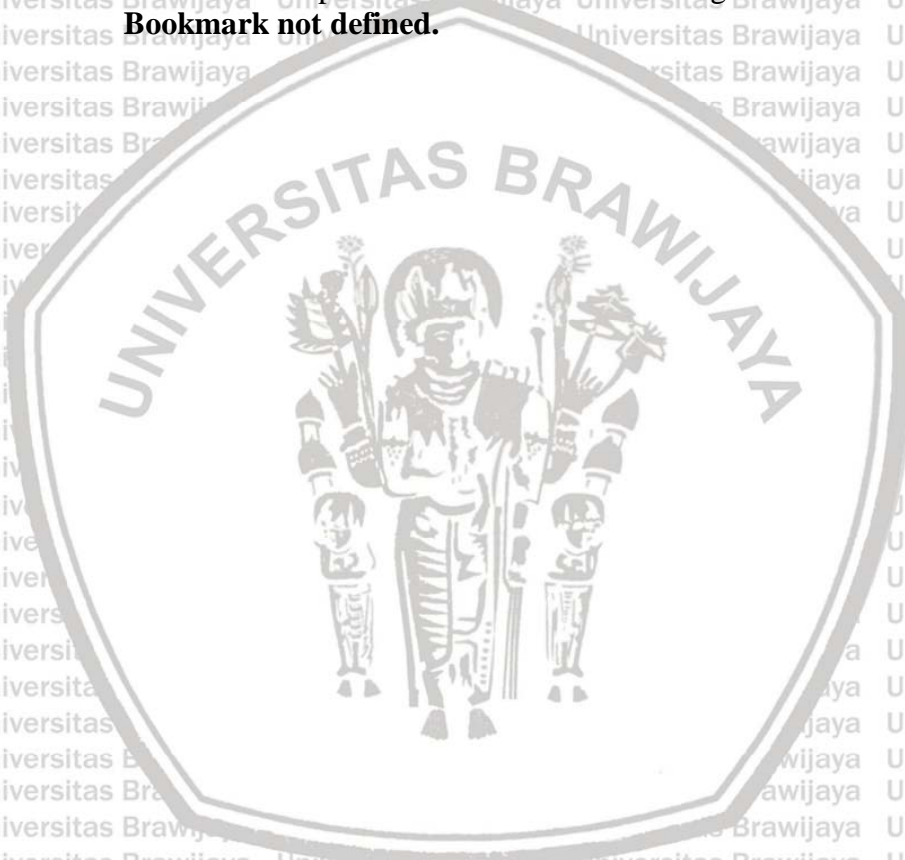
Figure 5.22 The output of power profile simulation on PV MPPT using FLC method in the first 3 s. **Error! Bookmark not defined.**

Figure 5.23 The output of power profile simulation on PV MPPT using FLC method in the first 100 ms. **Error! Bookmark not defined.**

Figure 5.24 Combined Matlab/Simulink PV MPPT circuit diagram for both P&O algorithm and FLC method. **Error! Bookmark not defined.**

Figure 5.25 Comparison between MPPT power profile using P&O algorithm and FLC method in the first 100 ms. **Error! Bookmark not defined.**

Figure 5.26 A detailed comparison result between P&O algorithm and FLC method. **Error! Bookmark not defined.**



CHAPTER I

PRELIMINARY

1.1 Background

Nowadays energy becomes crucial in everyday life. In recent times, the request for energy has significantly amplified all over the world. It caused for crisis of energy and alteration of climate.

Global warming and energy policies have become one of the biggest issues that globally facing now and a future concern for the ecosystem. The obviously clear that fossil fuels deteriorate climate, while renewable energy is in status quo. Currently, the majority of the developed countries have already switched over to solar energy by way of one of the major renewable energy sources.

So that makes most of scientific efforts recommends that the world desires for reducing emissions of greenhouse gas for at least 26% by 2020, and continuing for at least 81% by 2050. The basic process of exploitation of the solar power has been everywhere for eons and done in simple way.

The collectors of solar ray focus the sunlight that shines on them and change it to electricity. The solar power by today is a reasonable technique to enhance electricity power in urban and rural regions, where the running power lines cost increases. Recently, solar energy systems have been developed and become more available, especially for industrial or domestic uses as alternate energy resources.

Solar energy is one of renewable energy sources rapid developing due to its constant production cost reduction and the progress of its technology. The photovoltaic (PV) technology offers several benefits over fossil fuel, as it does not implicate fuel cost, does not contribute to pollution, requires tiny maintenance, low in noise, and presents good feasibility to install in distant sites. The charged particles produced by solar radiation in a PV cell are suitably detached to generate an electrical current by a proper strategy of the solar cell construction (Lynn, 2011). There are some PV main disadvantages, which consists of high manufacture cost, low efficiency of energy conversion, and nonlinear characteristics. The maximum power point (MPP) is a unique point on the power-voltage (P-V) curve. The PV array generates its maximum output power at this point. As the PV MPP power generation system is contingent on the temperature of array, the radiation received, and impedance of load, it is required for tracking the PV MPP continuously

(Abdulkadir, et al., 2013). A technique to sustain the PV array operating point at its MPP, known as the maximum power point tracking (MPPT), is required.

There have been known several MPPT method, including:

1. Incremental conductance (INC) (Al Nabulsi, et al., 2011);
2. Perturb and observe (P&O) (Rajendran & Smith, 2018);
3. Artificial neural network (ANN) with back propagation technique (Ramaprabha, et al., 2009);
4. The fuzzy logic controller (FLC) method with DC-DC converter (Mohamed, et al., 2012) (Aghoul, et al., 2013);
5. Ant colony optimization (ACO);
6. Genetic algorithm (GA) methods; and others.

Therefore, some research is done to optimize the use of PV module at its maximum power efficiency. Several studies have conducted experimental simulations with different methods, including FLC, P&O, and others. In this work, comparing and analyzing both FLC method and P&O algorithm on PV modules will be achieved to find MPPT. The photovoltaic system is a source of electrical energy derived from sunlight, can be directly used by electrical equipment, and can even be connected to public electricity.

This research tries to make comparison between P&O algorithm and FLC method implementation for MPPT. As the simplest and fastest method, P&O algorithm is chosen as the first method. While FLC has several basic advantages, it performs complex calculation that takes more computation power. Performance issues in FLC method implementation makes it as the second choice for comparison, to show the advantages over its complexity.

P&O algorithm is a classic control method that has been applied by the MPPT system so far, by measuring the voltage and current of a photovoltaic output, the voltage is always used to make measurements so that will always calculate if there is a change in the measured power. The main advantage of the P&O algorithm is its simplicity. But as P&O algorithm approaches MPP, it tends to oscillate around the point. From this problem, the various controller system of PV that using in MPPT can be determined. The control method is of P&O was chosen because it can track

maximum power quickly after changing environmental conditions. P&O is also an intelligent control of pulse width modulation (PWM) control in boost converter. To reduce oscillation around the MPP, P&O control is modified. In this case, the P&O control will look for MPP with an input state that is always changing.

P&O technique was also chosen for the simplicity and easy implementation (Sera, et al., 2013). PV voltage and current inputs are used as a reference for maximum power tracking. However, the main disadvantage of it is its failure to track the power under rapid changing of atmospheric conditions. Therefore, the P&O possesses limits, which decrease its MPPT efficiency, specifically:

1. The P-V curve flattens out when the amount of sunlight decreases; and
2. The P&O fluctuates around its MPP, as the technique becomes unbalanced with fast change in atmospheric conditions, especially in irradiance and temperature.

The FLC method-based MPPT has been used in the research carried out by Sun and Han. It had been based on the improvement of the more previous research using the proportional-integral (PI) control, resulting a fuzzified-PI (FLC-PI) method. The original PI method produced a rise time of 0.55 s, which was improved to 0.18 s using the fuzzified-PI method (Sun & Han, 2013).

Another MPPT technique using the FLC has been proposed by combining it with the proportional-integral-derivative (PID) control. A better performance in tracking speed has been obtained using the Fuzzy-PID control than applying conventional techniques such as P&O and ICond (Lee, et al., 2013).

In the research conducted by Huang, et al., the FLC method has been integrated into artificial neural network (ANN) to find the output error signal. The proposed fuzzified ANN (FLC-ANN) approach proved to be able to reach the MPP with output signal containing less than 2% error (Huang, et al., 2011).

As having been described previously, rarely a comparison between a pure FLC and other methods has been made. Another study analyzing only the application of the P&O algorithm on the PV MPPT has been conducted by Selmi, with the results show that the MPP can be tracked and almost be maintained, while the power output can be maximized (Selmi, et al., 2014).

The P&O technique has been widely implemented thanks to its ease implementation (Sera, et al., 2013). This algorithm is based on the “hill-climbing” principle, i.e. shifting the PV array point of operation in the course in which the power increases (Hohm & Ropp, 2003). Hill-climbing performs a perturbation on the duty cycle of the boost converter, while P&O executes a shifting in the DC link operating voltage between the PV array and boost converter (Esrām & Chapman, 2007) (Sivanandam, et al., 2007) (Rashid, 2011). PV voltage and current inputs are used as a reference for MPPT. However, the main P&O drawback is its failure on tracking the power under rapid atmospheric condition variation. This limitation specifically reduces the MPPT efficiency of the P&O method. The P-V plot gets flat out when the condition gets darker (Esrām & Chapman, 2007). The P&O fluctuates around the MPP, making this method unhinged with quick change in environment conditions, i.e. irradiance and temperature (Sivanandam, et al., 2007).

Based on this reason, an alternative MPPT technique is studied and deeply analyzed as comparison, to offer a better choice of possible MPPT techniques for a particular application. In this study, the chosen method to be compared to the P&O algorithm is the FLC method. The main problem to overcome with this alternative is that majority of the present MPPT algorithms undergo slow tracking, bringing about the reduction in their power efficiency. The lower efficiency of solar PV cells makes it difficult to determine the maximum point on the MPP path of the PV module and to give a better performance of the cell with lower oscillation during the MPPT operation. The results of comparison study is aimed to facilitate the choice among the high number of MPPT techniques available, and consequently to get a more reliable control of MPP in a PV system.

1.2 Formulations of Problem

Based on the background description of this study, it can be summarized that the MPPT technique in the solar cells adjusts the output voltage to extract the MPP. Therefore, the problem formulations of this study should include:

1. The choosing of PV MPPT implementation between P&O algorithm and FLC method;
2. The circuit models of P&O algorithm, FLC method, and combination of the two;
3. The simulation result of the models above; and
4. The analysis of performance between P&O algorithm and FLC method implementation as PV MPPT.

1.3 Objectives of Research

Based on the problem formulations described earlier, then the primary objectives of this research should include:

1. To select the common methods used in PV MPPT;
2. To design the entire circuit model of PV MPPT system for P&O algorithm, FLC method, and the combination of the two;
3. To perform simulation of PV MPPT using P&O algorithm, FLC method, and the combination of the two; and
4. To make analysis of result comparison between P&O algorithm and FLC method implementation as the PV MPPT.

1.4 Scopes of Problem

In accord of the research objectives, the research discussion is limited to the constraints as follows:

1. Matlab/Simulink system design simulation is used for MPPT technique to the connected PV cell in a combined system.
2. The solar panel model used is Kyocera Solar KC200GT type with 1000 W maximum power.
3. DC-DC converter used is boost converter.
4. Tracking methods used to compare are P&O algorithm and FLC method.
5. The solar irradiance level is set to $1000 \text{ W}\cdot\text{m}^{-2}$ and the ambient temperature is set to 25°C .
6. The result comparison to be analyzed consists of rise time, power efficiency, and quality of power output (power oscillation).

1.5 Benefits of Research

This project will obtain an optimal method of getting the maximum output value of the PV with faster tracking time, higher efficiency, and better power quality in PV uses in the future.

CHAPTER II

LITERATURE REVIEW

This chapter contains some of the previous relevant studies taken from scientific journals. Then followed by a discussion about the theoretical basics that supported the research concerning photovoltaic (PV) systems, maximum power point tracking (MPPT), boost converter, fuzzy logic control (FLC) method, and perturb and observe (P&O) algorithm.

MPPT technique uses because of its ease and to reduce the time to track the maximum power point (MPP). The MPP changes continuously under fast changing weather conditions (irradiance level and ambient temperature), sometimes ends up in calculating inaccurate MPP due to perturbation rather than that of the environmental change (Esram & Chapman, 2007).

1.1 Relevant Research Results

Several relevant studies related to the use of MPPT systems on PV include:

1. Sun and Han carried out research on the use of MPPT methods in 2013. The goal of the study was to employ solar energy because of its low efficiency in solar cells and the conditions of environmental change. MPPT engineering from the study stated that the boost type DC-DC converter uses FLC method to track MPP with a time of 0.18 s while without FLC takes 0.55 s, as a MPPT in PV has good tracking capability against changing external conditions compared to PI controllers, which have oscillation values at the MPP. The results show that the designed controller has better performance in terms of speed and stability (Sun & Han, 2013).
2. FLC and artificial neural networks (ANN) analysis has been performed by Keya Huang, et al., to test an MPPT application in 2011. Using of FLC and ANN is done to improve MPP determination discussed in MPPT research for the system. It was concluded that the principle of maximum power boost converter circuit and PV power generation method uses ANN, which was adopted and then compared with FLC. The results show only less than 2% of the output signal error, and indicate that the system is able to reach MPPT because the modified method uses ANN. The system also responds to environmental

variables both dynamic performance and steady performance with fast State (Huang, et al., 2011).

3. Chang-Uk Lee, et al., in 2013 also conducted research on MPPT using FLC. The purpose of the research is to combine two FLC and PI controllers to be applied to MPPT techniques. Cumulative integral calculus control on FLC and PI control problems also occur due to changes in operating conditions. The results obtained from this study that the performance of the FLC-PI controller (fuzzified-PI) has better results in terms of tracking speed compared to conventional methods such as P&O and ICond (Incremental conductance) (Lee, et al., 2013).
4. Selmi, et al., conducted another study that discusses the analysis of MPPT about PV that uses one diode and two diodes. The study aims at the effects of various values of PV irradiation on perturb and observe control. The results of the study show that MPP can be tracked and can almost be maintained. By using this method, power output can be maximized (Selmi, et al., 2014).

1.2 Solar Cell

1.2.1 Operating Principle

Most solar cells are made from silicon, therefore makes it the basic components of PV panels. The main benefits of the solar cells is the effect of some semiconductors to convert electromagnetic radiation directly into electrical current. The charged particles generated by the incident radiation are separated conveniently to create an electrical current by an appropriate design of the structure of the solar cell (Lynn, 2011).

A solar cell is basically a p-n junction which is made from two different layers of silicon doped with a small quantity of impurity atoms. In the case of the n-layer, the atoms consist of one more electron valence, called donors. In the case of the p-layer, the atoms consist of one less valence electron, known as acceptors. Generally, when the two layers are joined together, the free electrons of the n-layer are diffused in the p-side, leaving positively charged atoms by the donors. Similarly, the free holes in the p-layer are diffused in the n-side, leaving a region of negatively charged atoms by the acceptors. This creates an electrical field between the two sides that makes a potential barrier to further flow.

The equilibrium is reached in the junction when the electrons and holes cannot overcome that potential barrier and therefore they cannot move. This electric field pulls the electrons and holes in opposite directions so the current can flow in one way only: electrons can move from the p-side to the n-side and the holes in the opposite direction.

Figure 1.1 displays the p-n junction, which describes the effect of the electric field mentioned before. Metallic contacts are added at both sides to collect the electrons and holes so the current can flow. In another case of the n-layer, which is facing the solar irradiance, the contacts are in form of several metallic strips, as they must allow the light to pass to the solar cell.

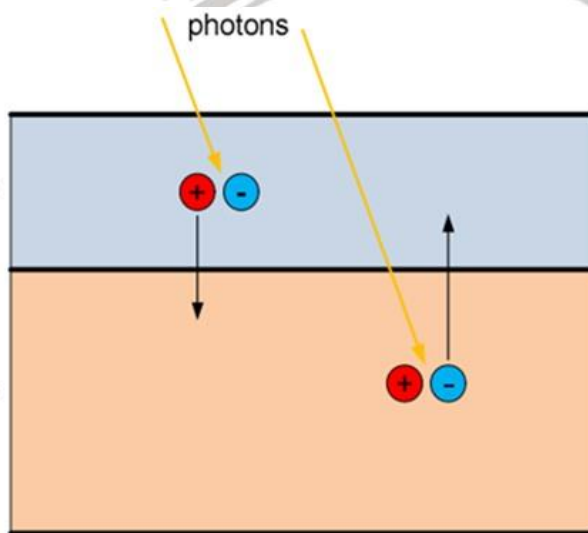


Figure 1.1 Solar cell basic principle operation.

When the photons of the solar radiation shine on the cell, three different cases can happen:

1. Some of the photons are reflected from the top surface of the cell and metal fingers. Those that are not reflected penetrate in the substrate;
2. Some of photons, usually the ones with less energy, pass through the cell without causing any effect; and
3. Only photons with energy level above the band gap of the silicon can create an electron-hole pair. These pairs are generated at both sides of the p-n junction.

The minority charges (electrons in the p-side, holes in the n-side) are diffused to the junction and swept away in opposite directions (electrons towards the n-side, holes towards the p-side) by

the electric field, generating a current in the cell, which is collected by the metal contacts at both sides. This is the light-generated current, which depends directly on the irradiation: if it is higher, then it contains more photons with enough energy to create more electron-hole pairs and consequently more current is generated by the solar cell.

1.2.2 Equivalent Circuit of Solar Cell

A general mathematical description of current-voltage (I-V) output characteristics for a PV cell has been studied for over the past four decades. Such an equivalent circuit-based model is mainly used for the MPPT technologies. The simplest equivalent circuit of the general model, which consists of a photocurrent, a diode, a parallel resistor expressing a leakage current, and a series resistor describing an internal resistance to the current flow, is shown in Figure 1.2 (Yusof, et al., 2004).

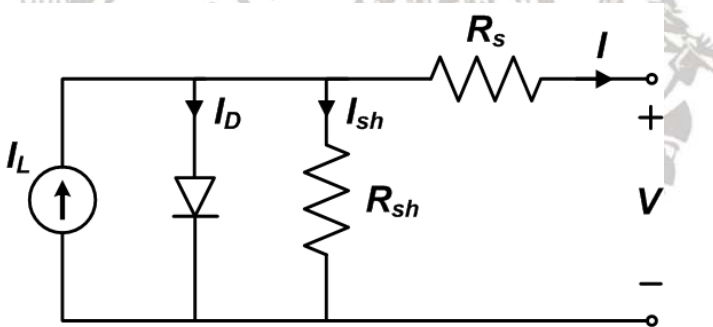


Figure 1.2 Equivalent circuit of solar cell.
Source : (Yusof, et al., 2004)

The output of the current source is directly proportional to the light falling on the cell (photocurrent I_{ph}). During darkness, the solar cell is not an active device, it works as a diode, i.e. a p-n junction, and produces neither current nor voltage. However, if it is connected to an external supply (large voltage), it generates current (I_D) called diode current or dark current. The diode determines the I-V characteristics of the cell. The I-V characteristic equation of an ideal solar cell is given in Equation (2-1) (Khouzam, et al., 1994).

$$I = I_{ph} - I_d \dots\dots\dots (2-1)$$

$$I = I_{ph} - I_d \cdot e^{\frac{V_q}{kT_a} - 1} \dots\dots\dots (2-2)$$

The Equation (2-2) describes the output current of the non-ideal practical PV cell, which was derived using Kirchhoff's current law as shown in Equation (2-3).

$$I = I_{ph} - I_d - I_{sh} \dots\dots\dots (2-3)$$

From Equation (2-3), the following Equation (2-4) can be determined.

$$I = I_{pv} - I_s \cdot \left(e^{\frac{q \cdot V + I \cdot R_s}{A \cdot K \cdot T_a}} - 1 - \frac{V + I \cdot R_s}{R_{sh}} \right) \dots\dots\dots (2-4)$$

Where:

I_{ph} = light-generated current or photocurrent (A)

I_d = reverse saturation current of diode (A)

q = elementary charge ($1.602 \cdot 10^{-19}$ C)

V = voltage across the diode (V)

K = Boltzmann's constant ($1.381 \cdot 10^{-23}$ J·K⁻¹)

T_a = junction temperature (K)

n = ideality factor of the diode

R_s = series resistance of diode (Ω)

R_{sh} = shunt resistance of diode (Ω)

The complete behavior of PV cells is described by five model parameters, which is a representative of the physical behavior of a PV module. These five parameters of PV module are in fact related to two environmental conditions, i.e. solar irradiance and ambient temperature.

The determination of these model parameters is not direct owing to non-linear nature of Equation (2-4). Based on Equation (2-4), the Matlab/Simulink model can then be developed. The above model includes two subsystems, one that calculates the PV cell photocurrent mainly depends on the solar irradiance and cell's working temperature, which is described as Equation (2-5).

$$I_{ph} = I_{sc} \cdot \frac{s}{1000} + C_T \cdot (T - T_{ref}) \dots\dots\dots (2-5)$$

Where:

I_{ph} = photon current (A)

I_{sc} = short circuit current at standard testing condition (A)

S = operating solar radiation ($W \cdot m^{-2}$)



- C_T = short-circuit current temperature coefficient ($0.0016 \text{ A}\cdot\text{K}^{-1}$)
- T = operating temperature (K)
- T_{ref} = solar cell absolute temperature at standard testing condition (293.15 K)

As Figure 1.2 shows the electric model of the PV cell, the output current of the PV cell is a result of subtraction of the photo current, the saturation current, and the current passing through the shunt resistance. There is a linear relation between the photo current and the solar irradiance as described in Equation (2-5). The photovoltaic I-V characteristics curve can be shown in Figure 1.3. Therefore, it can be noticed that there is a nonlinear relation between the output current and voltage of the PV cell.

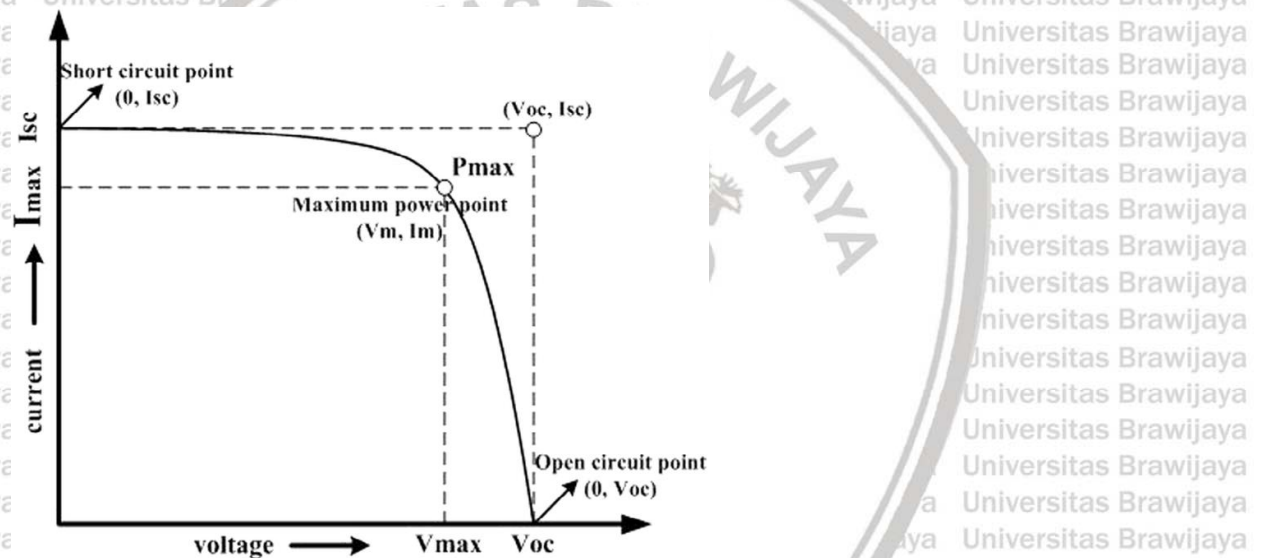


Figure 1.3 I-V characteristics for a PV module at specific atmospheric conditions.

Source : (Villalva, et al., 2009)

1.2.3 Short Circuit Current and Open-Circuit Voltage

There are two important points of the current-voltage characteristic, which are considered as:

1. The open circuit voltage (V_{oc}); and
2. The short circuit current (I_{sc}).

Therefore, when there is no current flows, then the output voltage is termed as the open circuit voltage as shown in Equation (2-6).

$$V_{oc} = \frac{K \cdot B \cdot T}{q} \cdot \ln\left(1 + \frac{I_{ph}}{I_o}\right) \dots \dots \dots (2-6)$$

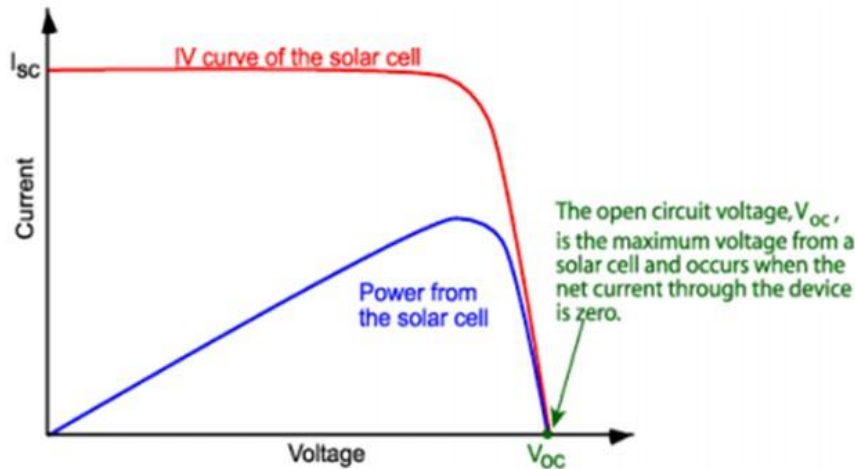


Figure 1.4 I-V characteristics of a solar cell showing the open-circuit voltage.

Source : (Wenham, et al., 2013)

At both points, the power generated is zero. The open circuit voltage can be approximated from Equation (2-1) when the output current of the cell is zero, i.e. when there is no current flows and the shunt resistance (R_{sh}) is neglected. It is represented by Equation (2-6).

The short circuit current is the current when there is no voltage and is approximately equal to the light generated current (I_L) as shown in Equation (2-7).

$$I_{sc} \approx I_L \dots \dots \dots (2-7)$$

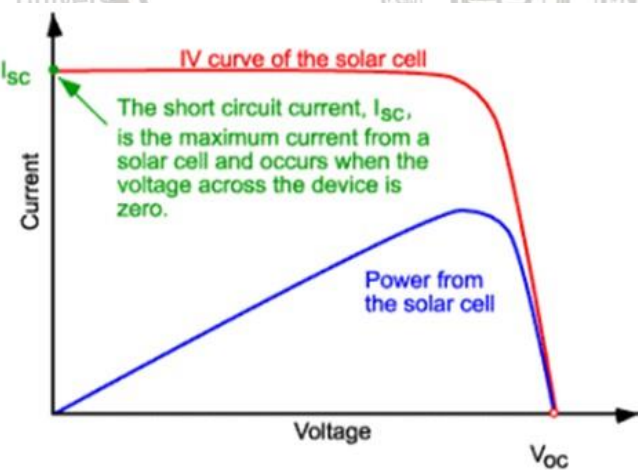


Figure 1.5 I-V characteristics of a solar cell showing the short-circuit current.

Source : (Wenham, et al., 2013)

The maximum power is generated by the solar cell at a point of the current-voltage characteristic where the I-V product is maximum. This point is known as the MPP and is unique, as can be seen in Figure 1.6, where the previous points are represented.

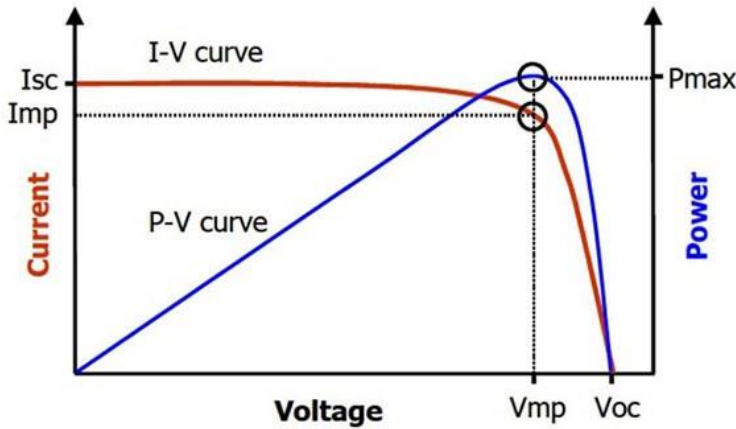


Figure 1.6 Important points in the characteristic curves of a solar panel.

Source : (Wenham, et al., 2013)

1.2.4 Fill Factor

The fill factor (FF) is defined as the ratio of the maximum power from the solar cell to the product of open circuit voltage and short circuit current. Graphically, as FF is a measurement of the I-V curve “squareness”, a solar cell with a higher voltage has a larger possible FF since the “rounded” portion of the I-V curve takes up less area, as shown in Figure 1.7. The variation in maximum FF can be important for solar cells made from different materials. The FF can be defined as Equation (2-8).

$$FF = \frac{I_{mp} \cdot V_{mp}}{I_{sc} \cdot V_{oc}} \quad (2-8)$$

The illustration of FF is shown on Figure 1.7.

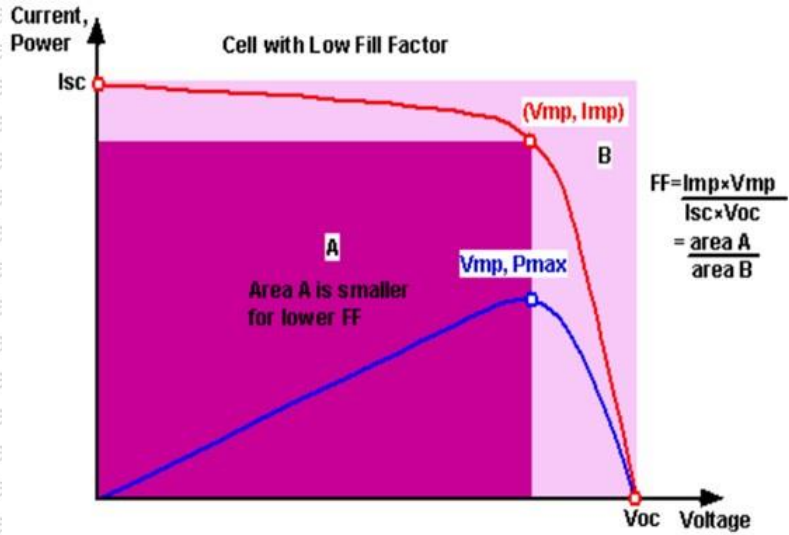


Figure 1.7 Fill factor of solar cell.

1.3 Power and Efficiency of a Photovoltaic System

Before knowing the momentary power produced, the energy received must be determined, which is the multiplication of the intensity of radiation received by the surface area, as shown in Equation (2-9).

$$E = I_r \cdot A \dots\dots\dots (2-9)$$

Where:

E = energy (J)

I_r = solar radiation intensity ($W \cdot m^{-2}$)

A = surface area (m^2)

The amount of instantaneous power is the multiplication of voltage and current produced by PV, which can be calculated using Equation (2-10).

$$P = V \cdot I \dots\dots\dots (2-10)$$

Where:

P = power (W)

V = potential difference (V)

I = current (A)

Efficiency of a PV system is a power comparison generated by photovoltaic with the input energy obtained from the efficiency used by the instantaneous efficiency at the time of data retrieval, regard to:

1. The efficiency of the PV panel (it is between 8% to 15% in commercial PV panels);
2. The efficiency of the inverter (95% to 98 %); and
3. The efficiency of the MPPT algorithm (which is over 98%).

Improving the efficiency of the PV panel and the inverter is not easy as it depends on the technology available. It requires high quality components, which can increase the cost of the installation.

$$\mu = \frac{V_{out}}{V_{in}} \cdot 100\% \dots\dots\dots (2-11)$$

Equation (2-11) describes the relation between input voltage, output voltage, and efficiency.

If the user wants a greater voltage or current, then PV can be arranged in series or in parallel or a combination of both. When PV is arranged in series, the voltage multiplies, but if it is arranged in parallel, the current is multiplied. The output of PV in the form of electric current can be directly used to supply the load. The electric current can also be used to charge the battery so that it can be used when needed, especially at nighttime due to the absence of sunlight.

If the PV is used for charging batteries, the amount of voltage produced must be above the batteries specifications. For example, if a battery used is 12 V, then the voltage generated by PV must be above 12 V to be able to charge. The unit of capacity of a battery is ampere-hour (Ah) and usually this characteristic is found on its label. A battery with 10 Ah capacity will be fully charged for 10 hours with a PV output current of 1 A.

1.4 Maximum Power Point Tracking (MPPT)

MPPT is a technique used to keep PV systems working around their MPP. Based on Figure 1.8, it can be seen that the MPP are at points E and F, which are affected by temperature and irradiation. As seen in the Figure 1.8, the irradiation is 500 W·m², while the temperature are set to 40° C and 80° C. Based on these graphs we can also find out the existence of an optimal point, so that maximum power is obtained. The working point is in V_{mp} and I_{mp} , which in turn produces MPP.

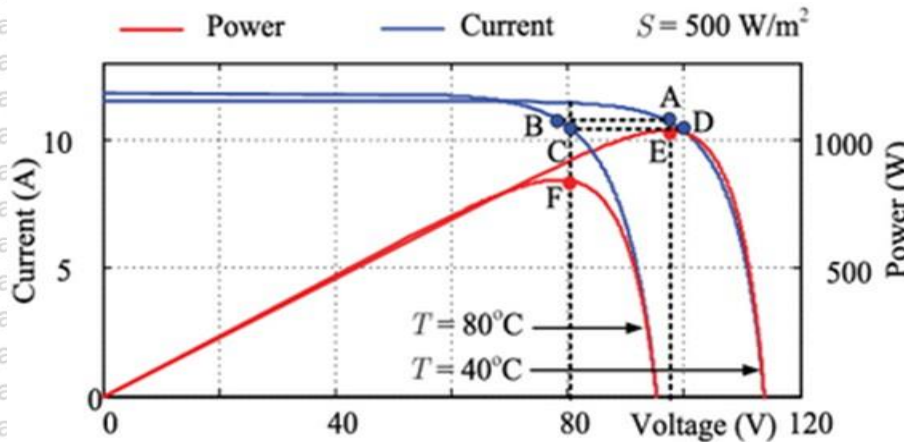


Figure 1.8 I-V curve and P-V curve showing MPP.

Source : (Kumar, et al., 2013)

MPPT is used to obtain optimal voltage and current values so that the maximum output power of a PV is obtained. This maximum output power will produce high efficiency and reduce losses of a PV.

The working principle of MPPT is to increase and decrease the photovoltaic working voltage. If in a PV system, the working voltage is also in the area to the left of V_{mp} (the working voltage is smaller than V_{mp}), then the PV working voltage will be increased until it reaches V_{mp} , and vice versa. After reaching the V_{mp} , the output power of the PV will also be maximum. A device used for increasing and decreasing the voltage is a DC-DC converter.

1.5 MPPT Techniques

There are some different techniques used to track the MPP and improve the solar energy efficiency. Few of the most popular techniques are:

1. Perturb and Observe (P&O), known as Hill Climbing Method;
2. Incremental Conductance Method (InCond);
3. Fractional Short Circuit Current;
4. Fractional Open Circuit Voltage;
5. Artificial Neural Networks (ANN); and
6. Fuzzy Logic Control (FLC).

Therefore, through the previous MPPT techniques literature review, researchers have seen the most common technique that have been used to obtaining MPP is P&O algorithm, due to its simple and easy implementation, but may fail under rapidly changing atmospheric conditions (Villalva, et al., 2009). The most popular intelligent control technique is using FLC method, known by its characteristic of multi rule based resolution and multivariable consideration. That is associated with an MPPT controller in order to improve energy conversion efficiency, which has the advantages of working with imprecise inputs, no need to have accurate mathematical model, and it can handle the nonlinearity (Engineering, 2013). It can also be used to select the optimized value of MPP (Souza, et al., 2005).

1.5.1 Hill-Climbing Method

Both P&O and InCond algorithms are based on the hill-climbing principle, which consists of moving the operation point of the PV array in the direction in which power increases (Hohm & Ropp, 2003). Hill-climbing technique is the most popular MPPT methods due to its ease of implementation and good performance when the irradiation is constant. The advantages of both methods are the simplicity and low computational power they require. The shortcomings are also well known: oscillations around the MPP and they can get lost and track the MPP in the wrong direction during rapid change of atmospheric conditions (Hohm & Ropp, 2003).

The P&O algorithm is also called hill climbing, but both names are related to the same algorithm depending on how it is implemented. Hill climbing involves a perturbation on the duty cycle of the power converter, whilst P&O trigs a perturbation in the operating voltage of the DC link between the PV array and the power converter (Esrasm & Chapman, 2007).

If there is an increment in the power, then the perturbation should be kept in the same direction. If the power decreases, then the perturbation should be in the opposite direction. Based on these facts, the algorithm is implemented (Esrasm & Chapman, 2007). The process is repeated until the MPP is reached, then the operating point oscillates around the MPP. This problem is also common to the InCond method, as mentioned earlier. A scheme of both algorithms is shown in Figure 1.9.

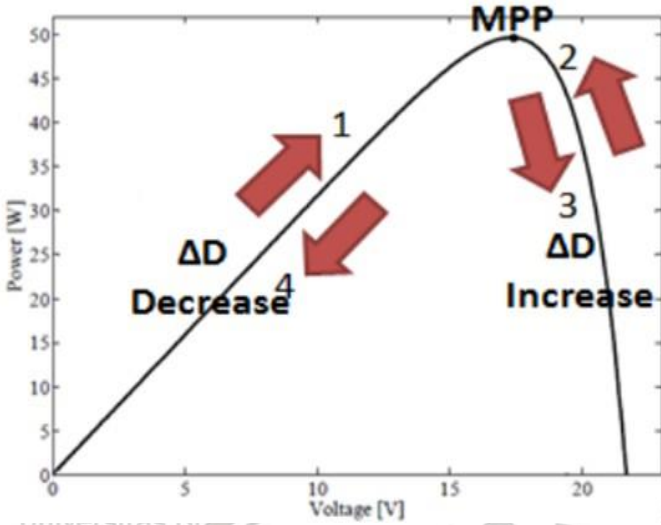


Figure 1.9 A scheme of hill-climbing technique in PV MPPT.

In Figure 1.10, the flowchart of P&O algorithm is shown, as it describes following steps sequence:

1. Measurement of voltage and current;
2. Power calculation;
3. Initialization as new power;
4. Initialization of power sum new and past power;
5. Initialize the new voltage addition and the previous voltage;
6. Initialize the new voltage addition and the previous voltage; and
7. Initialization of the sum of new currents and past flows to 8, 9, or 10, according to addition or subtraction of values for duty cycle.

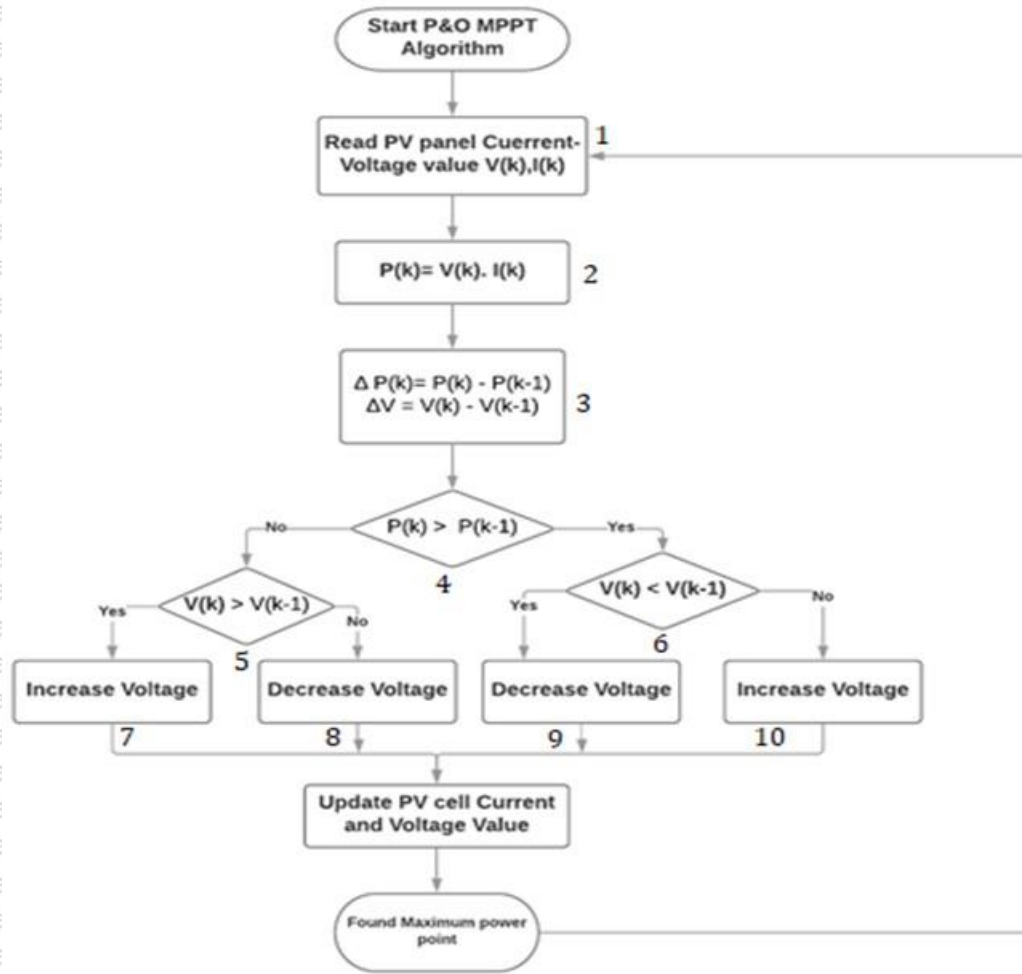


Figure 1.10 Flowchart of P&O algorithm.

Source : (Esrarn & Chapman, 2007)

Oscillations around the MPP generated by P&O algorithm is explained in Figure 1.11. The P&O algorithm was developed based on Figure 1.11, which is in a steady state condition if the positive slope is to the left of MPP (A-B) and the negative slope is to the right (B-C).

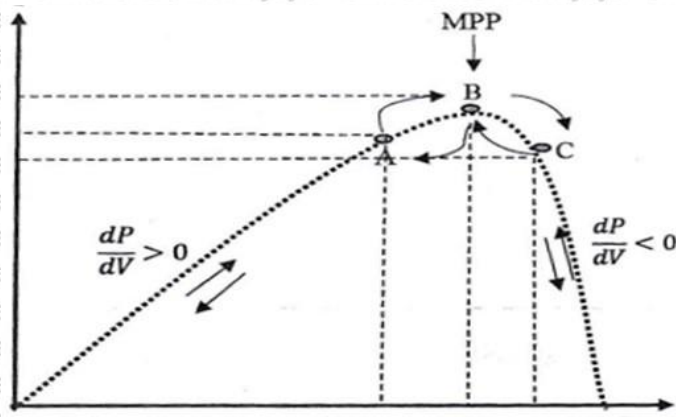


Figure 1.11 P&O MPPT technique.

1.5.2 Fuzzy Logic

Recently, the FLC method has been introduced in the tracking of the MPP in PV systems. As it has the advantages to be robust and relatively simple to design, the use of FLC method has become popular over the last decade. Moreover, this method deals with imprecise inputs, does not need an accurate mathematical model, and can handle nonlinearity very well. Microcontrollers have also helped in the popularization of FLC method (Esram & Chapman, 2007). The basic of FLC method generally consists of three stages:

1. Fuzzification;
2. Rule Base Evaluation (Rule Table Lookup Process); and
3. Defuzzification.

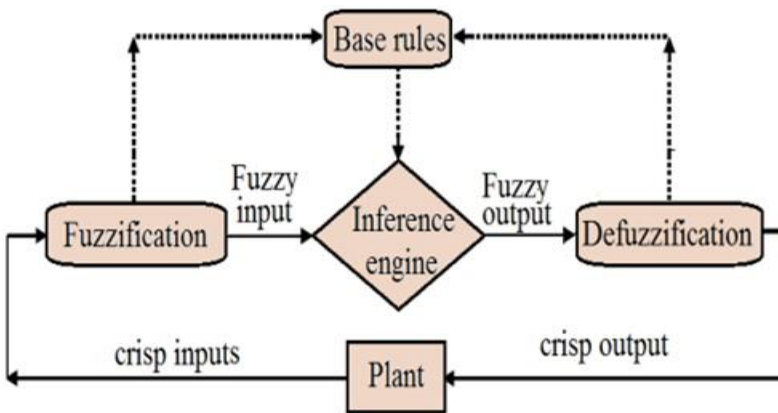


Figure 1.12 Stages of an FLC method.

In fuzzification process, the numerical input variables are converted into linguistic variables based on a membership function. For the purpose of this project, seven fuzzy levels as linguistic variables will be used, namely:

1. NB (Negative Big);
2. NM (Negative Medium);
3. NS (Negative Small);
4. ZE (Zero);
5. PS (Positive Small);
6. PM (Positive Medium); and
7. PB (Positive Big).

Illustration of membership function in Figure 1.13, states that the values of a , b , and c are based on the range of the numerical input variables (Sivanandam, et al., 2007).

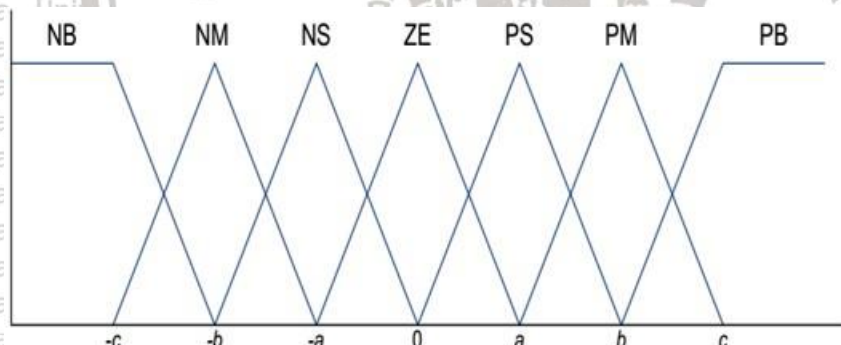


Figure 1.13 Membership functions for inputs and output of FLC.

Membership function is a curve that defines how each point in the input space is mapped to a membership value (degree of membership) between 0 and 1. The input space is sometimes referred to as the universe of discourse.

Fuzzy rule set and inference engine are designed to make controller achieves zero error signal ($E = 0$) at the steady state of the MPP. The main idea of the fuzzy rule set is a collection of IF-THEN rules that contain all the information for the controlled parameters. Therefore, in case of MPPT, the role of fuzzy rule set is to bring operating point to the MPP by increasing or decreasing the duty cycle ratio, depending on the position of the operating point from the MPP. Therefore,

when the operating point is deviating from the MPP, the duty cycle ratio will be increased or decreased (Sivanandam, et al., 2007).

About the fuzzy inference engine, an operating method formulates a logical decision based on the fuzzy rule setting and transforms the fuzzy rule base into fuzzy linguistic output. There are some known methods for the inference engine, such as Mamdani, Sugeno, Larsen, and so on. The Mamdani method is the most commonly used that will be used in this work (Sivanandam, et al., 2007) (Esram & Chapman, 2007).

After evaluating the fuzzy rule, the output will be converted from linguistic variable to numerical crisp once again using membership function, a process called defuzzification. The last operation of the controller generates output of precise value of duty cycle ratio, commonly called as control action.

In case of MPPT, the inputs for FLC method are two derivative values, a change in solar power (ΔP), and a change in solar voltage (ΔV). The derivative values are the difference between present value and previous value, as described in Equation (2-12) for power and Equation (2-13) for voltage.

$$\Delta P = P_n - P_{n-1} \dots\dots\dots(2-12)$$

$$\Delta V = V_n - V_{n-1} \dots\dots\dots(2-13)$$

Where:

ΔP = power derivative (W)

P_n = present value of power (W)

P_{n-1} = previous value of power (W)

ΔV = voltage derivative (V)

V_n = present value of voltage (V)

V_{n-1} = previous value of voltage (V)

The two derivative values are then translated into linguistic variables via membership functions, which describe the perturbation intensity. The linguistic variables are then tested in the fuzzy rule set to calculate the weight of fuzzy control. The output membership functions are used for translating the linguistic output variable, to a crisp numerical variable as control action.



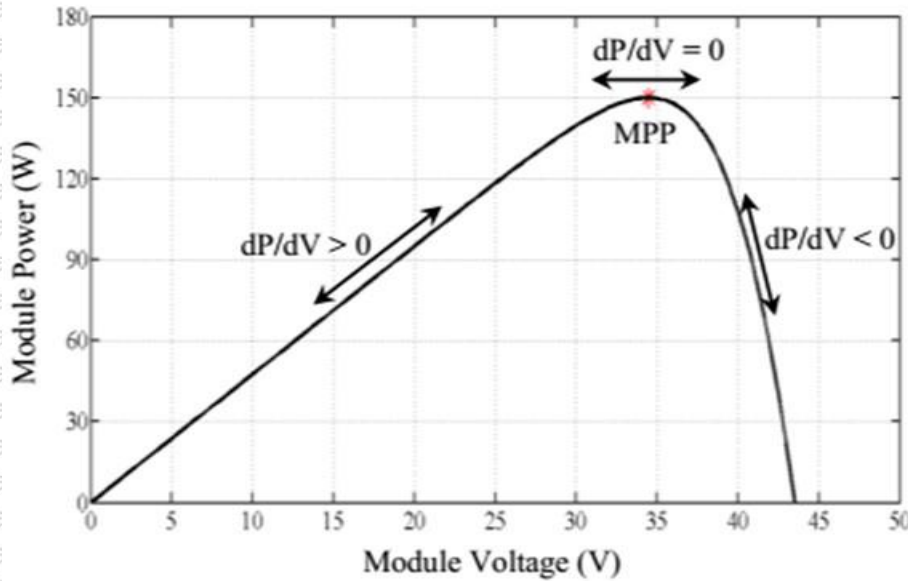


Figure 1.14 The slope of P-V curve of PV module in accordance to power derivative and voltage derivative.

Figure 1.14 shows the relation between power derivative and voltage derivative detected as inputs to be the FLC strategy in finding MPP. In order to map the control action as the output, the slope division of each area in P-V curve can be determined with linguistic variable as shown in

Figure 1.15.

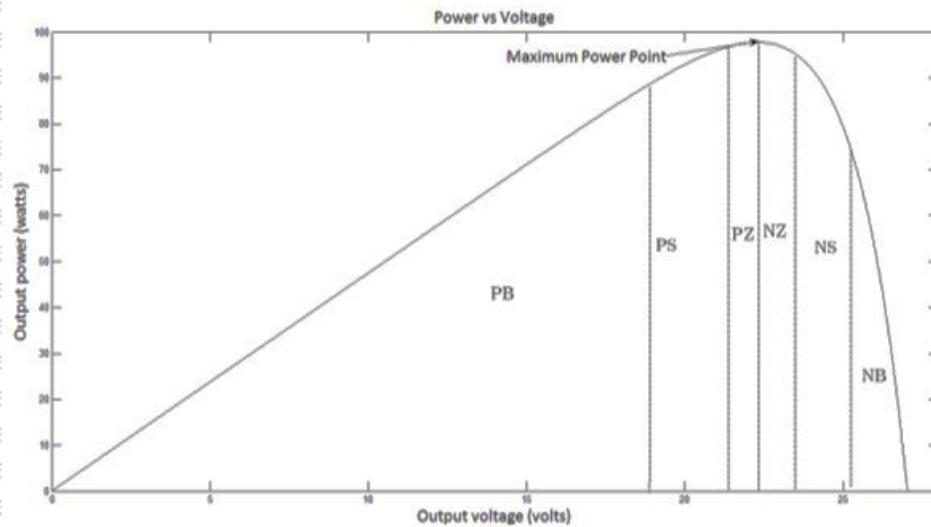


Figure 1.15 The P-V curve area division as named by linguistic variables.

In Figure 1.16, it is described that the general FLC method receives inputs to convert into linguistic variables, then inspected in fuzzy rule table, and finally convert back to the crisp values as the outputs.

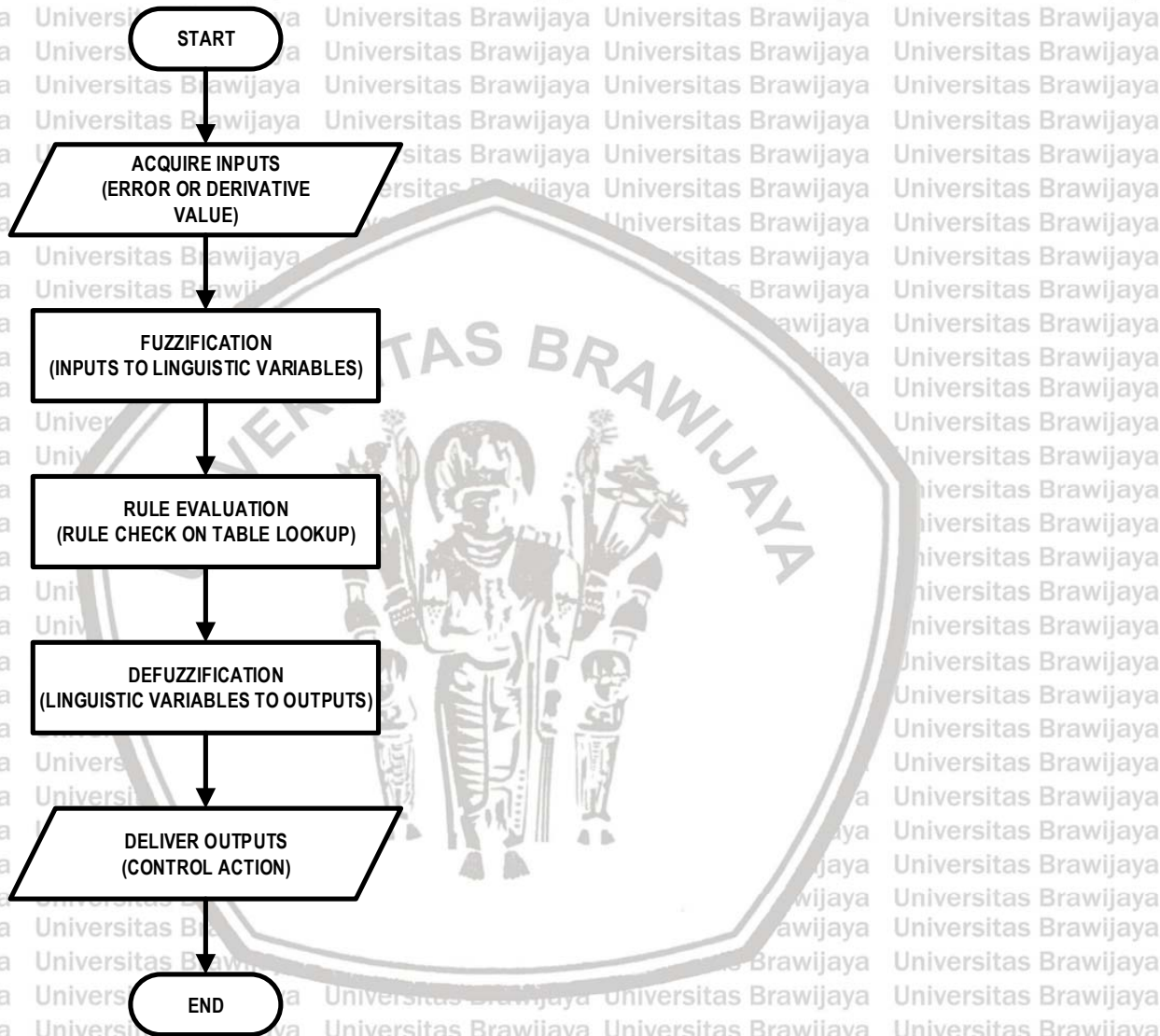


Figure 1.16 The flowchart of general FLC method.

The variable crisp value of control action (as duty cycle ratio) will make sure that the controller perturbs a smaller value as approaching MPP, in the contrary with P&O that has constant control value regardless the distance from MPP. Fuzzy inference engine used in this study is Mamdani method, and the defuzzification is using center of gravity technique. This output is then given to the PWM generator to generate PWM signal for DC-DC power converter.

1.6 Pulse Width Modulation (PWM)

Pulse-width modulation (PWM) is a method of reducing the average power delivered by an electrical signal, by effectively chopping it up into discrete parts. The average value of voltage (and current) fed to the load is controlled by turning the switch between supply and load on and off at a fast rate. The longer the switch is on compared to the off periods, the higher the total power supplied to the load. Along with MPPT, it is one of the primary methods of reducing the output of solar panels to that which can be utilized by a battery. PWM is particularly suited for running inertial loads such as motors, which are not as easily affected by this discrete switching. Because they have inertia, they react slower. The PWM switching frequency has to be high enough not to affect the load, which is to say that the resultant waveform perceived by the load must be as smooth as possible.

In this study, the output waveform of PWM generator is then supplied to MOSFET in the boost converter. The MOSFET in boost converter acts as a digital switch, driven by voltage delivered by PWM generator to make the circuit closes and opens in high frequency.

1.7 DC-DC Converter

DC-DC converters are devices for transforming DC voltage into higher or lower values, whether it is boost converter (Kumar & Tripathi, 2012), buck-boost converters (Rashid, et al., 2011), or buck converters (Mrabti, et al., 2009). Boost converter transforms DC voltage into higher value, while buck converter transforms into lower value. As the name suggests, buck-boost converter can both increase and decrease the DC voltage.

DC-DC converters are considered the main element in the MPPT process and without those, the maximum power could not be achieved. In this study, boost converter is used change the terminal voltage of the PV array to higher voltage, hence the MPP can be achieved.

1.7.1 Boost Converter

A boost converter steps up voltage and steps down current from its input (supply) to its output (load). It is a class of switched-mode power supply containing at least two semiconductors (a diode and a transistor) and at least one energy storage element: a capacitor, inductor, or the two in combination. To reduce voltage ripple, filters made of capacitors (sometimes in combination with

inductors) are normally added to such a converter's output (load-side filter) and input (supply-side filter).

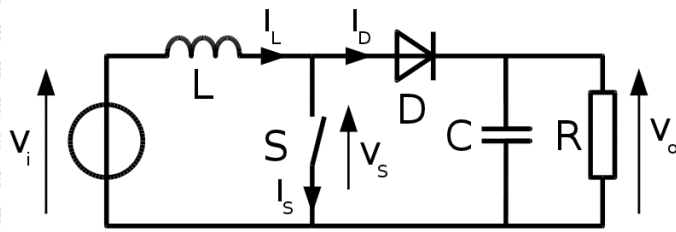


Figure 1.17 Schematic of a boost converter.

Figure 1.17 shows the schematic of a boost converter, which consists of an inductor L , a switch S (can be built by MOSFET, IGBT, or BJT), a diode D , and a capacitor C . Input voltage comes from supply in V_i , while the output voltage will be supplied to load R .

The key principle that drives the boost converter is the tendency of an inductor to resist changes in current by creating and destroying a magnetic field. In a boost converter, the output voltage is always higher than the input voltage. The PWM waveform from PWM generator makes the switch close and open in high frequency, with duty cycle define how many volts the voltage increasing in the output.

CHAPTER III RESEARCH CONCEPTUAL FRAMEWORK

1.1 Framework of the Research

As described on of the problem based on the background and literature review, this research is focused on maximizing the efficiency output of PV energy sources, namely solar cell by using two kinds of technologies, namely P&O algorithm and FLC method. Those connected with DC step up transformer (boost converter), where the output voltage and photovoltaic current are connected to MPPT control that can be perceived in next framework on Figure 1.1. Consequently, the option to use boost converter is because it has a function to produce an output voltage that is higher than the input voltage.

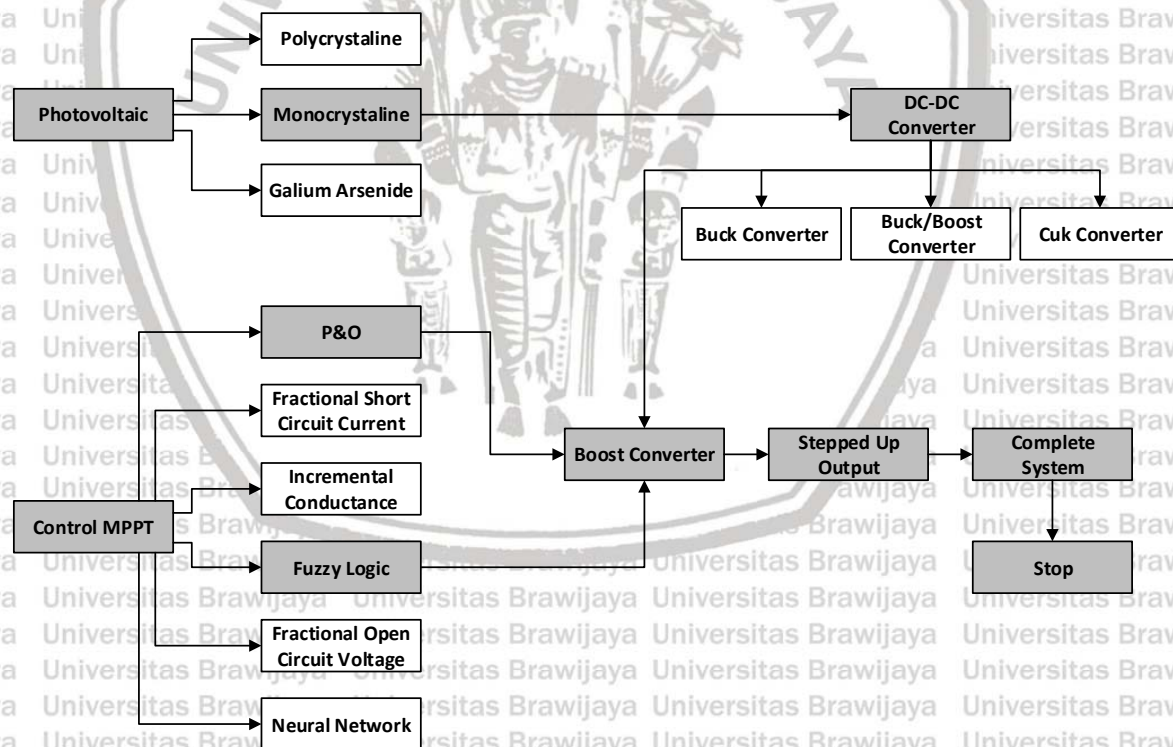


Figure 1.1 Block system concept framework that will be created. The grayed boxes are the parts that will be done in this study.

Implementation of P&O algorithm and FLC method generate output namely as duty cycle. The output controls PWM signal for closing and opening MOSFET switch in boost converter in

rapid succession. Constrained value of the duty cycle is required to prevent MOSFET from continuously open or continuously close, which makes boost converter ineffective.

1.2 The MPP Control Principles using P&O Algorithm and FLC Method

The comparison study of the P&O and FLC methods are to be performed through simulation approach. The schemas of the MPP control using the P&O algorithm and the FLC method are given in Figure 1.2 and Figure 1.3, subsequently.

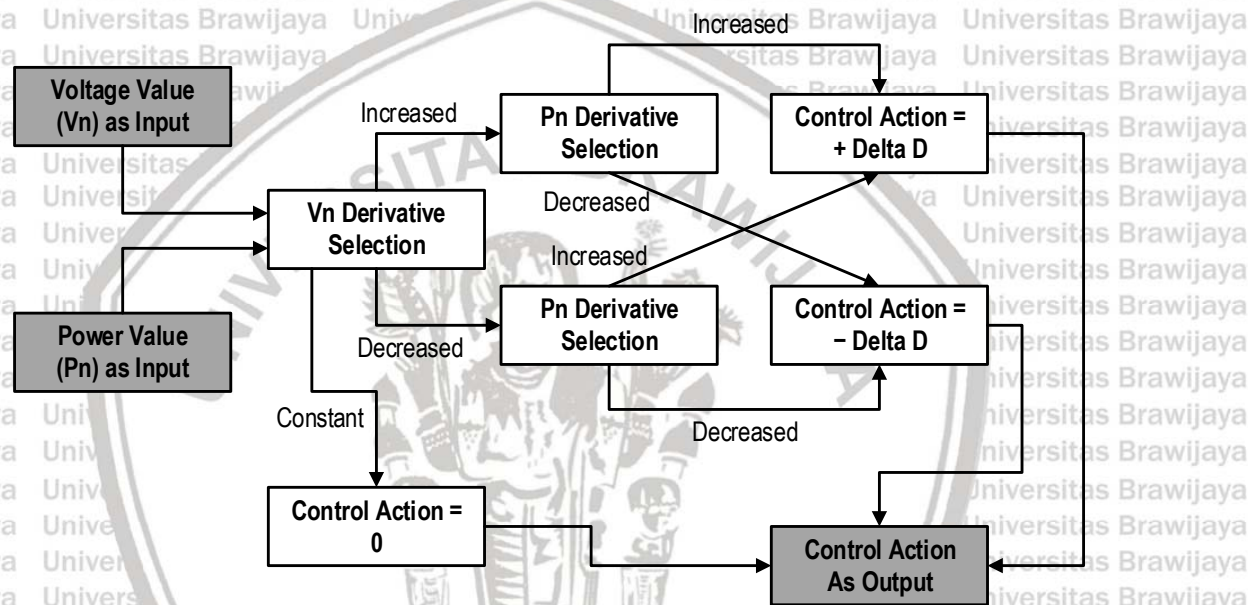


Figure 1.2 The principle of MPPT controller using P&O algorithm.

Basically, P&O algorithm is very simple. As shown in Figure 1.2, voltage value (V_n) and power value (P_n) are both inputs which are then compared to their previous values, generated derivative values (ΔV and ΔP). The algorithm then checks the voltage derivative value: if it has a zero value then the control action is set to zero; otherwise if it has a positive value then the control action is set to ΔD with the sign equals to the ΔP ; otherwise if it has a negative value then the control action is set to ΔD with the sign being opposite to the ΔP . The value of ΔD is set constant.

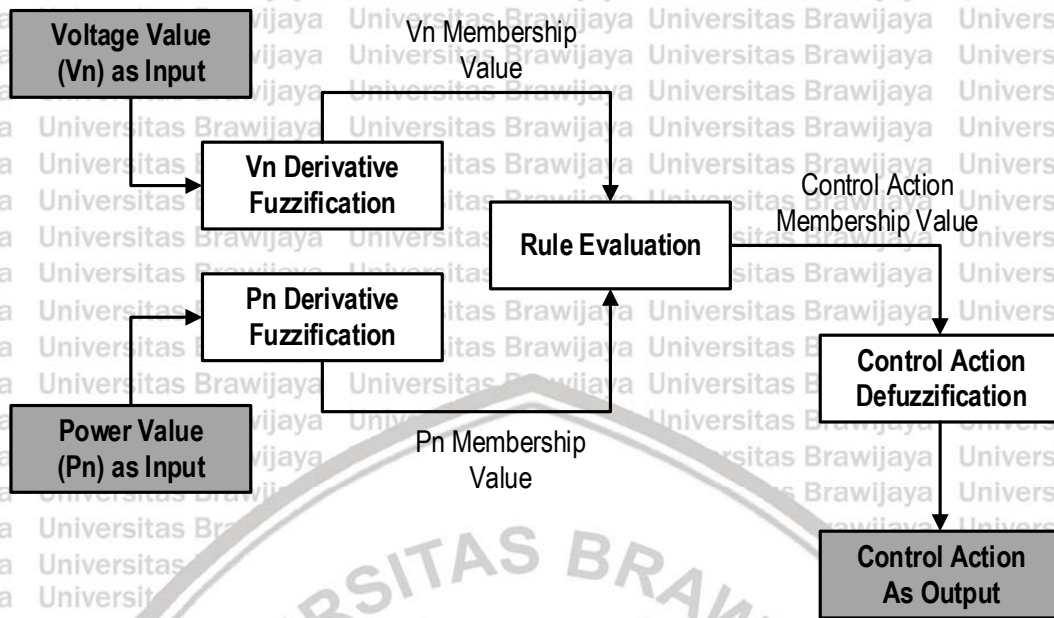


Figure 1.3 The principle of MPPT controller using FLC method.

On the other hand, the FLC method explained in Figure 1.3 comprises three main computation blocks. Just as in P&O, V_n and P_n are inputs in FLC, which are then compared to their previous values, generated derivative values (ΔV and ΔP). The derivative values are converted into fuzzy memberships previously prepared, a process called fuzzification. In the rule evaluation process, the membership values are then used as lookup keys in the rule table to determine the control action membership value. Final step is to convert back the control action membership value into crisp value, an opposite process called defuzzification. The crisp value is then fed into the output as a control action. The value of ΔD in this method is not constant, but varies according to the present output distance from MPP. As the present state approaching MPP, the ΔD value approaches to zero.

1.3 Modeling of the PV System

The model of PV module used in this research is given in Figure 1.4. It is based on datasheet and research by Pendem on 2018, representing the Kyocera Solar KC200GT type which has a maximum power of about 1000 W (Kyocera, 2009) (Pendem & Mikkili, 2018). The main parameters of the Kyocera solar module at 25°C and 1,000 W·m⁻² comprise the open-circuit voltage V_{oc} of 32.9 V and the short-circuit current I_{sc} of 8.21 A. In the PV model, the parameters influencing the PV operation are to be known.

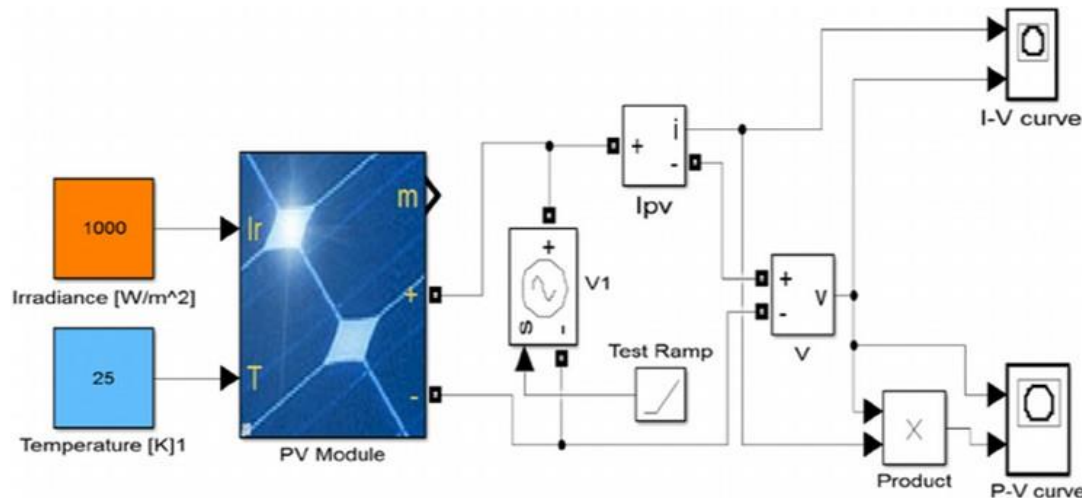


Figure 1.4 Kyocera Solar KC200GT PV module modeling in Matlab/Simulink.

Source : (Pendem & Mikkili, 2018)

As seen in Figure 1.4, the photovoltaic block diagram includes the solar cell, with the positive and negative terminal will be connected to boost converter. The other terminal acts as feedback, is connected to the controller, whether implements P&O algorithm or FLC method. The difference between the two blocks besides receiving standard parameter signals from photovoltaic blocks (temperature and irradiation), MOSFET in the boost converter will also receive signals from P&O algorithm and FLC method, then performs MPPT by varying the output voltage. At the MPP condition, the photovoltaic produces the voltage of 26.3 V and the current of 7.61 A, giving the maximum power of 200.14 W (Kyocera, 2009).

1.4 Determination of the Common Simulation Parameters

There are two types of simulation to perform. The first one is the MPPT simulation using P&O algorithm, while the second one is the MPPT simulation using the FLC method. The simulations will be run under common parameters below:

1. Irradiance level is defined to $1,000 \text{ W}\cdot\text{m}^{-2}$.
2. Ambient temperature of solar panel is determined as 25°C .
3. PWM generator switching frequency is set to 31,000 Hz.
4. Capacitor capacitance before the boost converter is set to $1,150 \mu\text{F}$.
5. Inductance in the boost converter is set to $45 \mu\text{H}$.

6. MOSFET in the boost converter has a FET resistance of 0.1Ω , internal diode inductance of 0 H , internal diode resistance of 0.01Ω , internal diode forward voltage of 0 V , snubber resistance of $100,000 \Omega$, and snubber capacitance of infinity.
7. Diode in the boost converter has a resistance of 0.001Ω , inductance of 0 H , forward voltage of 0.004 V , snubber resistance of 750Ω , and snubber capacitance of $0.25 \mu\text{F}$.
8. Capacitor in the boost converter is set to $2,500 \mu\text{F}$.
9. Load after the boost converter has a nominal voltage of 28.5 V , nominal frequency of 50 Hz , active power of 120 W , inductive reactive power of 0 VAR , and capacitive reactive power of 0 VAR . The load flow model is set to constant current.
10. Duty cycle constrains from both methods are limited to minimum of 0.02 and maximum of 0.98 .

For each of the simulation performed, the period is set to 3 s , while the data sampling time of the plotting is set to 0.0001 s ($100 \mu\text{s}$).

1.5 Hypothesis

A hypothesis can be defined, that it will provide a comparison assessment of the two methods, so it is known which one has the best rising time, power efficiency, and power quality.

CHAPTER IV RESEARCH METHODS

1.1 The Methods Comparison Study

This study performs a detail comparison between pure P&O algorithm and pure FLC method to inspect all output aspects, including rise time, power efficiency, and power quality (oscillation).

Prior to the comparison, both P&O algorithm and FLC method parameters undergo a fine-tuning procedure to display their best performance.

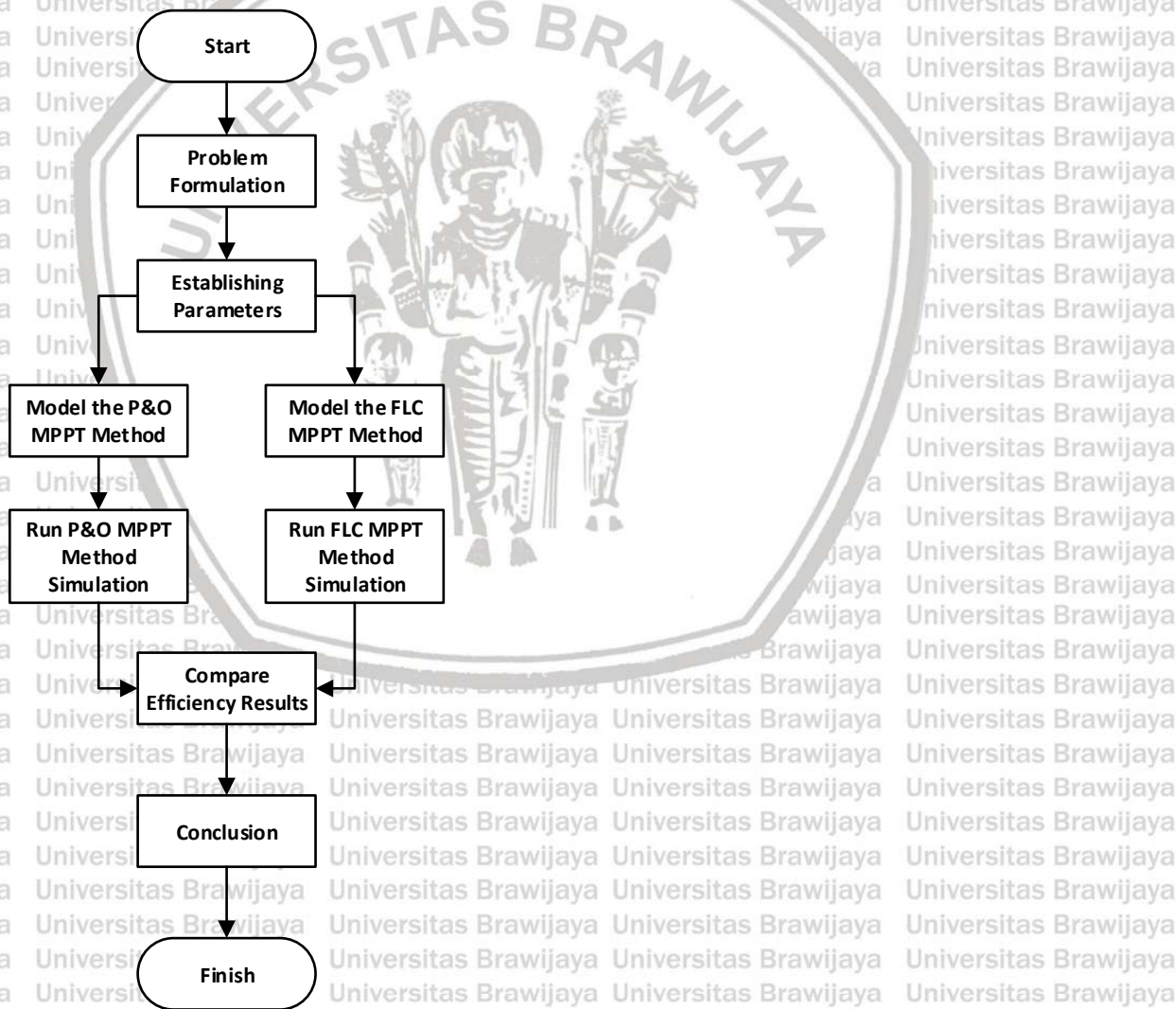


Figure 1.1 Flowchart of the research methodology.

The study is performed in several steps, which is mainly focused in the simulation using Matlab/Simulink and the related results analysis. The first stage is to define all variables to be analysis, which consist of rise time, oscillation amplitude, and average output power. The next step is to design the model of each simulation, based on the basic principles of P&O algorithm and FLC method. The step is then followed by creating common parameters in which both simulations are to be conducted, i.e. the irradiance and temperature of PV, PWM generator, boost converter, and the load. It is important to make sure that the parameters are identical for a fair comparison.

The next step is to execute the simulations in order to find the optimum output for each method, followed by running (executing) both simulations under common parameters prepared previously. After the results are acquired, the final step is to make a deep analysis of every outcomes and to make comparison between the two methods, as well as a general comparison with the results of other previous researches. (Sun & Han, 2013) (Lee, et al., 2013) (Huang, et al., 2011) (Selmi, et al., 2014) (Sera, et al., 2013) (Hohm & Ropp, 2003) (Esrasm & Chapman, 2007) (Sivanandam, et al., 2007) (Rashid, 2011) (Kyocera, 2009) (Pendem & Mikkili, 2018)

1.1.1 Problem Formulation

As the first step to take in this study, problem formulation has the most important role to define objectives. This step focuses in the key issues trying to address and determines their importance. Efficiency factor of the PV system is the current topic in this study, while the MPPT as the methods for achieving MPP is required to be compared each other. This study determines that P&O algorithm as the simplest method needs to be compared against more advance one, namely FLC method.

The model of the two methods are then implemented in the form of Matlab/Simulink simulation and then executed in order to get results. A comparison will be performed using several aspects, namely rise time (the time required to reach MPP), oscillation (amplitude between upper bound and lower bound of power), and power efficiency (proximity of the power resulted against MPP).

1.1.2 Establishing Parameters

The variables involved as the comparison result need to be tuned prior to simulation. Both P&O algorithm and FLC method must be performed on their best condition to make a fair

comparison. First, the PV type and configuration will be set to single parameter. Second, the environmental condition should be determined in a common manner, i.e.:

1. Solar irradiance; and
2. Ambient temperature.

Third, as the device that drives the output voltage, the parameters of every component in boost converter must be determined for the same between two simulations. It consists of:

1. The FET resistance of MOSFET inside boost converter as the main switch;
2. The inductance of main inductor of boost converter;
3. The resistance and forward voltage of diode inside boost converter;
4. The switching frequency of PWM which drives the MOSFET;
5. Upper limit and lower limit of duty cycle for MOSFET; and
6. The parameters of load.

Fourth, for the comparison between the two methods, simulations result must be constrained for:

1. Simulation sampling time; and
2. The period of each simulation.

1.1.3 Modeling the Methods for Simulation

The next step after determining all parameters is to make model of P&O algorithm and FLC method in Matlab/Simulink. All resources in Matlab/Simulink for constructing the model can be performed by writing Matlab source code of function or by using Simulink blocks.

The P&O algorithm will be implemented in Matlab using function created directly with source code. The input consists of two values: voltage value (V_n) and power value (P_n). Both will be compared to their previous values, generated derivative values (ΔV and ΔP). The algorithm then checks the voltage derivative value. If ΔV has a zero value then the control action is set to zero. If it has a positive value then the control action is set to ΔD with the sign equals to the ΔP ; otherwise

if it has a negative value then the control action is set to ΔD with the sign being opposite to the ΔP . The value of ΔD is set constant.

In contrast, the FLC method will be implemented in the form of Simulink blocks. It consists of three main computation blocks. The input consists of two values, V_n and P_n . The values are compared to their previous values, generated derivative values (ΔV and ΔP). The derivative values are converted into fuzzy memberships previously prepared in fuzzification process. In the rule evaluation process, the membership values are then used as lookup keys in the rule table to determine the control action membership value. Final step is to convert back the control action membership value into crisp value in an opposite process called defuzzification. The crisp value is then fed into the output as a control action. The value of ΔD in this method is not constant, but varies according to the present output distance from MPP. As the present state approaching MPP, the ΔD value approaches to zero.

To analyze one by one of each simulation, separate model must be developed, i.e. for the P&O algorithm and FLC method. The third model must also be developed to compare simulation result directly in numerical and visual form, i.e. the combination of P&O algorithm and FLC method.

1.1.4 Executing, Analyzing, and Comparing the Simulations

After preparing the models, the simulations are then executed under the common parameters as described previously. The numerical results are then plotted in the graphical form to make visual comparison. One of the graphic will be constrained for rise time analysis; while the other for oscillation and power efficiency analysis.

Numerical comparison for rise time is done by analyzing time taken for the power to reach the first lower bound of the next oscillation. The oscillation comparison can be done by observing the power distance between lower and upper bound. The power efficiency comparison can be done by observing the average power in oscillation.

1.1.5 Making Conclusions

The conclusions can be determined after the study makes comparisons on every variables involved. Both quantitative and qualitative forms of the comparison result should be includes in the conclusions.

1.2 The Expected Result of this Research

The expected result of this research is an extensive simulation for both techniques that is going to be done by the assistance of Matlab/Simulink. The results is going to present with a comparison between fuzzy logic and P&O controllers MPPT controllers and will know the best method for give the smooth power profile, less oscillation, also who is the better stable operating point.



CHAPTER V RESULTS AND ANALYSIS

1.1 The Photovoltaic Parameters

This sub chapter describes the characteristic of PV model used, i.e. the module type of Kyocera Solar KC200GT. The PV modules are then constructed in single panel configuration in order to be able to generate maximum output power around 200 W. As presented in Figure 1.1 and Figure 1.2, it is known from the datasheets that the MPP on PV modules is 200.14 W, with generated voltage of 26.3 V and current of 7.61 A under constant $1,000 \text{ W}\cdot\text{m}^{-2}$ irradiance and 25°C of temperature (Kyocera, 2009).

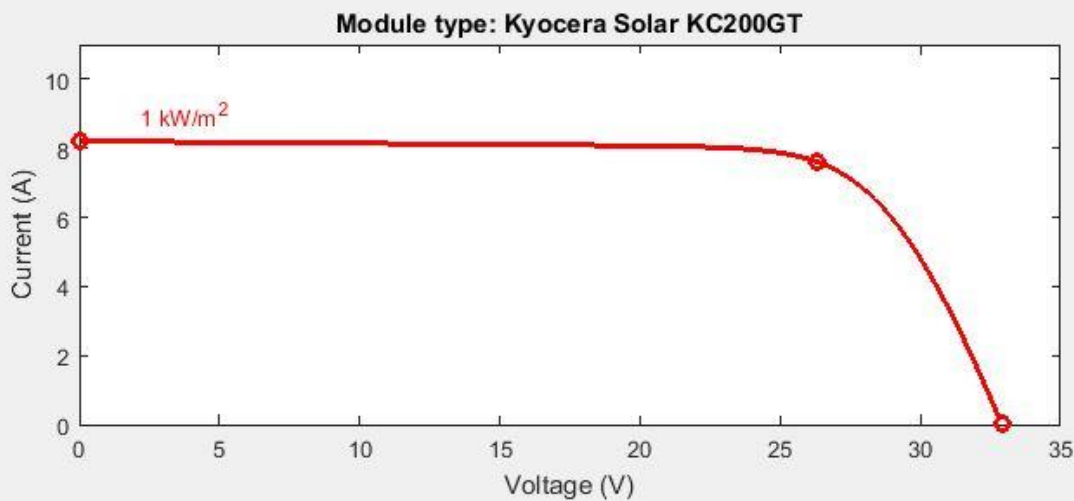


Figure 1.1 Kyocera Solar KC200GT I-V curve, with $1,000 \text{ W}\cdot\text{m}^{-2}$ irradiance and 25°C temperature.

Source : (Kyocera, 2009)

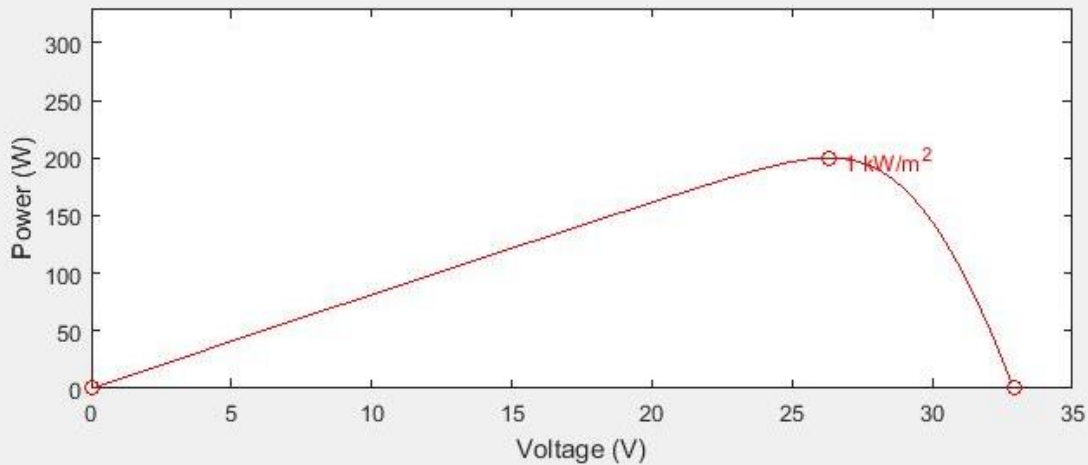


Figure 1.2 Kyocera Solar KC200GT P-V curve, with $1,000 \text{ W} \cdot \text{m}^{-2}$ irradiance and 25°C temperature.

Source : (Kyocera, 2009)

1.2 Photovoltaic Testing without MPPT Implementation

Preceding both methods operation, there is a testing for knowing the PV modules output without MPPT implementation. This testing will be conducted under constant irradiance ($1,000 \text{ W} \cdot \text{m}^{-2}$) and temperature condition (25°C), as shown in Figure 1.3, in order to identify the power output on different load.

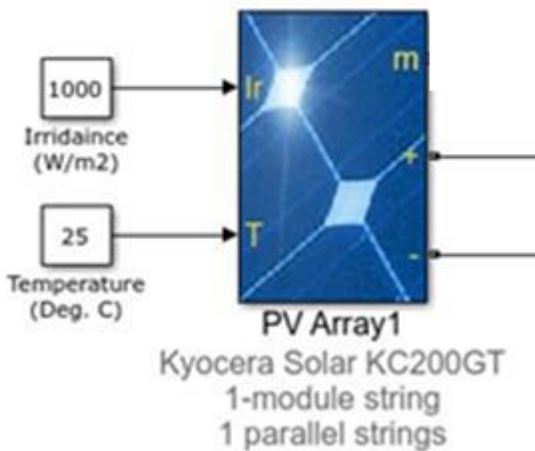


Figure 1.3 Simulink PV circuit diagram without MPPT implementation.

Source : (Pendem & Mikkili, 2018)

The result of this preceding testing is displayed in voltage plot only, since the power output must be known only after the load is applied, i.e. beyond the boost converter. Both the voltage and current as the output of the PV can be measured, then the values are fed to the MPPT method as

inputs. As the load change, voltage and current generated by the PV will also change, following specific P-V curve.

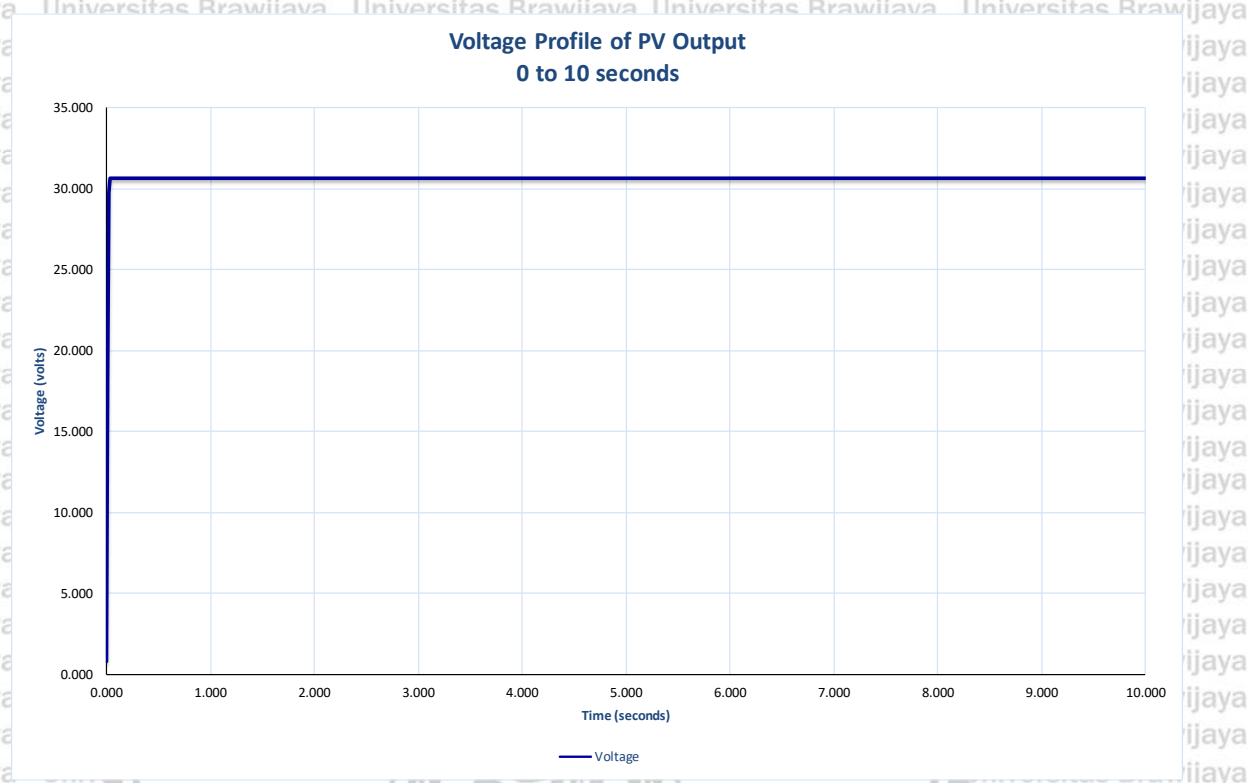


Figure 1.4 The output voltage profile on PV, without the MPPT.

According to the testing result on Figure 1.4, the voltage output generated by PV modules under $1,000 \text{ W}\cdot\text{m}^{-2}$ irradiance and 25°C temperature is on 30.627 V, far beyond MPP at 26.3 V.

1.3 General Simulation Parameters

There are three types of simulation that will be performed. First type is the MPPT simulation using P&O algorithm, while the second type is the MPPT simulation using FLC method. The last type will be using both P&O algorithm and FLC method on single simulation, and will be performed to confirm previous results. All methods generated duty cycle to PWM generator, which will control MOSFET in boost converter. The simulation will be run under common parameters below:

1. Irradiance Level

The irradiance level for solar panel surface is set to $1,000 \text{ W}\cdot\text{m}^{-2}$.

2. Ambient Temperature

The ambient temperature of solar panel is set to 25°C.

3. PWM Generator

The PWM generator switching frequency is set to 31,000 Hz.

4. Capacitor before Boost Converter (between Solar Panel output and Boost Converter)

This capacitor's capacitance is set to 1,150 μF .

5. Inductor in Boost Converter

This inductor's inductance is set to 45 μH .

6. MOSFET in Boost Converter

This MOSFET has FET resistance at 0.1 Ω , internal diode inductance of 0 H, internal diode resistance of 0.01 Ω , internal diode forward voltage of 0 V, snubber resistance at 100,000 Ω , and snubber capacitance at infinity.

7. Diode in Boost Converter

This diode has resistance at 0.001 Ω , inductance at 0 H, forward voltage of 0.004 V, snubber resistance at 750 Ω , and snubber capacitance of 0.25 μF .

8. Capacitor in Boost Converter

This capacitor's capacitance is set to 2,500 μF .

9. Load after Boost Converter

This load has nominal voltage of 28.5 V, nominal frequency at 50 Hz, active power of 120 W, inductive reactive power on 0 var, and capacitive reactive power on 0 var. The load flow model is set to constant current.

10. Duty Cycle Constrains

The duty cycle from both method are limited to minimum of 0.02 and maximum of 0.98.

For all the simulation performed, the period is set to 3 s, while the data sampling time is set to 0.0001 s (100 μs).

1.4 Perturb and Observe Algorithm MPPT Simulation

1.4.1 The P&O Algorithm Model and Parameters

This MPPT testing is performed by implementing P&O algorithm. The testing is done by making simulation of $1,000 \text{ W}\cdot\text{m}^{-2}$ solar radiance perpendicular to solar panel surface, and the temperature is set to 25°C .

Perturb and Observe MPPT Controller for Solar PV

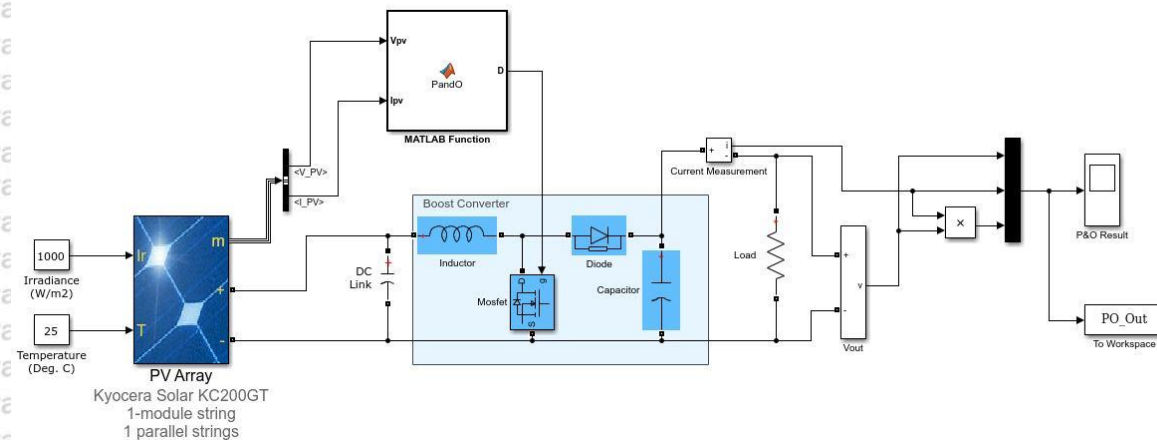


Figure 1.5 Matlab/Simulink PV MPPT circuit diagram for P&O algorithm.

Figure 1.5 shows the circuit diagram of PV MPPT using P&O algorithm in Matlab/Simulink, which the result data will be analyzed. The inputs of the function are voltage and current from the PV. Both the voltage and current can be used to compute power. All values of input and output from the previous pass are stored in memory in order to generate their derivatives. The method is implemented by a function named **PandO** as in source code below, that replaces the duty cycle value for PWM generator.

```
function D = PandO(Vpv, Ipv)
persistent Dprev Pprev Vprev
if isempty(Dprev)
    Dprev = 0.7;
    Vprev = 32.5;
    Pprev = 135;
end
deltaD = 0.0025;
Ppv = Vpv * Ipv;
```

```

if (Ppv - Pprev) ~= 0
    if (Ppv - Pprev) > 0
        if (Vpv - Vprev) > 0
            D = Dprev - deltaD;
        else
            D = Dprev + deltaD;
        end
    else
        if (Vpv - Vprev) > 0
            D = Dprev + deltaD;
        else
            D = Dprev - deltaD;
        end
    end
end
else
    D = Dprev;
end
end

if (D < 0.02)
    D = 0.02;
end

if (D > 0.98)
    D = 0.98;
end

end

Dprev = D;
Vprev = Vpv;
Pprev = Ppv;
    
```

As shown in the code above, the only P&O parameter is **deltaD** (ΔD), i.e. the increment or decrement of duty cycle during one pass of the function. The parameter is chosen to 0.0025 after several trials to deliver minimum oscillation around maximum power point and the best rise time. For filtering from giving excessive duty cycle value, the output is constrained within 0.02 and 0.98. The output will be supplied to the PWM generator; therefore, the control for MOSFET in boost converter can be handled.

The following steps described explanations of PV MPPT implementation using P&O algorithm, with one example from the data result in Table 1.1 for the row number 6 with time of 0.5 millisecond ($V_{pv} = 0.645$, $I_{pv} = 0.095$, $P_{pv} = 0.061$, $V_{prev} = 0.4$, $P_{prev} = 0.024$, and assuming $D_{prev} = 0.02$):

1. The input stage is to accept voltage value and current value from PV.
 - a. The voltage is assigned to V_{pv} variable.

$$V_{pv} \leftarrow input_1$$

Example: $V_{pv} = 0.645$

- b. The current is assigned to I_{pv} variable.

$$I_{pv} \leftarrow \text{input}_2$$

Example: $I_{pv} = 0.095$

2. If the process is the first passing, then assign the previous value of duty cycle (D_{prev}), previous value of voltage (V_{prev}), and previous value of power (P_{prev}) with initial values. All initial values could be random, but have to be within acceptable range. The duty cycle must be fallen within 0.02 to 0.98, while the voltage could be any values between 0 to 50 volts, and the power would be from 0 to 150 watts. For example, the initial value for the duty cycle would assigned to 0.7, the voltage would assigned to 32.5, and the power would assigned to 135.

$$D_{prev} \leftarrow 0.7$$

$$V_{prev} \leftarrow 32.5$$

$$P_{prev} \leftarrow 135$$

3. The first process stage is intended to calculate the derivative of voltage and the derivative of power.
- a. Determine the ΔD as constant value of 0.0025. This value will be added or subtracted to the previous duty cycle to form the new value of duty cycle.

$$\Delta D \leftarrow 0.0025$$

- b. Calculate present value of power (P_{pv}) as a multiplication between present value of voltage (V_{pv}) and present value of current (I_{pv}).

$$P_{pv} \leftarrow V_{pv} \cdot I_{pv}$$

Example: $P_{pv} = 0.645 \cdot 0.095 = 0.061$

- c. Calculate derivative of power (ΔP) as P_{pv} subtracted by previous value of power (P_{prev}). The ΔP value is defined as the severity of power increasing or decreasing against the previous one.

$$\Delta P \leftarrow P_{pv} - P_{prev}$$

Example: $\Delta P = 0.061 - 0.024 = 0.037$

- d. Calculate derivative of voltage (ΔV) as V_{pv} subtracted by previous value of voltage (V_{prev}). The ΔV value is defined as the severity of voltage increasing or decreasing against the previous one.

$$\Delta V \leftarrow V_{pv} - V_{prev}$$

Example: $\Delta V = 0.645 - 0.04 = 0.245$

4. The second process stage is intended to get the value of duty cycle. It is the main process for P&O algorithm. The previous duty cycle will be added or subtracted by ΔD with the following conditions:

- If ΔP is zero, then set D as D_{prev} .
- If ΔP is positive and ΔV is positive, then set D as D_{prev} added by ΔD .
- If ΔP is positive and ΔV is negative, then set D as D_{prev} subtracted by ΔD .
- If ΔP is negative and ΔV is positive, then set D as D_{prev} subtracted by ΔD .
- If ΔP is negative and ΔV is negative, then set D as D_{prev} added by ΔD .

if ($\Delta P = 0$) *then*

$$D \leftarrow D_{prev}$$

else

if ($\Delta P > 0$) *then*

if ($\Delta V > 0$) *then*

$$D \leftarrow D_{prev} + \Delta D$$

else

$$D \leftarrow D_{prev} - \Delta D$$

end if



```

else
if ( $\Delta V > 0$ ) then

```

```

     $D \leftarrow D_{prev} - \Delta D$ 

```

```

else

```

```

     $D \leftarrow D_{prev} + \Delta D$ 

```

```

end if

```

```

end if

```

```

end if

```

Example: $D = 0.02 + 0.0025 = 0.0225$

5. The output stage is to prepare D as the duty cycle for the PWM generator and to prepare the next process passing.

a. Make the value of D constrained in the range between 0.02 and 0.98.

```

if ( $D < 0.02$ ) then

```

```

     $D \leftarrow 0.02$ 

```

```

end if

```

```

if ( $D > 0.98$ ) then

```

```

     $D \leftarrow 0.98$ 

```

```

end if

```

Example: $D = 0.0225$

b. Assign all present values to the previous values for the next passing:

```

 $D_{prev} \leftarrow D$ 

```

```

 $V_{prev} \leftarrow V_{pv}$ 

```

```

 $P_{prev} \leftarrow P_{pv}$ 

```

Example: $D_{prev} = 0.0225$, $V_{prev} = 0.645$, and $P_{prev} = 0.061$

6. In this point, the output value of duty cycle (D) is ready to transfer to the PWM generator, therefore drives the MOSFET in boost converter.

An example of P&O algorithm result from the calculation within the first 3 milliseconds is presented in Table 1.1, consisting of time, voltage, current, and power.

Table 1.1
Example of P&O Algorithm Calculation Result from 0 Millisecond to 3 Milliseconds

No.	Time (millisecond)	P&O		
		Voltage (volt)	Current (ampere)	Power (watt)
1	0.0	0.000	0.000	0.000
2	0.1	0.009	0.001	0.000
3	0.2	0.067	0.010	0.001
4	0.3	0.198	0.029	0.006
5	0.4	0.400	0.059	0.024
6	0.5	0.645	0.095	0.061
7	0.6	0.894	0.132	0.118
8	0.7	1.103	0.163	0.180
9	0.8	1.265	0.187	0.236
10	0.9	1.400	0.207	0.290
11	1.0	1.511	0.223	0.337
12	1.1	1.593	0.235	0.375
13	1.2	1.659	0.245	0.407
14	1.3	1.715	0.253	0.434
15	1.4	1.769	0.261	0.462
16	1.5	1.828	0.270	0.493
17	1.6	1.896	0.280	0.531
18	1.7	1.978	0.292	0.578
19	1.8	2.083	0.308	0.641
20	1.9	2.197	0.325	0.713
21	2.0	2.323	0.343	0.797
22	2.1	2.441	0.361	0.880
23	2.2	2.555	0.377	0.964
24	2.3	2.662	0.393	1.047
25	2.4	2.763	0.408	1.128
26	2.5	2.853	0.422	1.203
27	2.6	2.937	0.434	1.275
28	2.7	3.020	0.446	1.347
29	2.8	3.105	0.459	1.425
30	2.9	3.193	0.472	1.506
31	3.0	3.285	0.485	1.595

The graphical P&O algorithm representation result above is presented in Figure 1.6 with the data labels on every 0.5 millisecond. As the visual representation, the blue line represents voltage in volt, while the red line denotes current in ampere, and the green line denotes power in watt. In this example, the power has lower values compared to the voltage, since the current values are below 1 ampere. For the current value greater than 1 ampere, the power will have values above voltage, which is shown beyond Figure 1.6.

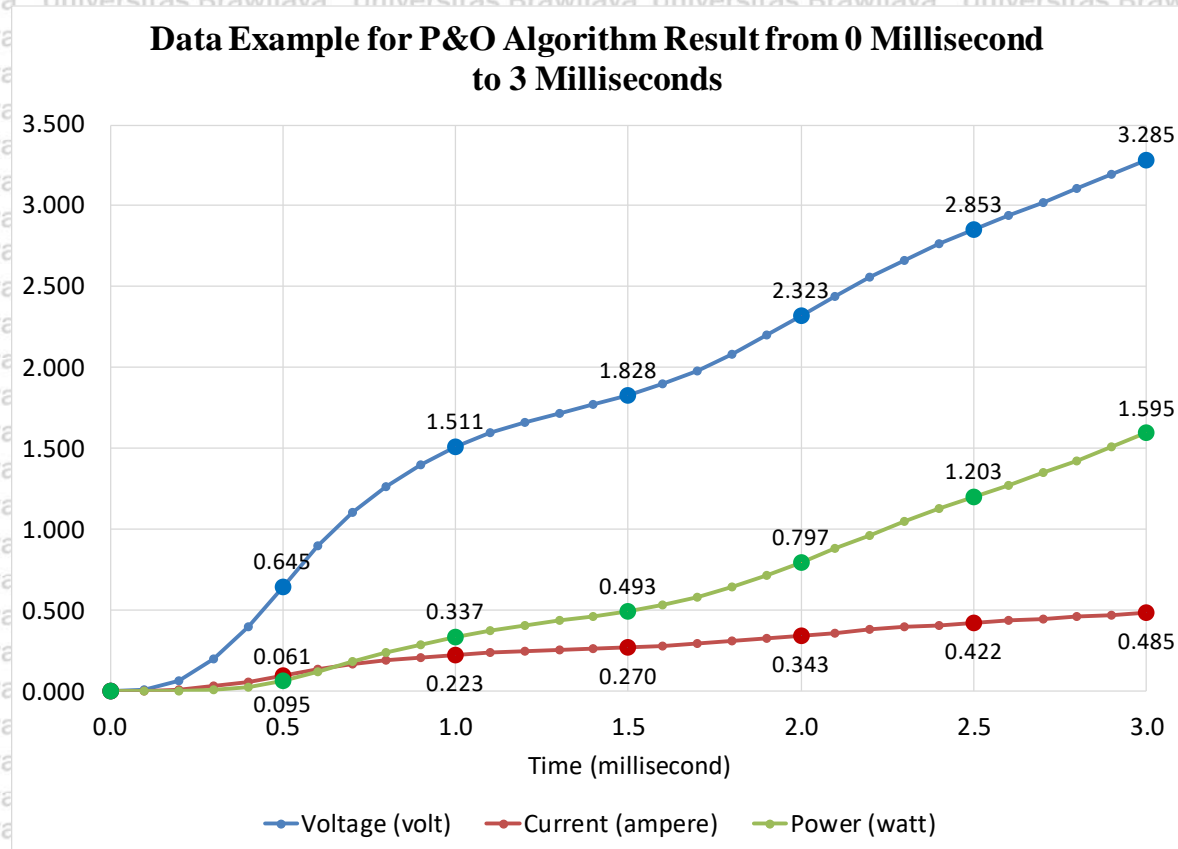


Figure 1.6 The graphical representation of the example of P&O algorithm result from 0 millisecond to 3 milliseconds.

1.4.2 The P&O Algorithm Simulation Result

For this simulation, a data plotting with 100 μ s (0.0001 s) sample rate is chosen. Starting from zero condition, the simulation duration is set to 3 s.

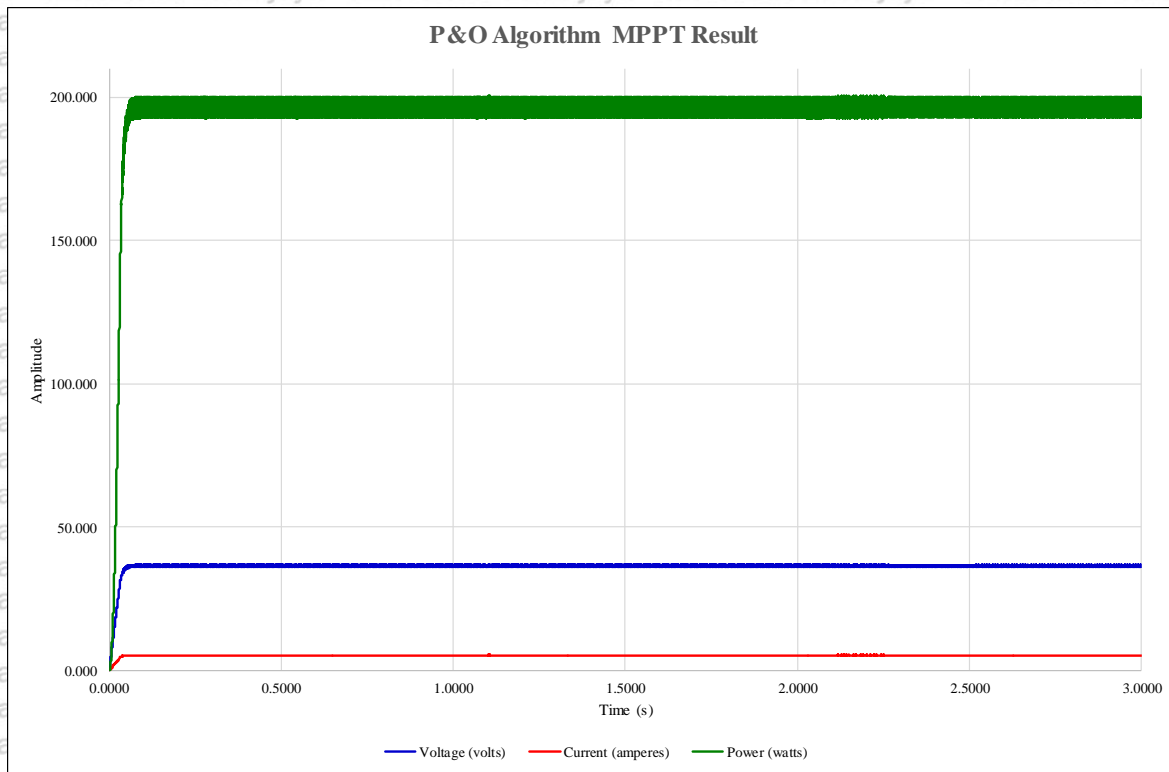


Figure 1.7 The output of voltage, current, and power profile simulation on PV MPPT using P&O algorithm in the first 3 s.

The result of voltage, current, and power profile against time using P&O algorithm can be seen in Figure 1.7. Visually, the power profile is copying both voltage and current profile.

According to the numerical data, P&O algorithm produces rise time at 0.0482 second. For the voltage profile in a single graph, an adjusted y-axis scale is shown in Figure 1.8.

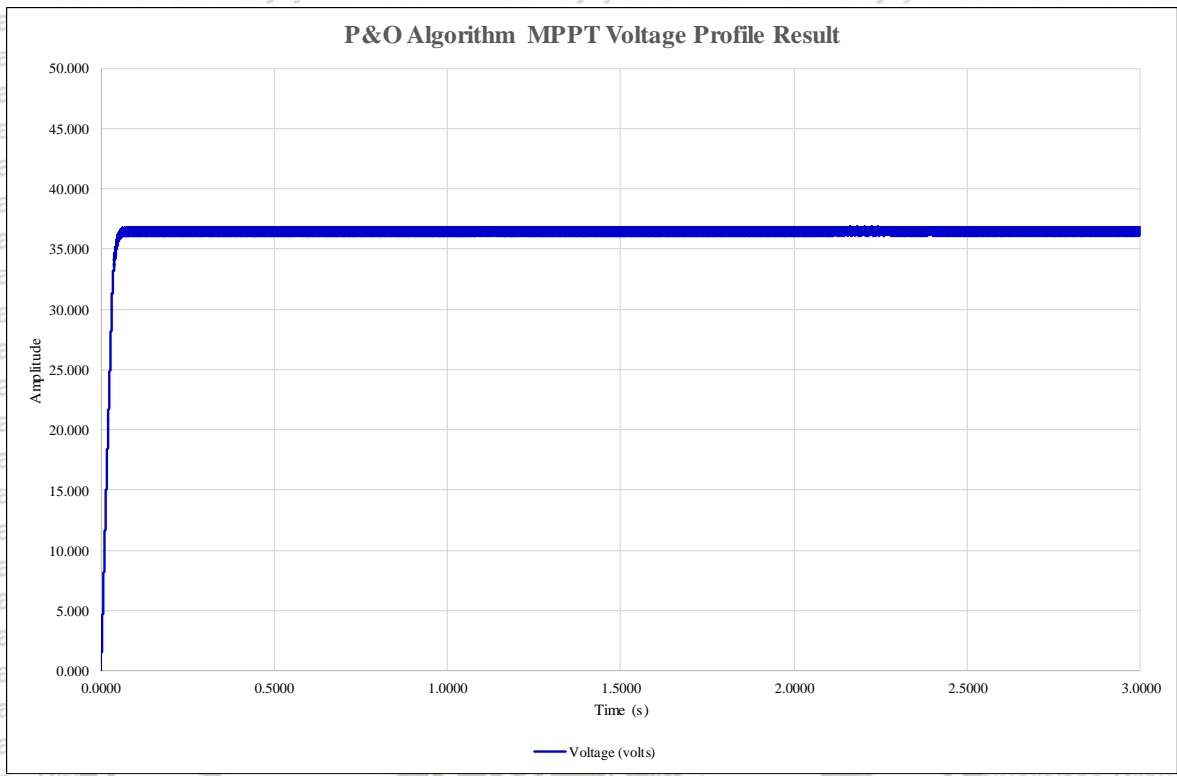


Figure 1.8 The output voltage profile simulation on PV MPPT using P&O algorithm in the first 3 s.

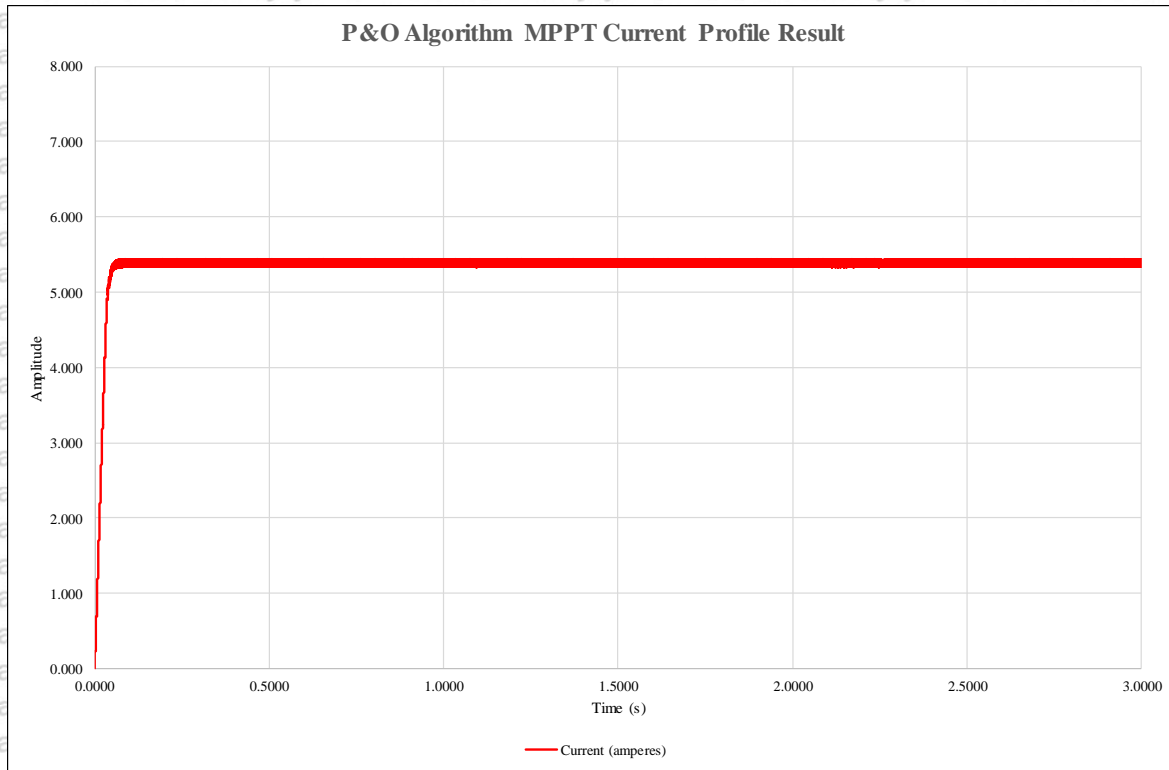


Figure 1.9 The output current profile simulation on PV MPPT using P&O algorithm in the first 3 s.

Figure 1.8 shows that after 100 ms, the voltage reaches steady state in average 36.455 V, with minimum value of 36.104 V and maximum value of 36.834 V. It is a 0.73 VPP oscillation.

Figure 1.9 shows that after 100 ms, the current reaches steady state in average 5.386 A, with minimum value of 5.334 A and maximum value of 5.442 A. It is a 0.108 APP oscillation.

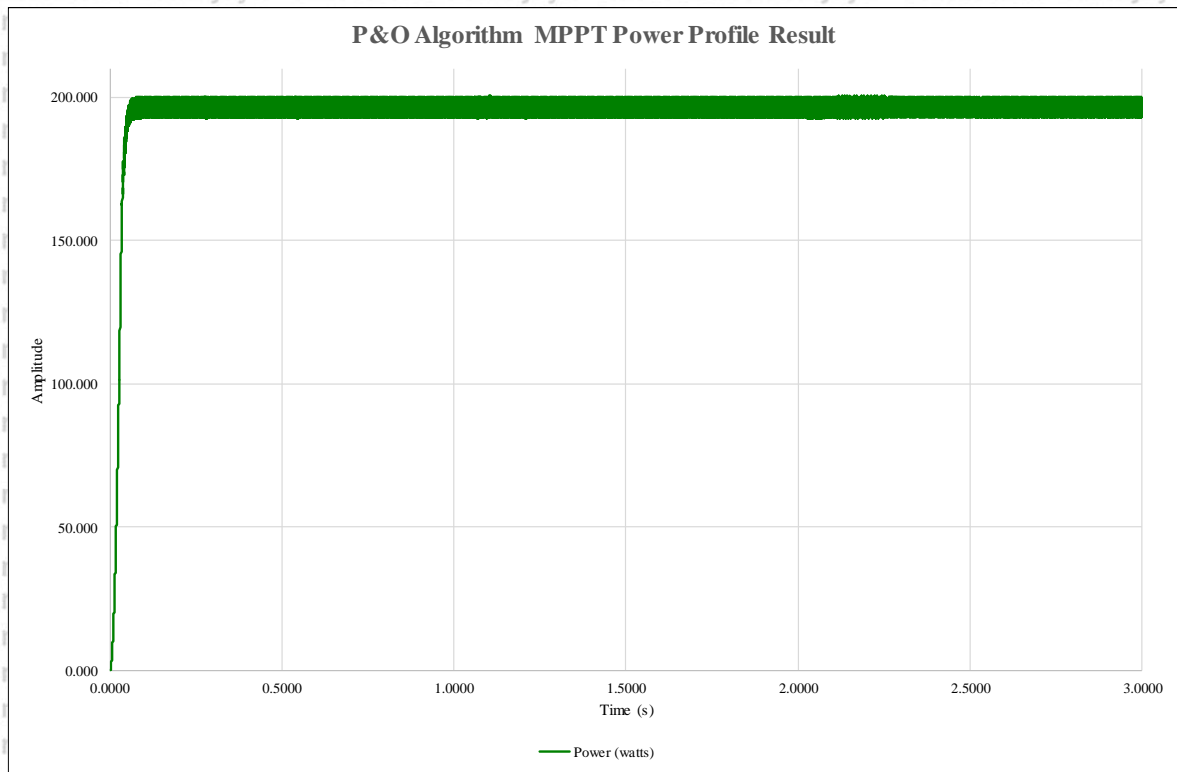


Figure 1.10 The output power profile simulation on PV MPPT using P&O algorithm in the first 3 seconds.

Figure 1.10 shows only power profile of P&O algorithm, with the average power output value of 196.347 W, minimum power of 192.573 W, and maximum power of 200.44 W. The oscillation, hence, has peak to peak amplitude of 7.867 W. A zoomed version of the first 100 ms power profile is revealed in Figure 1.11. The power reaches minimum steady state value (192.573 W) for the first time in 0.0482 s (48.2 ms).

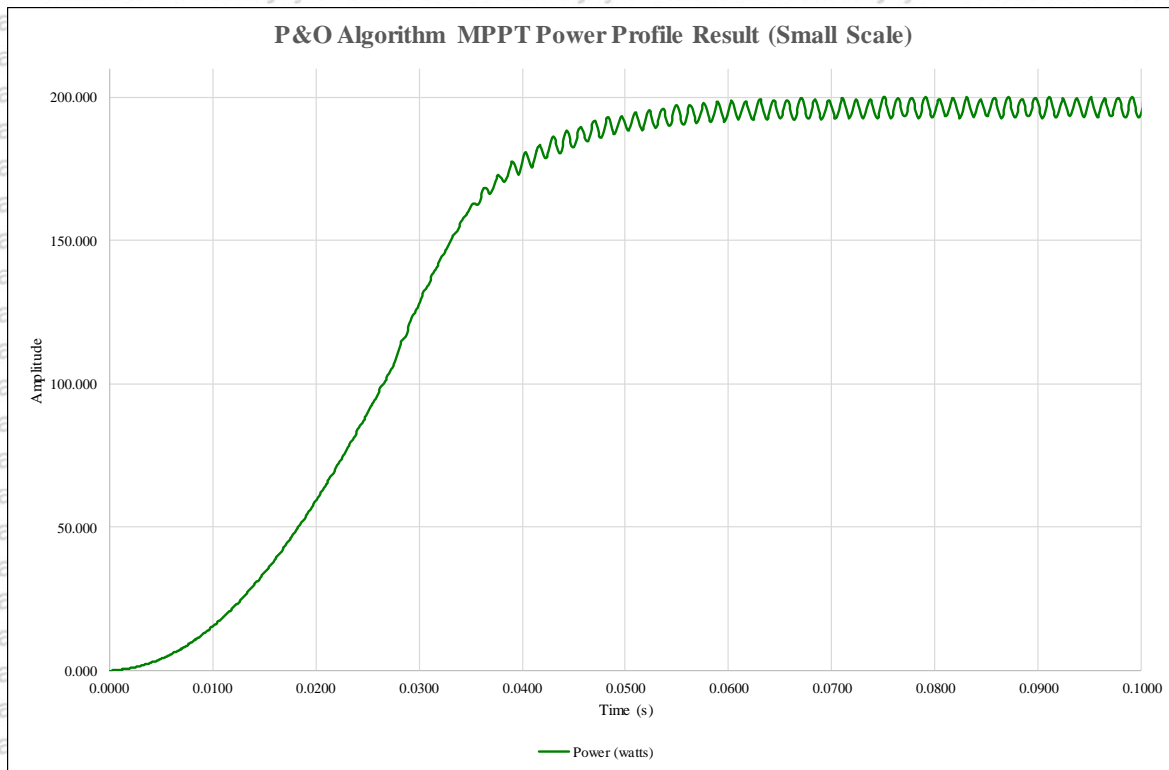


Figure 1.11 The output of power profile simulation on PV MPPT using P&O algorithm in the first 100 ms.

1.5 Fuzzy Logic Control Method MPPT Simulation

1.5.1 The FLC Method Model and Parameters

The final MPPT testing is performed by implementing FLC. For making the testing identical and fair, it is done by making simulation of $1000 \text{ W} \cdot \text{m}^{-2}$ solar radiance perpendicular to solar panel surface, and the temperature is set to 25°C degrees Celsius.

Fuzzy Logic MPPT Controller for Solar PV System

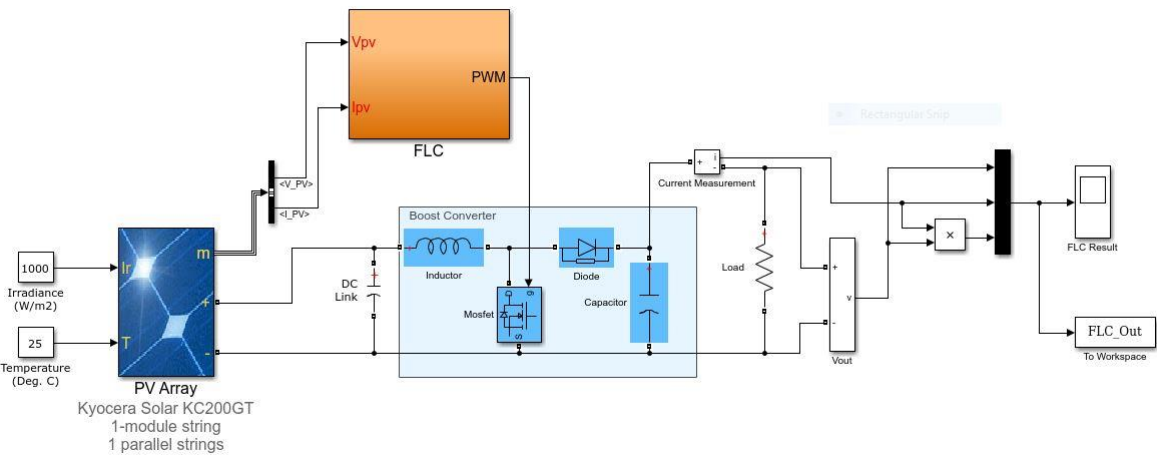


Figure 1.12 Matlab/Simulink PV MPPT circuit diagram for FLC method.

Figure 1.12 displays the circuit diagram of PV MPPT using FLC in Matlab/Simulink, which the result data will be analyzed. For more detail on FLC block in orange box is accessible in Figure 1.13.

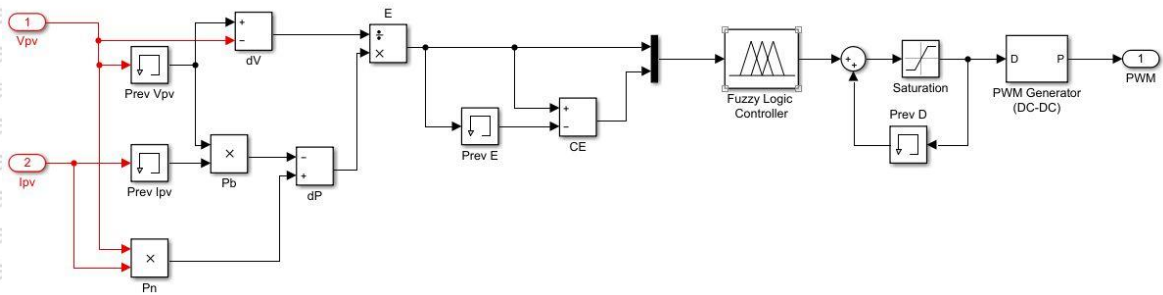


Figure 1.13 Simulink PV MPPT detailed circuit diagram for FLC method.

As in the P&O algorithm, the inputs consist of present voltage (V_n) and present current (I_n) provided by the PV, which converted to voltage derivative (ΔV) and power derivative (ΔP).

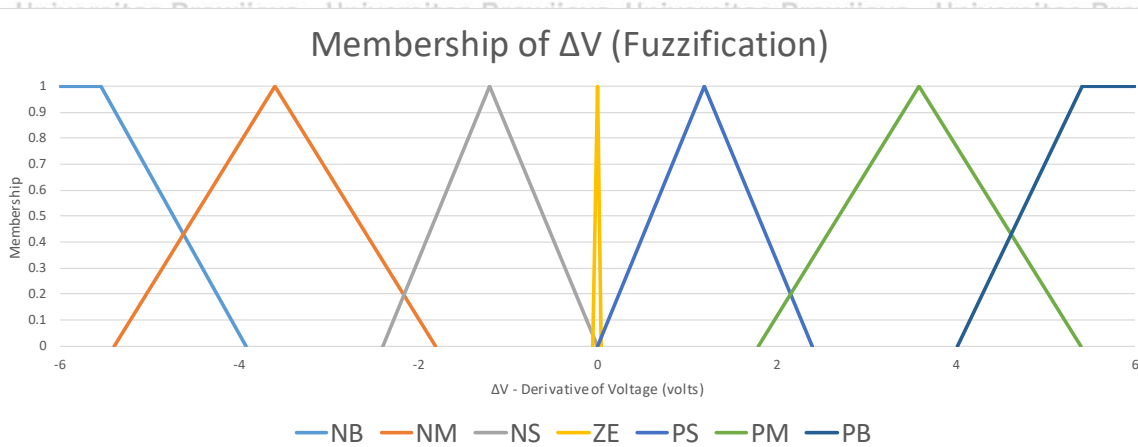


Figure 1.14 Membership functions of voltage derivative (ΔV).

While Figure 1.14 shows in graphical style, in Matlab FIS (fuzzy inference system) parameter, the membership function of ΔV is written as follow:

```
NB = ZMF [-5.54 -3.921]
NM = TRMF [-5.4 -3.6 -1.8]
NS = TRMF [-2.4 -1.2 0]
ZE = TRMF [-0.4 0 0.4]
PS = TRMF [0 1.2 2.4]
PM = TRMF [1.8 3.6 5.4]
PB = SMF [4.016 5.41]
```

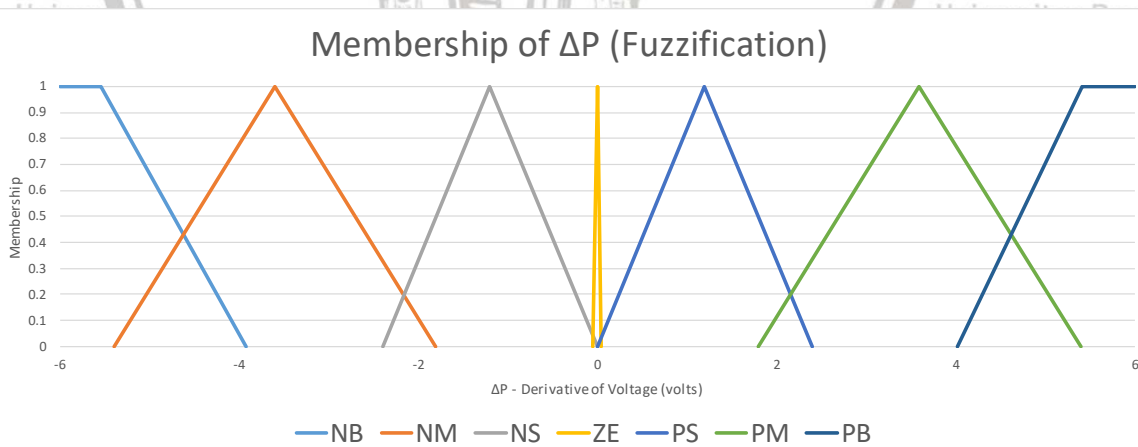


Figure 1.15 Membership functions of power derivative (ΔP).

Figure 1.15 shows membership function of ΔP in graphical style, and in Matlab FIS parameter, it is written as follow:

```
NB = ZMF [-5.37 -3.984]
```

NM = TRIMF [-5.4 -3.6 -1.8]
 NS = TRIMF [-2.4 -1.2 0]
 ZE = TRIMF [-0.3 0 0.3]
 PS = TRIMF [0 1.2 2.4]
 PM = TRIMF [1.8 3.6 5.4]
 PB = SMF [4.02 5.317]

After the membership of ΔV and ΔP are determined, FLC process goes into the rule evaluation to decide control action taken. The FLC rule is set into table type as in Table 1.2.

Table 1.2
 FLC Rule for MPPT

dV \ dP	NB	NM	NS	ZE	PS	PM	PB
NB	PB	PM	PS	NS	NS	NM	NB
NM	PM	PS	PS	NS	NS	NM	NB
NS	PS	PS	PS	PS	NS	NS	NM
ZE	NS	NS	NS	ZE	PS	PS	PS
PS	NS	NS	NS	ZE	PS	PS	PS
PM	NM	NS	NS	NS	PS	PS	PM
PB	NB	NM	NS	NS	PS	PS	PB

Under the rule table at Table 1.2, control action can be decided. The action taken can be fallen into more than one membership of control action. The inference engine chooses minimum membership value between ΔP and ΔV , and gives the value to the action membership as weight. Once the weight of every action are known, then the weights are summed up into each action membership. This process then undergoes “centering” between defuzzification memberships into center of gravity method.

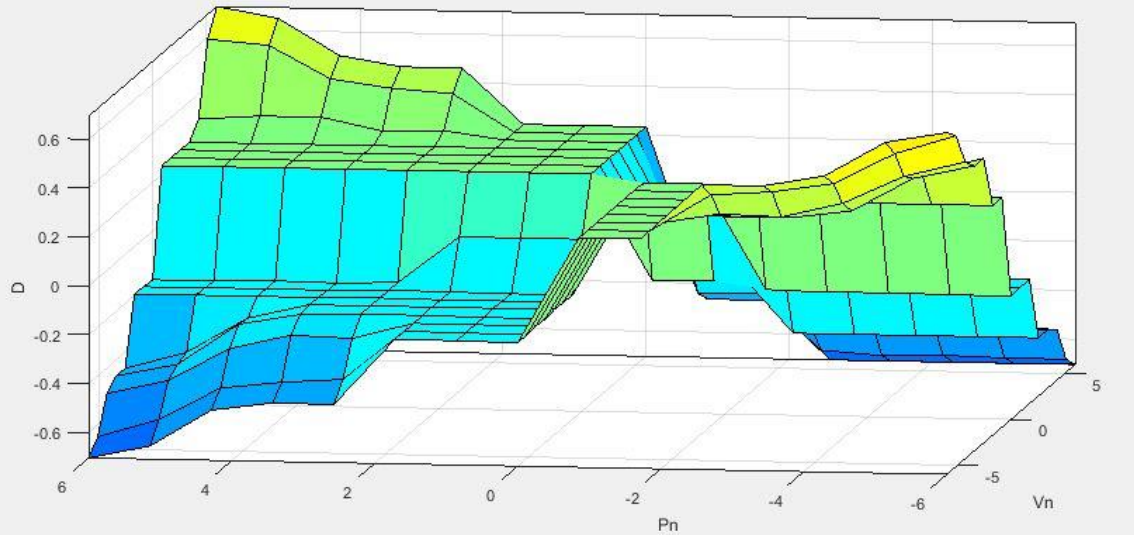


Figure 1.16 The surface view of FLC rules for MPPT.

Next, in the Figure 1.17, the memberships of control action are shown. The membership functions are the defuzzification to generate severity of duty cycle rate of change. After the centering process, memberships of control action are determined, and finally the value of duty cycle can be updated by the defuzzification value. As in P&O, the duty cycle generated is constrained within the value of 0.02 to 0.98.

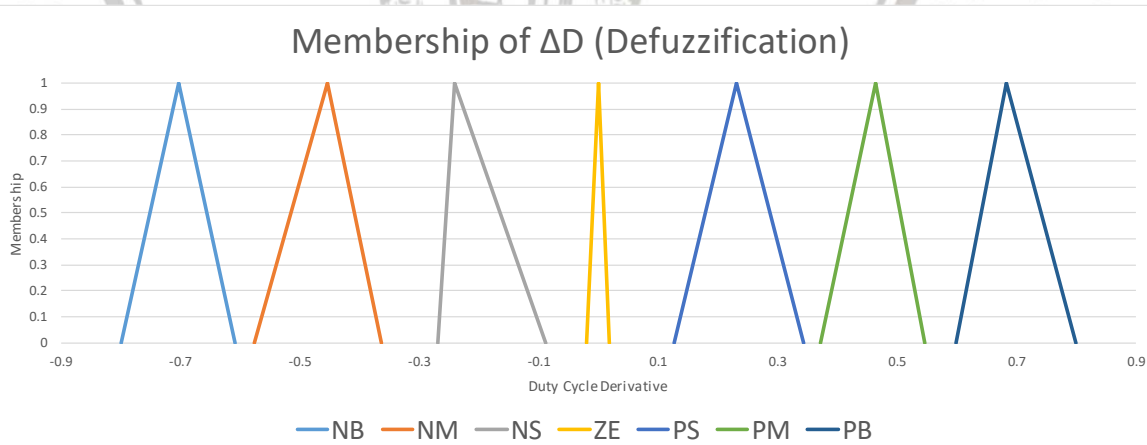


Figure 1.17 Membership functions of duty cycle action (ΔD) as control action.

By Matlab FIS parameter, the membership function of ΔD in Figure 1.17 is written as follow:

```

NB = TRIMF [-0.8 -0.702 -0.608]
NM = TRIMF [-0.576 -0.454 -0.3632]
NS = TRIMF [-0.2688 -0.24 -0.088]
    
```

```

ZE = TRIMF [-0.005 0 0.005]
PS = TRIMF [0.128 0.232 0.344]
PM = TRIMF [0.3728 0.464 0.548]
PB = SMF [0.6 0.6832 0.8]
    
```

The 3 dimension visualization of relation between fuzzification, rule evaluation, and defuzzification process can be represented as the control surface in Figure 1.16, with the horizontal axis denotes input of ΔP and ΔV , and the vertical axis denotes output of ΔD . The FLC equivalent Matlab source code is presented in Appendix 3.

The following steps described explanations of PV MPPT implementation using FLC method, with one example from the data result in Table 1.5 for the row number 6 with time of 0.5 millisecond ($V_{pv} = 0.893$, $I_{pv} = 0.132$, $P_{pv} = 0.118$, $V_{prev} = 0.521$, $P_{prev} = 0.040$, and assuming $D_{prev} = 0.02$):

1. The input stage is to accept voltage value and current value from PV.

a. The voltage is assigned to V_{pv} variable.

$$V_{pv} \leftarrow input_1$$

Example: $V_{pv} = 0.893$

b. The current is assigned to I_{pv} variable.

$$I_{pv} \leftarrow input_2$$

Example: $I_{pv} = 0.132$

2. If the process is the first passing, then assign the previous value of duty cycle (D_{prev}), previous value of voltage (V_{prev}), and previous value of power (P_{prev}) with initial values. All initial values could be random, but have to be within acceptable range.

$$D_{prev} \leftarrow 0.7$$

$$V_{prev} \leftarrow 32.5$$

$$P_{prev} \leftarrow 135$$

3. The first process stage is intended to calculate the derivative of voltage and the derivative of power.

- a. Calculate present value of power (P_{pv}) as a multiplication between present value of voltage (V_{pv}) and present value of current (I_{pv}).

$$P_{pv} \leftarrow V_{pv} \cdot I_{pv}$$

Example: $P_{pv} = 0.893 \cdot 0.132 = 0.118$

- b. Calculate derivative of power (ΔP) as P_{pv} subtracted by previous value of power (P_{prev}). The ΔP value is defined as the severity of power increasing or decreasing against the previous one.

$$\Delta P \leftarrow P_{pv} - P_{prev}$$

Example: $\Delta P = 0.118 - 0.040 = 0.078$

- c. Calculate derivative of voltage (ΔV) as V_{pv} subtracted by previous value of voltage (V_{prev}). The ΔV value is defined as the severity of voltage increasing or decreasing against the previous one.

$$\Delta V \leftarrow V_{pv} - V_{prev}$$

Example: $\Delta V = 0.893 - 0.521 = 0.372$

4. The second process stage is the main procedure of FLC method. The first step of FLC method is to perform fuzzification for two prepared input, i.e. ΔP and ΔV .

- a. Calculate each membership of ΔP for NB, NM, NS, ZE, PS, PM, and PB. The FIS model based on the fuzzification of the first input does this process internally. Each value for NB, NM, NS, ZE, PS, PM, and PB will be determined in this process.

Example:

$$NB(\Delta P) = 0.000$$

$$NM(\Delta P) = 0.000$$

$$NS(\Delta P) = 0.000$$

$$ZE(\Delta P) = 0.740$$

$$PS(\Delta P) = 0.065$$

$$PM(\Delta P) = 0.000$$

$$PB(\Delta P) = 0.000$$

- b. Calculate each membership of ΔV for NB, NM, NS, ZE, PS, PM, and PB. The FIS model based on the fuzzification of the second input does this process internally.

Each value for NB, NM, NS, ZE, PS, PM, and PB will be determined in this process.

Example:

$$NB(\Delta V) = 0.000$$

$$NM(\Delta V) = 0.000$$

$$NS(\Delta V) = 0.000$$

$$ZE(\Delta V) = 0.070$$

$$PS(\Delta V) = 0.310$$

$$PM(\Delta V) = 0.000$$

$$PB(\Delta V) = 0.000$$

5. The second step of FLC method is to perform rule evaluation based on the rule table, by the following procedures:

Table 1.3
 FLC Weight Values Example for $\Delta P = 0.078$ and $\Delta V = 0.372$

dV \ dP	NB	NM	NS	ZE	PS	PM	PB
NB	Min (0.000, 0.000) = 0.000	Min (0.000, 0.000) = 0.000	Min (0.000, 0.000) = 0.000	Min (0.000, 0.740) = 0.000	Min (0.000, 0.065) = 0.000	Min (0.000, 0.000) = 0.000	Min (0.000, 0.000) = 0.000
NM	Min (0.000, 0.000) = 0.000	Min (0.000, 0.000) = 0.000	Min (0.000, 0.000) = 0.000	Min (0.000, 0.740) = 0.000	Min (0.000, 0.065) = 0.000	Min (0.000, 0.000) = 0.000	Min (0.000, 0.000) = 0.000
NS	Min (0.000, 0.000) = 0.000	Min (0.000, 0.000) = 0.000	Min (0.000, 0.000) = 0.000	Min (0.000, 0.740) = 0.000	Min (0.000, 0.065) = 0.000	Min (0.000, 0.000) = 0.000	Min (0.000, 0.000) = 0.000
ZE	Min (0.070, 0.000) = 0.000	Min (0.070, 0.000) = 0.000	Min (0.070, 0.000) = 0.000	Min (0.070, 0.740) = 0.070	Min (0.070, 0.065) = 0.065	Min (0.070, 0.000) = 0.000	Min (0.070, 0.000) = 0.000
PS	Min (0.310, 0.000) = 0.000	Min (0.310, 0.000) = 0.000	Min (0.310, 0.000) = 0.000	Min (0.310, 0.740) = 0.310	Min (0.310, 0.065) = 0.065	Min (0.310, 0.000) = 0.000	Min (0.310, 0.000) = 0.000
PM	Min (0.000, 0.000) = 0.000	Min (0.000, 0.000) = 0.000	Min (0.000, 0.000) = 0.000	Min (0.000, 0.740) = 0.000	Min (0.000, 0.065) = 0.000	Min (0.000, 0.000) = 0.000	Min (0.000, 0.000) = 0.000
PB	Min (0.000, 0.000) = 0.000	Min (0.000, 0.000) = 0.000	Min (0.000, 0.000) = 0.000	Min (0.000, 0.740) = 0.000	Min (0.000, 0.065) = 0.000	Min (0.000, 0.000) = 0.000	Min (0.000, 0.000) = 0.000

- a. Calculate the weight of 49-cell in rule table, and multiplied by minimum value between membership of ΔP and ΔV , according to the lookup table data of defuzzification value. The FIS model based on the rule evaluation of the fuzzification values does this process internally.

Example as in Table 1.3:

$$SumWeight = \sum(Weight) = 0.070 + 0.065 + 0.310 + 0.065 = 0.51$$



Table 1.4

FLC Weight Multiplied by Control Action Crisp Values Example for $\Delta P = 0.078$ and $\Delta V = 0.372$

dV dP	NB	NM	NS	ZE	PS	PM	PB
NB	0.000	0.000	0.000	0.000	0.000	0.000	0.000
	x	x	x	x	x	x	x
	0.6832	0.464	0.232	-0.240	-0.240	-0.454	-0.702
	=	=	=	=	=	=	=
NM	0.000	0.000	0.000	0.000	0.000	0.000	0.000
	x	x	x	x	x	x	x
	0.464	0.232	0.232	-0.240	-0.240	-0.454	-0.702
	=	=	=	=	=	=	=
NS	0.000	0.000	0.000	0.000	0.000	0.000	0.000
	x	x	x	x	x	x	x
	0.232	0.232	0.232	0.232	-0.240	-0.240	-0.454
	=	=	=	=	=	=	=
ZE	0.000	0.000	0.000	0.070	0.065	0.000	0.000
	x	x	x	x	x	x	x
	-0.240	-0.240	-0.240	0.000	0.232	0.232	0.232
	=	=	=	=	=	=	=
PS	0.000	0.000	0.000	0.310	0.065	0.000	0.000
	x	x	x	x	x	x	x
	-0.240	-0.240	-0.240	0.000	0.232	0.232	0.232
	=	=	=	=	=	=	=
PM	0.000	0.000	0.000	0.000	0.000	0.000	0.000
	x	x	x	x	x	x	x
	-0.454	-0.240	-0.240	-0.240	0.232	0.232	0.464
	=	=	=	=	=	=	=
PB	0.000	0.000	0.000	0.000	0.000	0.000	0.000
	x	x	x	x	x	x	x
	-0.702	-0.454	-0.240	-0.240	0.232	0.232	0.6832
	=	=	=	=	=	=	=
	0.000	0.000	0.000	0.000	0.000	0.000	0.000

- b. Sum the product of weight and minimum value between memberships of ΔP and ΔV to generate center value of defuzzification. The FIS model based on the rule evaluation of the fuzzification values does this process internally.

Example as in Table 1.4:

$$SumWeightCrisp = \sum(WeightCrisp) = 0.01508 + 0.01508 = 0.03016$$

6. The third step of FLC method is to perform defuzzification to generate crisp value from the fuzzy value, as described in the following procedures:

- a. Calculate ΔD as inverted membership of center value of defuzzification from NB, NM, NS, ZE, PS, PM, and PB. The FIS model based on the defuzzification of the fuzzy values does this process internally.

$$\Delta D \leftarrow \frac{SumWeightCrisp}{SumWeight}$$

Example: $\Delta D = 0.03016 / 0.51 = 0.05914$

- b. Add ΔD for the value of D from their previous duty cycle value of D_{prev} .

$$D \leftarrow D_{prev} + \Delta D$$

Example: $D = 0.02 + 0.05914 = 0.07914$

7. The output stage is to prepare D as the duty cycle for the PWM generator and to prepare the next process passing.

- a. Make the value of D constrained in the range between 0.02 and 0.98.

if ($D < 0.02$) *then*

$$D \leftarrow 0.02$$

end if

if ($D > 0.98$) *then*

$$D \leftarrow 0.98$$

end if

Example: $D = 0.07914$

- b. Assign all present values to the previous values for the next passing:

$$D_{prev} \leftarrow D$$

$$V_{prev} \leftarrow V_{pv}$$

$$P_{prev} \leftarrow P_{pv}$$



Example: $D_{prev} = 0.07914$, $V_{prev} = 0.893$, and $P_{prev} = 0.118$

8. In this point, the output value of duty cycle (D) is ready to be fed to the PWM generator, therefore drives the MOSFET in boost converter.

An example of FLC method result from the calculation within the first 3 milliseconds is presented in Table 1.5, consisting of time, voltage, current, and power.



Table 1.5
Example of FLC Method Calculation Result from 0 Millisecond to 3 Milliseconds

No.	Time (millisecond)	FLC		
		Voltage (volt)	Current (ampere)	Power (watt)
1	0.0	0.000	0.000	0.000
2	0.1	0.010	0.001	0.000
3	0.2	0.077	0.011	0.001
4	0.3	0.243	0.036	0.009
5	0.4	0.521	0.077	0.040
6	0.5	0.893	0.132	0.118
7	0.6	1.318	0.195	0.257
8	0.7	1.740	0.257	0.447
9	0.8	2.107	0.311	0.656
10	0.9	2.379	0.351	0.836
11	1.0	2.541	0.375	0.954
12	1.1	2.609	0.385	1.005
13	1.2	2.620	0.387	1.014
14	1.3	2.628	0.388	1.020
15	1.4	2.687	0.397	1.067
16	1.5	2.837	0.419	1.189
17	1.6	3.095	0.457	1.415
18	1.7	3.444	0.509	1.752
19	1.8	3.850	0.569	2.190
20	1.9	4.256	0.629	2.676
21	2.0	4.612	0.681	3.142
22	2.1	4.875	0.720	3.511
23	2.2	5.032	0.743	3.741
24	2.3	5.093	0.752	3.833
25	2.4	5.097	0.753	3.839
26	2.5	5.099	0.753	3.841
27	2.6	5.153	0.761	3.922
28	2.7	5.296	0.782	4.144
29	2.8	5.545	0.819	4.542
30	2.9	5.882	0.869	5.111
31	3.0	6.273	0.927	5.813

The graphical form of the FLC method result above is presented in Figure 1.18 with the data labels on every 0.5 millisecond. As the visual representation, the blue line signifies voltage in volt, while the red line embodies current in ampere, and the green line denotes power in watt. In this example, the power has lower values compared to the voltage, since the current values are below



1 ampere. For the current value greater than 1 ampere, the power will have values above voltage, which is shown beyond Figure 1.18.

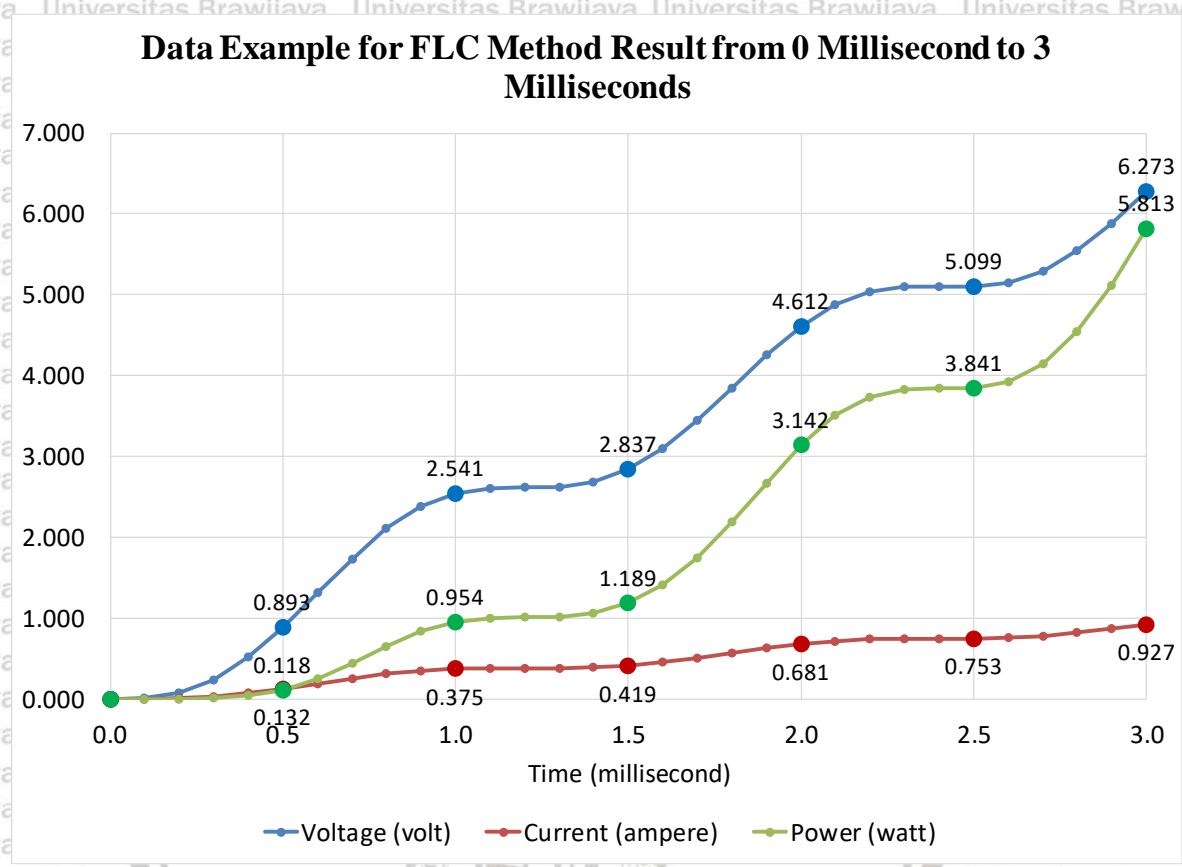


Figure 1.18 The graphical representation of the example of FLC method result from 0 millisecond to 3 milliseconds.

1.5.2 The FLC Method Simulation Result

For this simulation, a data plotting with 100 μ s sample rate is chosen. Starting from zero condition, the simulation duration is set to 3 s.

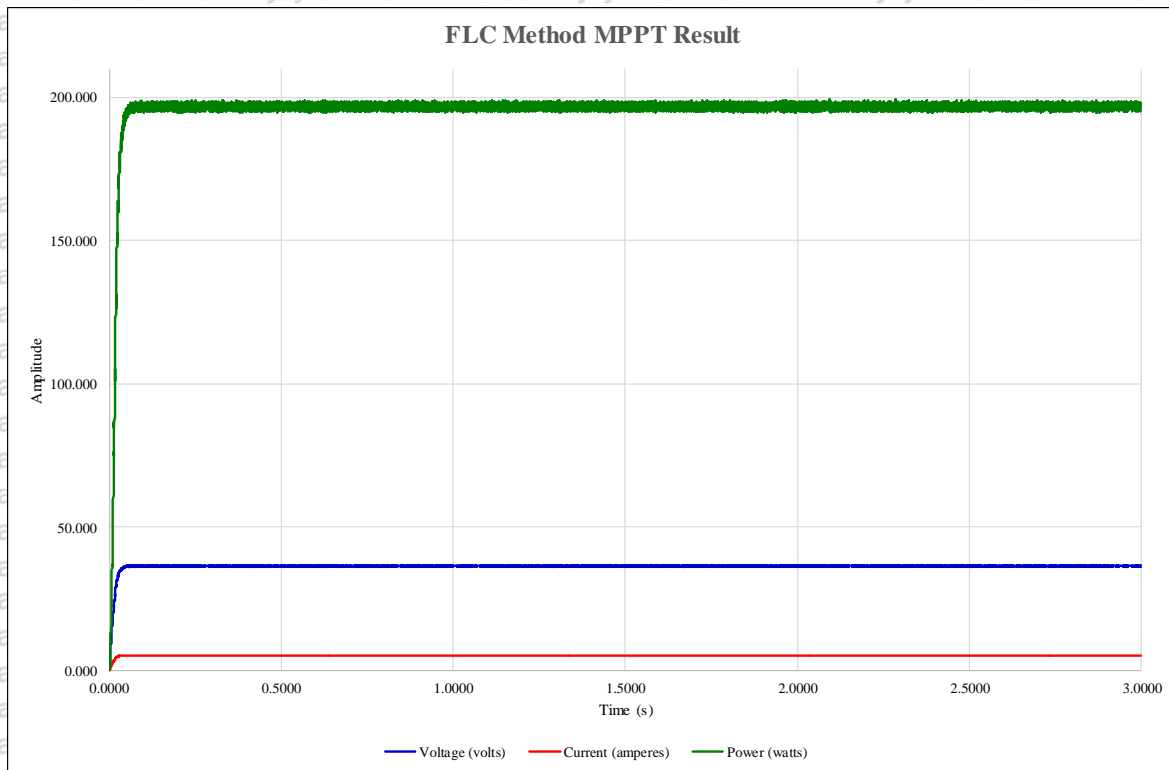


Figure 1.19 The output of voltage, current, and power profile simulation on PV MPPT using FLC method in the first 3 s.

The result of voltage, current, and power profile against time using FLC method is shown in Figure 1.19. Visually, the power profile is copying both voltage and current profile. According to the numerical data, FLC method produces rise time at 0.0454 s. For the voltage profile in a single graph, an adjusted y-axis scale is shown in Figure 1.20.

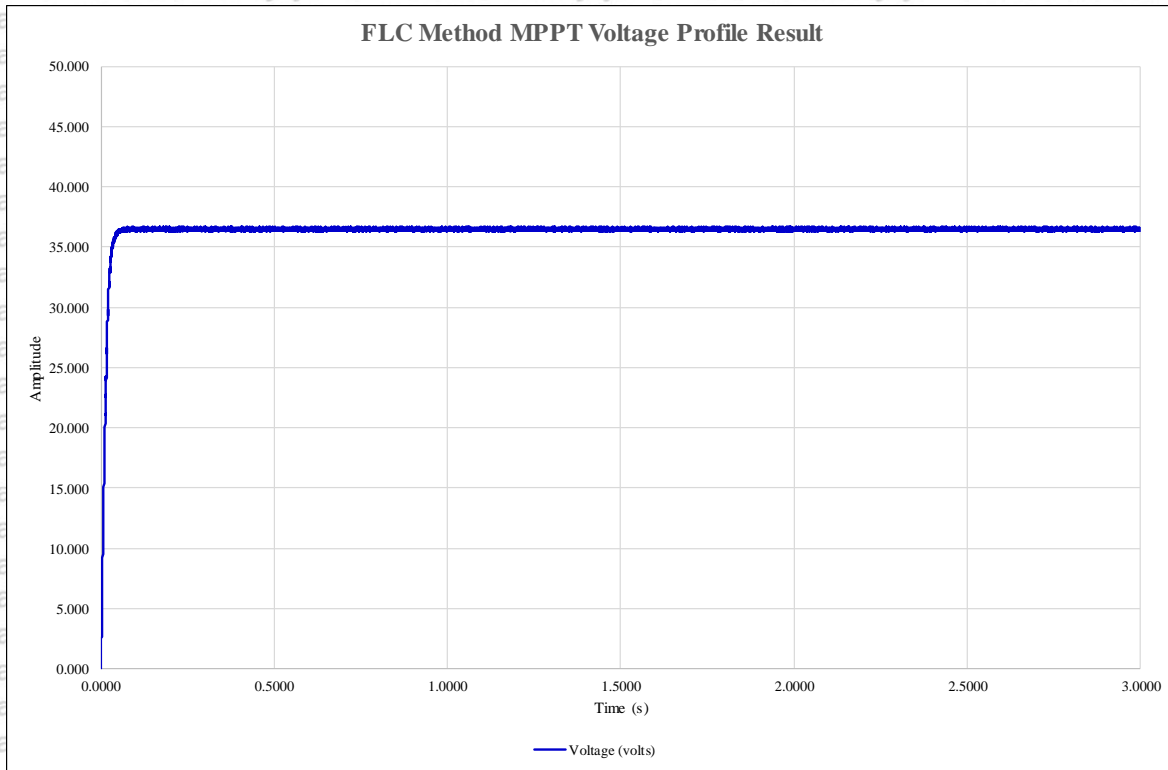


Figure 1.20 The output of voltage profile simulation on PV MPPT using FLC method in the first 3 s.

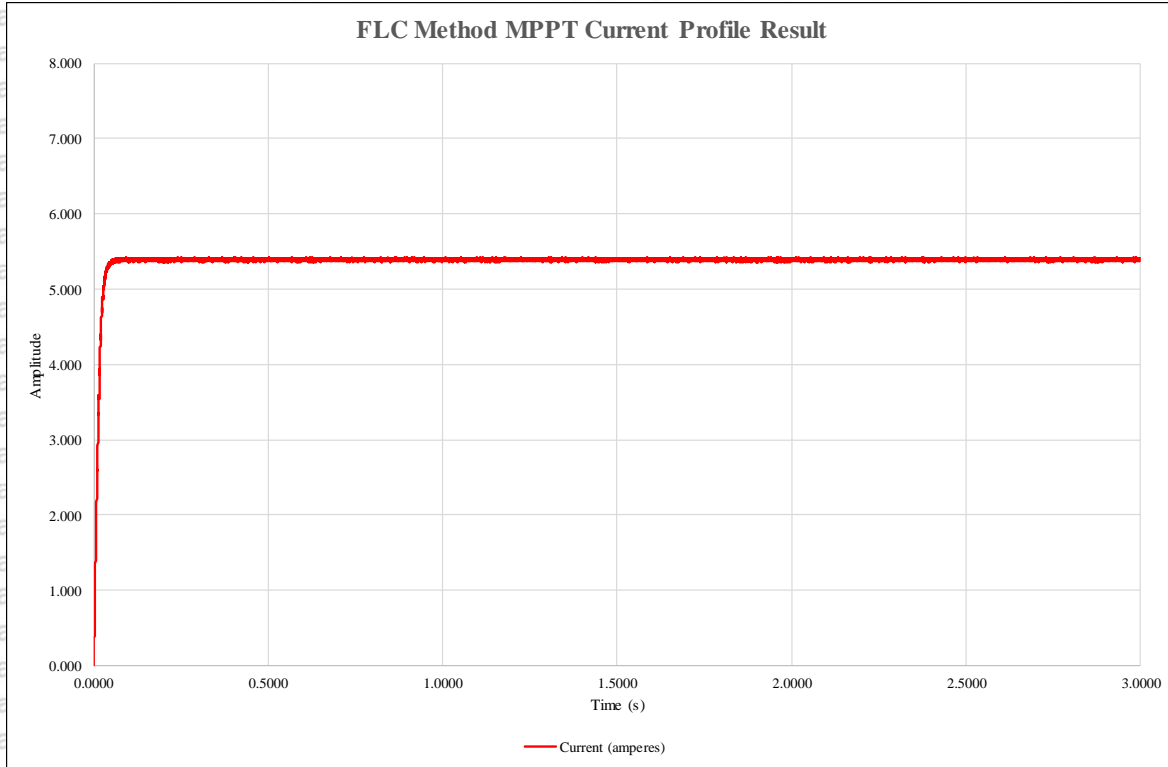


Figure 1.21 The output of current profile simulation on PV MPPT using FLC method in the first 3 s.

Figure 1.20 shows that after 100 ms, the voltage reaches steady state in average 36.516 V, with minimum value of 36.288 V and maximum value of 36.710 V. It is a 0.422 VPP oscillation.

Figure 1.21 shows that after 100 ms, the current reaches steady state in average 5.395 A, with minimum value of 5.361 A and maximum value of 5.423 A. It is a 0.062 APP oscillation.

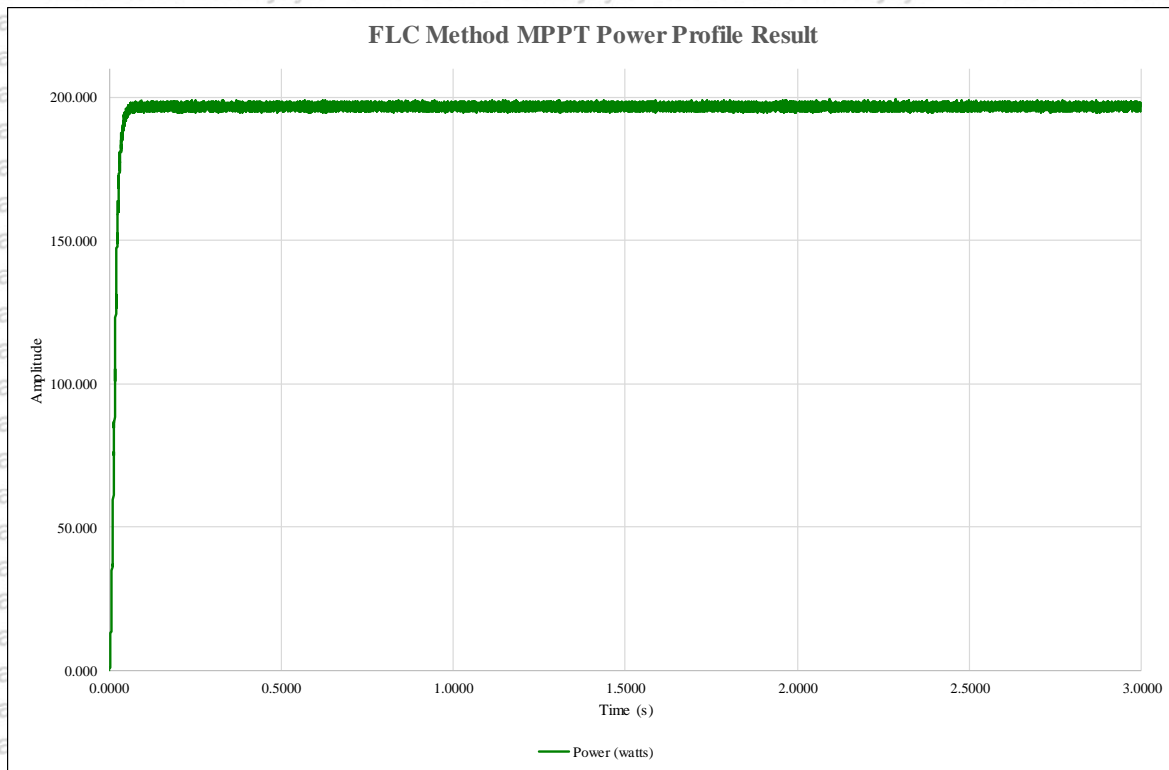


Figure 1.22 The output of power profile simulation on PV MPPT using FLC method in the first 3 s.

Figure 1.22 shows only power profile of FLC method, with the average power output value of 196.996 W, minimum power of 194.545 W, and maximum power of 199.091 W. The oscillation, hence, has peak to peak amplitude of 4.546 W. A zoomed version of the first 100 ms power profile is exposed in Figure 1.23. The power reaches minimum steady state value (194.545 W) for the first time in 0.0454 s (45.4 ms).

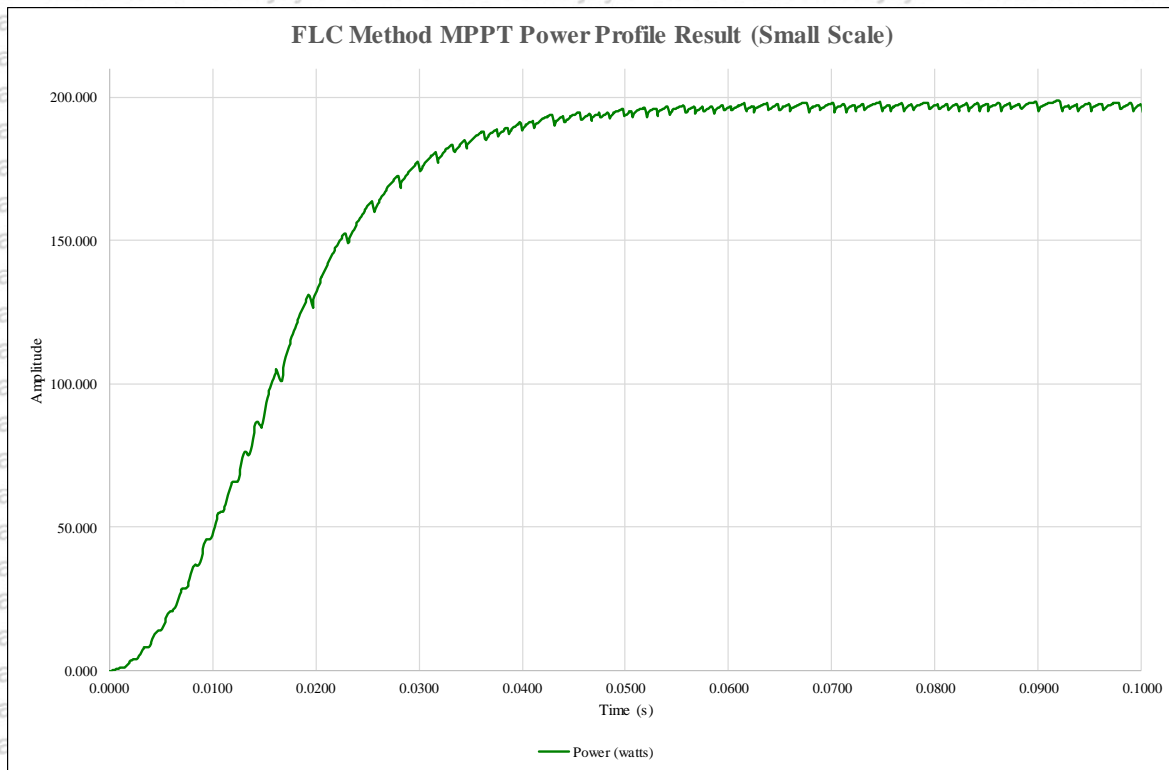


Figure 1.23 The output of power profile simulation on PV MPPT using FLC method in the first 100 ms.

1.6 Analysis of Result Comparison between P&O Algorithm and FLC Method

For the confirmation purpose, a combination of P&O algorithm and FLC method for MPPT is created in a single simulation project. With the same parameters as the separate simulations previously, the simulation runs in the same starting time and the data collected within the same sampling time, i.e. 100 μ s.

Comparison Between P&O Algorithm and FLC Method MPPT Controllers

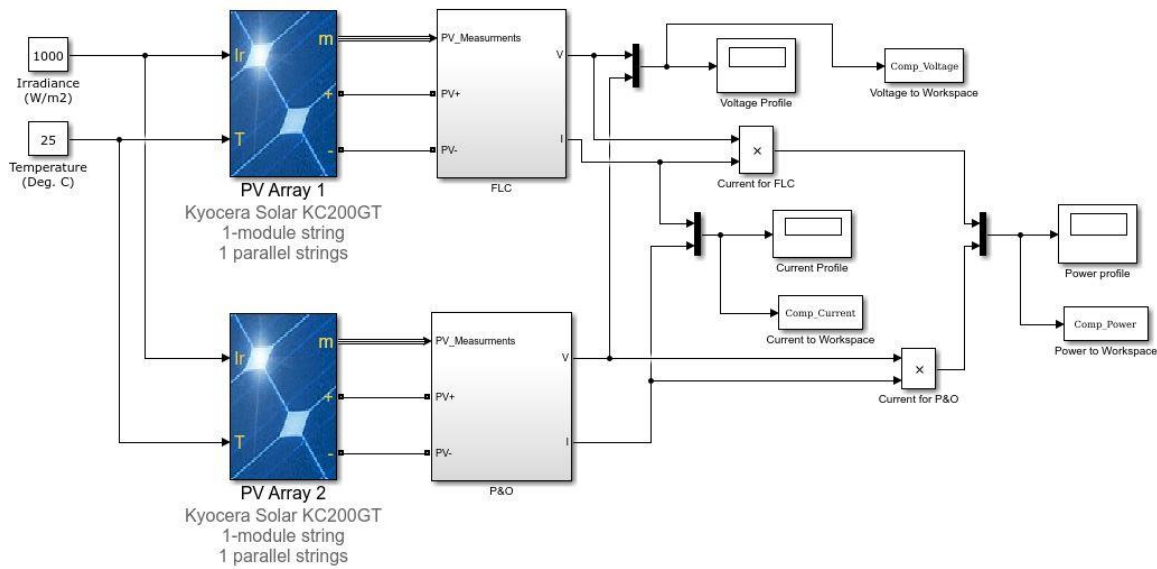


Figure 1.24 Combined Matlab/Simulink PV MPPT circuit diagram for both P&O algorithm and FLC method.

Figure 1.24 shows the combined simulation diagram for P&O algorithm and FLC method altogether. It uses separate PV array but fed with the common irradiance level and ambient temperature. After the simulation is performed, it is known that the data plots the same value as two previous simulations, therefore confirms their validity. Comparison between P&O algorithm and FLC method for MPPT is shown in Figure 1.25 and Figure 1.26.

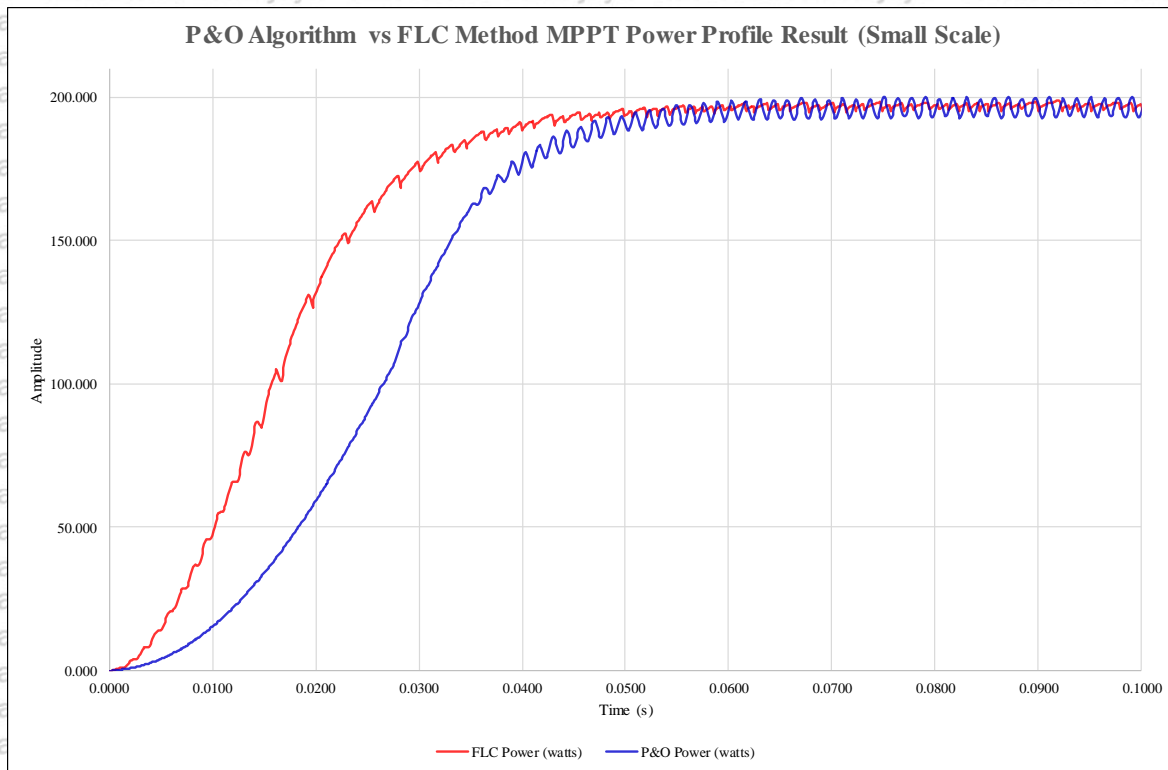


Figure 1.25 Comparison between MPPT power profile using P&O algorithm and FLC method in the first 100 ms.

For the first 100 ms, the P&O algorithm takes a bit longer rising time from zero to reach the stability point, while FLC method gives the rapid one, as seen on Figure 1.25. The ΔD of P&O algorithm plays special role in rising time and oscillation near the MPP. When a big ΔD value selected, then rapid rising time will be achieved, with a consequence of a large oscillation around MPP. In the other case, when a tiny ΔD value is selected, then oscillation around MPP will be suppressed while it needs longer time of rise time. In this simulation case, the value of ΔD is chosen at 0.0025. The P&O algorithm uses constant ΔD , therefore the increasing or decreasing value of duty cycle during one pass of the function is fixed at 0.0025.

On the other hand, FLC method uses various value of ΔD , based on input. Voltage and power change as inputs are converted into fuzzy value membership, and based on the rule table the output of ΔD is then determined through the defuzzification. Hence, the wildness of duty cycle changing depends on the voltage distance from MPP.

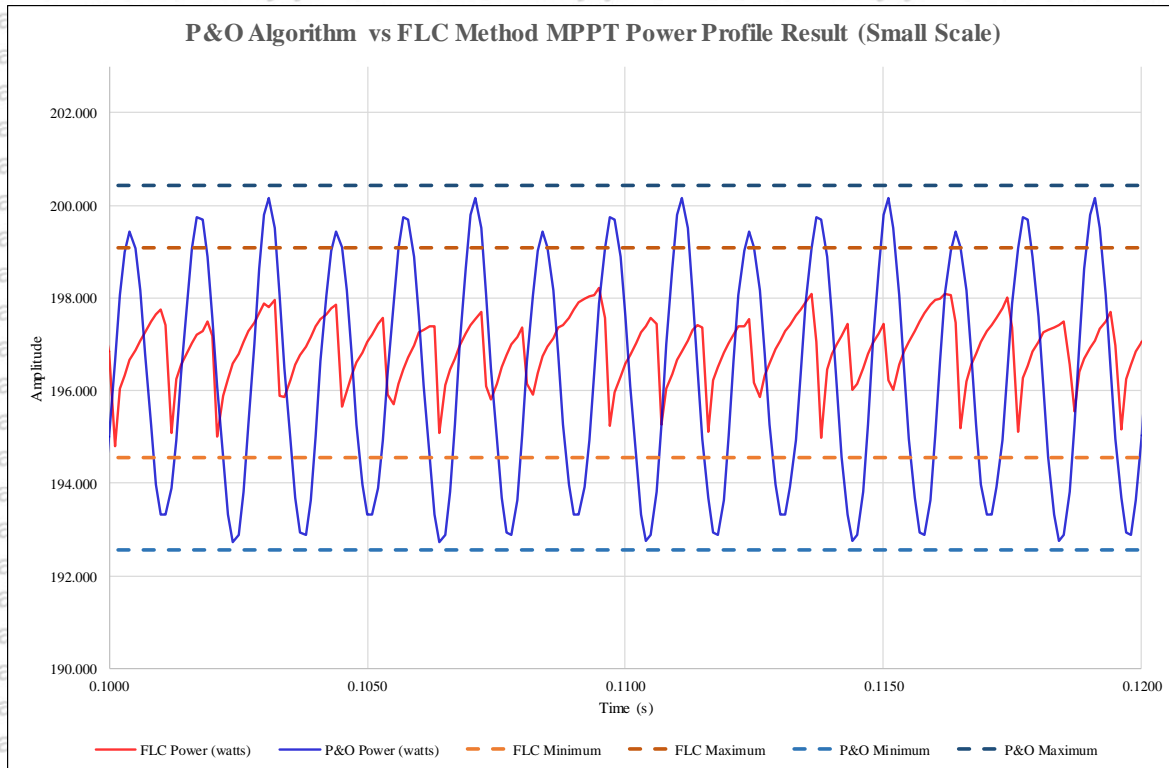


Figure 1.26 A detailed comparison result between P&O algorithm and FLC method.

A sample of power profile between 100 ms and 120 ms is provided in Figure 1.26, which shows both P&O algorithm (plotted in blue line) and FLC method result (plotted in red line). As the nature of constant duty cycle changing in P&O algorithm, it tends to oscillate larger than FLC method ones. Theoretically, FLC method can achieve zero oscillation. The nature of boost converter and PWM generator, however, produces a slight oscillation. The oscillation in the simulations shows peak-to-peak ripple of 7.867 WPP under P&O algorithm and 4.546 WPP under FLC method.

Summary of both methods result is shown in Table 1.6. It tells the difference between the P&O algorithm and FLC method.

Table 1.6
Summary of P&O Algorithm and FLC Method on Photovoltaic MPPT

Description	P&O Algorithm	FLC Method
Rising time	0.0482 s	0.0454 s
Minimum power on oscillation after 100 milliseconds	192.573 W	194.545 W
Maximum power on oscillation after 100 milliseconds	200.44 W	199.091 W
Average power after 100 milliseconds	196.347 W	196.996 W
Peak-to-peak oscillation after 100 milliseconds	7.867 WPP	4.546 WPP
Method efficiency (compared to 200.14 watts in datasheet)	98.105%	98.429%
Average voltage	36.455 V	36.516 V
Average current	5.386 A	5.395 A

As the summary on Table 1.6, FLC method gets 98.429% efficiency, slightly better than P&O algorithm on 98.105%. FLC method also has slightly better rising time on 45.4 ms, compared to the 48.2 ms for P&O algorithm. The oscillation generated by FLC method is also lower in just 4.546 WPP, compared to the 7.867 WPP for P&O algorithm. It concludes that in those three aspect (the effective power, rising time, and oscillation), FLC method can perform better than P&O algorithm.

Being compared to some previous studies results, Sun and Han achieved 0.18 s of rise time in FLC-PI method (Sun & Han, 2013), while this study can make 0.0454 s of rise time in the pure FLC method. Huang achieved less than 2% of signal error, which corresponds to at least 98% power efficiency in the implementation of FLC-ANN into MPPT (Huang, et al., 2011), while this research delivers 98.429% power efficiency in pure FLC method.

According to this study, those better results have been reached because of several factors, including:

1. A fine-tuning procedure is performed to find optimum performance of each method before conducting simulation for comparison.
2. The adjustment of FLC parameters in FIS module is performed, especially the reducing of defuzzification membership values.

3. A setting of frequency in PWM generator is executed for the optimum voltage build-up based on the inductor's inductance in boost converter.





CHAPTER VI

CONCLUSIONS AND PROPOSITIONS

1.1 Conclusions

Based on the deep analysis undertaken of the results in this study, some conclusions are to be taken as following:

1. Photovoltaic MPPT simulations have been successfully built using Matlab and Simulink, constructed by the P&O algorithm and the FLC method, by the circuit models designed.
2. Photovoltaic MPPT based on P&O algorithm produces 98.105% of efficiency, compared to the FLC method that delivers 98.429% of efficiency, under irradiance of $1,000 \text{ W}\cdot\text{m}^{-2}$ and temperature of 25°C .
3. The FLC method efficiency, rising time, and oscillation are superior than P&O algorithm in photovoltaic MPPT. From this result, the FLC method should be selected over P&O algorithm as the PV MPPT implementation.

1.2 Propositions

Some suggestions that can be put forward so that there will be developments in the future research, include:

1. Operation of a real-world model for the artificial neural network MPPT technique by utilize microcontrollers, and make the testing on a real PV panel.
2. Making comparisons across many MPPT techniques and the proposed neural network one.
3. Simulation with variance in irradiance and temperature conditions.



BIBLIOGRAPHY

- Abdulkadir, M., Samosir, A., Yatim, A., & Yusuf, S. (2013). A New Approach of Modelling, Simulation of MPPT for Photovoltaic System in Simulink Model. *ARNP Journal of Engineering and Applied Sciences*, 8(7), 488–494.
- Afghoul, H., Chikouche, D., Krim, F., & Beddar, A. (2013). A novel implementation of MPPT sliding mode controller for PV generation systems. *IEEE EuroCon 2013*, (pp. 789–794). Retrieved from <https://doi.org/10.1109/EUROCON.2013.6625073>
- Al Nabulsi, A., Dhaouadi, R., & Rehman, H. (2011). Single input fuzzy controller (SFLC) based maximum power point tracking. In *Modeling, Simulation and Applied Optimization (ICMSAO), 2011 4th International Conference* (pp. 1-5). IEEE.
- Engineering, I. (2013). Design and Simulation of Intelligent Control MPPT Technique for PV Module Using MATLAB / SIMSCAPE.
- Esrarn, T., & Chapman, P. (2007). Comparison of photovoltaic array maximum power point tracking techniques. *IEEE Transactions on Energy Conversion*, 22(2), 439–449.
- Hohm, D., & Ropp, M. (2003). Comparative study of maximum power point tracking algorithms. *Progress in Photovoltaics: Research and Applications*, 11(1), 47–62.
- Huang, K., Li, W., & Huang, X. (2011). MPPT of solar energy generating system with fuzzy control and artificial neural network. *Proceedings - 2011 International Conference of Information Technology, Computer Engineering and Management Sciences, ICM 2011, 1*, pp. 230–233. Retrieved from <https://doi.org/10.1109/ICM.2011.56>
- Khouzam, K., Koh, C., Ly, C., & Yong, N. (1994). Simulation and Real-Time Modelling of Space Photovoltaic Systems. *IEEE 1st World Conference on Photovoltaic Energy Conversion*, 2, pp. 2038–2041.
- Kumar, H., & Tripathi, R. (2012). Simulation of variable incremental conductance method with direct control method using boost converter. In *Engineering and Systems (SCES), 2012 Students Conference* (pp. 1-5). IEEE.
- Kumar, S., Student, K., Kumar, M., & Senior, M. (2013). Novel Adaptive P & O MPPT Algorithm for Photovoltaic System Considering Sudden Changes in Weather Condition. *Clean Electrical Power (ICCEP), 2013 International Conference*, (pp. 653-658). Retrieved from <https://doi.org/10.1109/ICCEP.2013.6586955>
- Kyocera. (2009). High-efficiency multi-crystal photovoltaic module KC200GT.
- Lee, C., Ko, J., Seo, T., & Chung, D. (2013). MPPT control of photovoltaic system using FLC-PI controller. *International Conference on Control, Automation, and Systems*, 5, pp. 437–439. Retrieved from <https://doi.org/10.1109/ICCAS.2013.6703970>
- Lynn, P. (2011). *Electricity from sunlight: an introduction to photovoltaics*. John Wiley & Sons.
- Mohamed, T., Kasa, A., & Taha, M. (2012). Fuzzy Logic System for Slope Stability Prediction. *IJASEIT*, 2(2), 151-155.

- Mrabti, T., Ouariachi, M., Tidhaf, B., Kassmi, K., & Chadli, E. (2009). Regulation of Electric Power of Photovoltaic Generators With DC-DC Converter (Buck Type) And MPPT Command. 0-4.
- Pendem, S., & Mikkili, S. (2018). Modeling, simulation and performance analysis of solar PV array configurations (Series, Series-Parallel and Honey-Comb) to extract maximum power under Partial Shading Conditions. *Energy Report*, (pp. 274-287). Retrieved from <https://doi.org/10.1016/j.egy.2018.03.003>
- Raedani, R., & Hanif, M. (2004). *Design, Testing and Comparison of P & O, IC and VSSIR MPPT Techniques*.
- Rajendran, P., & Smith, H. (2018). Experimental Study of Solar Module & Maximum Power Point Tracking System under Controlled Temperature Conditions. *IJASEIT*, 8(4), 1147-1153.
- Ramaprabha, R., Mathur, B., & Sharanya, M. (2009). Solar array modeling and simulation of MPPT using neural network. In *Control, Automation, Communication and Energy Conservation, 2009 (INCACEC 2009)* (pp. 1-5). IEEE.
- Rashid, M. (2011). *Circuits, Devices, and Applications*. Electrical and Computer Engineering, University of West Florida.
- Rashid, M., Pena, J., Brito, M., Melo, G., & Canesin, C. (2011). A comparative study of MPPT strategies and a novel single-phase integrated buck-boost inverter for small wind energy conversion systems. 458-465.
- Selmi, T., Abdul-niby, M., & Davis, A. (2014). *P & O MPPT Implementation Using MATLAB / Simulink*.
- Sera, D., Mathe, L., Kerekes, T., Spataru, S., & Teodorescu, R. (2013). On the perturb-and-observe and incremental conductance mppt methods for PV systems. *IEEE Journal of Photovoltaics*, 3(3), 1070-1078. Retrieved from <https://doi.org/10.1109/JPHOTOV.2013.2261118>
- Sivanandam, S., Sumathi, S., & Deepa, S. (2007). *Introduction to fuzzy logic using MATLAB* (Vol. 1). Springer.
- Souza, N., Lopes, L., & Liu, X. (2005). An Intelligent Maximum Power Point Tracker using Peak Current Control. *2005 IEEE 36th Power Electronics Specialists Conference*, (p. 172). Retrieved from <https://doi.org/10.1109/PESC.2005.1581620>
- Sun, L., & Han, F. (2013). Study on MPPT approach in photovoltaic system based on fuzzy control. In *Industrial Electronics and Applications (ICIEA), 2013 8th IEEE Conference* (pp. 1259-1263). IEEE.
- Sun, L., & Han, F. (2015). Comprehensive analysis of maximum power point tracking techniques in solar photovoltaic systems under uniform insolation and partial shaded condition. In *Industrial Electronics and Applications (ICIEA), 2015 IEEE Conference*. IEEE. Retrieved from <https://doi.org/10.1063/1.4926844>
- Villalva, M., Gazoli, J., & Filho, E. (2009). Comprehensive Approach to Modeling and Simulation of Photovoltaic Arrays. *IEEE Transactions on Power Electronics*, 24(5), 1198-1208.

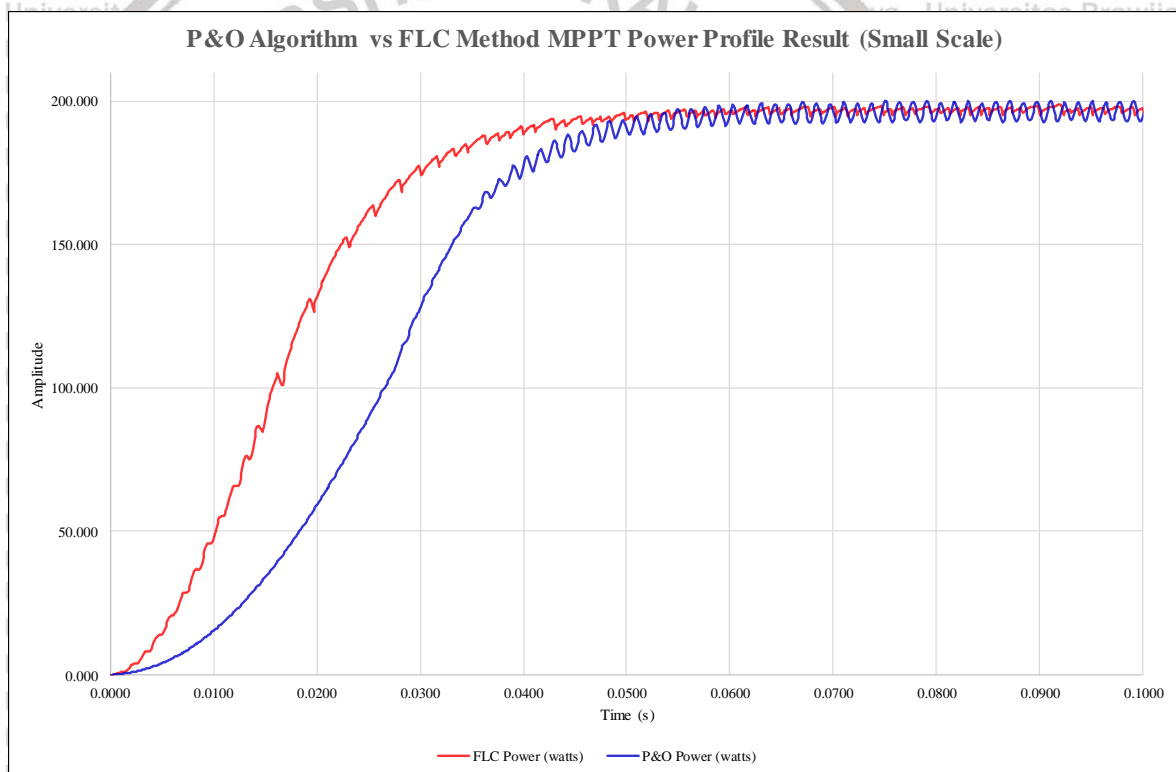
Wenham, S., Green, M., Watt, M., Corkish, R., & Sproul, A. (2013). *Applied Photovoltaics*. Abingdon, UK: Routledge.

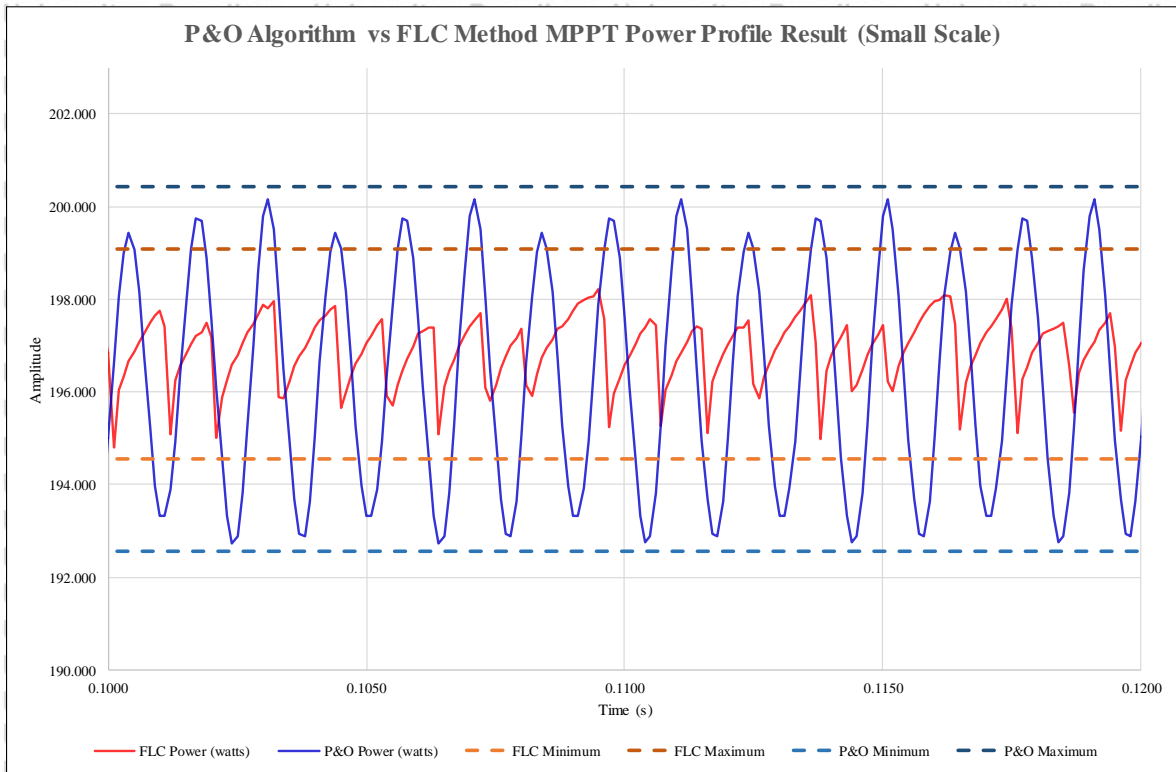
Yusof, Y., Sayuti, S., Latif, M., Zamri, M., & Wanik, C. (2004). Modeling and Simulation of Maximum Power Point Tracker for Photovoltaic System. *National Power and Energy Conference* (pp. 88-93). Kuala Lumpur: IEEE.



APPENDIX I COMPARISON DATA AND CHART

Description	P&O Algorithm	FLC Method
Rising time	0.0482 second	0.0454 second
Minimum power on oscillation after 100 milliseconds	192.573 watts	194.545 watts
Maximum power on oscillation after 100 milliseconds	200.44 watts	199.091 watts
Average power after 100 milliseconds	196.347 watts	196.996 watts
Peak-to-peak oscillation after 100 milliseconds	7.867 watts	4.546 watts
Method efficiency (compared to 200.14 watts in datasheet)	98.105%	98.429%





APPENDIX II

PERTURB AND OBSERVE ALGORITHM SOURCE CODE

Main Function (PandO)

```
function D = PandO(Vpv, Ipv)

// prepares the persistent variables for previous (memorized) values
persistent Dprev Pprev Vprev

// initializes all previous values in the first time
if isempty(Dprev)
    Dprev = 0.7;
    Vprev = 32.5;
    Pprev = 135;
end

// sets the delta D to a constant value
deltaD = 0.0025;

// calculates the present value of power
Ppv = Vpv * Ipv;

// checks the power derivative
if (Ppv - Pprev) ~= 0
    // these lines will be executed when the power is changing
    if (Ppv - Pprev) > 0
        // these lines will be executed when the power is rising
        if (Vpv - Vprev) > 0
            // these lines will be executed when the voltage is rising
            D = Dprev - deltaD;
        else
            // these lines will be executed when the voltage is falling
            D = Dprev + deltaD;
        end
    else
        // these lines will be executed when the power is falling
        if (Vpv - Vprev) > 0
            // these lines will be executed when the voltage is rising
            D = Dprev + deltaD;
        else
            // these lines will be executed when the voltage is falling
            D = Dprev - deltaD;
        end
    end
end
else
    // these lines will be executed when the power is unchanging
    D = Dprev;
end

// keeps the duty cycle from falling below 0.02
if (D < 0.02)
    D = 0.02;
end

// keeps the duty cycle from exceeding 0.98
if (D > 0.98)
    D = 0.98;
end
```


APPENDIX III

FUZZY LOGIC CONTROL METHOD SOURCE CODE

Main Function (FLC)

```

function D = FLC(Vpv, Ipv)

persistent Dprev Pprev Vprev

if isempty(Dprev)
    Dprev = 0.7;
    Vprev = 32.5;
    Pprev = 135;
end

Ppv = Vpv * Ipv;

Perr = Ppv - Pprev;
Verr = Vpv - Vprev;

MV_err(0) = ZMF(Verr, -5.54, -3.921);
MV_err(1) = TRIMF(Verr, -5.4, -3.6, -1.8);
MV_err(2) = TRIMF(Verr, -2.4, -1.2, 0);
MV_err(3) = TRIMF(Verr, -0.4, 0, 0.4);
MV_err(4) = TRIMF(Verr, 0, 1.2, 2.4);
MV_err(5) = TRIMF(Verr, 1.8, 3.6, 5.4);
MV_err(6) = SMF(Verr, 4.016, 5.41);

MP_err(0) = ZMF(Perr, -5.37, -3.984);
MP_err(1) = TRIMF(Perr, -5.4, -3.6, -1.8);
MP_err(2) = TRIMF(Perr, -2.4, -1.2, 0);
MP_err(3) = TRIMF(Perr, -0.3, 0, 0.3);
MP_err(4) = TRIMF(Perr, 0, 1.2, 2.4);
MP_err(5) = TRIMF(Perr, 1.8, 3.6, 5.4);
MP_err(6) = SMF(Perr, 4.02, 5.317);

for i = 0:6
    for j = 0:6
        RULE_WEIGHT(i, j) = min(MV_err(i), PV_err(j));
    end
end

SUM_OF_WEIGHT = 0.0;
SUM_OF_WEIGHT_TIMES_CRISP = 0.0;
for i = 0:6
    for j = 0:6
        SUM_OF_WEIGHT = SUM_OF_WEIGHT + RULE_WEIGHT(i, j);
        SUM_OF_WEIGHT_TIMES_CRISP = SUM_OF_WEIGHT_TIMES_CRISP +
            RULE_WEIGHT(i, j) * RULE_INDEX(i, j);
    end
end

deltaD = SUM_OF_WEIGHT_TIMES_CRISP / SUM_OF_WEIGHT;
D = D + deltaD;

if (D < 0.02)
    D = 0.02;
end

```



```
if (D > 0.98)  
  D = 0.98;  
end
```

```
Dprev = D;  
Vprev = Vpv;  
Pprev = Ppv;
```



Triangle Membership Function (TRIMF)

```
function M = TRIMF(error, A, B, C)
    if (error <= A) || (error >= C)
        M = 0;
    end

    if (error > A) && (error <= B)
        M = (error - A) / (B - A);
    end

    if (err > A) && (err < C)
        M = 1 - (err - B) / (C - B);
    end
end
```



Left Trapezoid Membership Function (ZMF)

```
function M = ZMF(error, A, B)
    if error <= A
        M = 1;
    end
    if (error > A) && (error < B)
        M = 1 - (error - A) / (B - A);
    end
    if (error >= B)
        M = 0;
    end
end
```



Right Trapezoid Membership Function (SMF)

```
function M = SMF(error, A, B)
    if error >= B
        M = 1;
    end
    if (error < A) && (error > B)
        M = 1 - (error - B) / (A - B);
    end
    if (error <= A)
        M = 0;
    end
end
```

